

Biogeochemistry of Pb in the Northeastern Subarctic
Pacific Ocean and the Beaufort Sea of the Arctic Ocean

by

Jeffrey William Charters

B.Sc., Trent University, 2008

A THESIS SUBMITTED IN PARTIAL FULFILLMENT OF
THE REQUIREMENTS FOR THE DEGREE OF

MASTER OF SCIENCE

in

THE FACULTY OF GRADUATE STUDIES

(Earth and Ocean Science)

The University of British Columbia

(Vancouver)

September 2012

© 2012 Jeffrey William Charters

Abstract

Using a method which simultaneously concentrates and isolates Pb from seawater, a total of 208 samples collected using trace-metal clean techniques were determined for dissolved Pb concentration in the subarctic Northeast Pacific and the Canada Basin of the southwestern Arctic Ocean. The analytical method found good agreement between determined values and consensus values of several seawater standards. Concentration in seawater was generally dictated by proximity to pollution sources which appeared to provide Pb via aeolian deposition and by proximity to primary productivity or freshly precipitated mineral phases which scavenged Pb to lower levels than expected based on previous research. Over the entire dataset, concentration ranged from 1.8 pmol/kg to 81.3 pmol/kg, with the highest values occurring just below the permanent mixed layer in the northeast Pacific and was of unknown origin. The lowest level was found in the Pacific water mass of the southern Beaufort Sea, which may be the result of interactions with sediment during transit through the Bering and Chukchi Seas. When samples that were expected to be contaminated are discounted, Pb levels were generally lowest in the Arctic, below 30 pmol/kg. Samples taken from three eddies along the British Columbian and southern Alaskan coasts found low [Pb] within the eddy relative to reference stations, though in two of the eddies a phytoplankton bloom had not occurred, suggesting that either the source water was low in Pb or scavenging had occurred by sorption onto precipitated mineral phases during estuarine processes. A low-resolution time series between 1992 and 2010 at Ocean Station Papa (OSP; 50 °N, 145 °W) found that Pb concentration at this location has remained quite steady over time, in contrast with the North Atlantic Ocean which showed a drastic decrease in concentration over the same time period. The difference may be attributed to formation of the water mass in the Sea of Okhotsk during the winter when atmospheric conditions would transport most Asian pollution away from the region where the water mass subducts and advects towards OSP, along with a different history of Pb pollution upwind of the Atlantic and Pacific Oceans.

Table of Contents

Abstract.....	ii
Table of Contents.....	iii
List of Tables.....	v
List of Figures.....	vi
List of Abbreviations.....	viii
Acknowledgements.....	x
Dedication.....	xi
1. Introduction to Pb, the northeast Pacific and the southwestern Arctic Ocean.....	1
1.1. Pb pollution and environmental behaviour.....	1
1.1.1. History of Pb pollution.....	1
1.1.2. Sources of Pb to the environment.....	1
1.1.3. Biogeochemical behaviour of Pb in seawater.....	2
1.2. Lead in the Pacific Ocean.....	5
1.2.1. The subarctic northeast Pacific Ocean.....	5
1.2.2. Spiciness in the northeast Pacific.....	6
1.2.3. Mesoscale eddies in the Gulf of Alaska.....	8
1.2.4. Lead in the North Pacific Ocean.....	9
1.3. The polar seas.....	10
1.3.1. Hydrography of the western Arctic Ocean.....	10
1.3.2. Lead trends in the Southern Ocean.....	12
1.4. Aims of thesis.....	13
2. Distribution of Pb in the upper waters of the subarctic northeast Pacific Ocean.....	14
2.1. Introduction.....	14
2.2. Methods.....	15

2.3. Results and discussion.....	18
2.4 Conclusions.....	28
3.A synoptic survey of Pb in three eddies in the Gulf of Alaska.....	30
3.1. Introduction.....	30
3.2. Methods.....	31
3.3. Results.....	33
3.4. Discussion.....	35
3.4.1. Haida eddy.....	36
3.4.2. Sitka and Yakutat eddies.....	38
3.5. Conclusions.....	39
4. A first look at dissolved Pb in the Canada Basin of the western Arctic Ocean.....	41
4.1. Introduction.....	41
4.2. Methods.....	43
4.3. Results.....	45
4.4. Discussion.....	46
4.5 Conclusions.....	49
5. Conclusion.....	50
References.....	53
Appendix I.....	61
Isotope dilution mass spectrometry method.....	61
Appendix II.....	65
Data Tables.....	65

List of Tables

Table 2.1. Typical operating conditions during ICP-MS analysis.....	22
Table 2.2. Comparison of certified or agreement values of reference materials and determination by ID-MS. Asterisk denotes a certified value. Error for all values except CASS-4 is 1 standard deviation, error for CASS-4 is 95% confidence interval.....	22
Table 2.3. Results of Pb determination for stations along Line P including historic data from archived samples collected in 1992 and 2003. Depth is reported in meters (m), potential density ($\sigma\text{-0}$) and spiciness are presented in units of kg/m^3 and [Pb] is reported as pmol/kg . Duplicate and triplicate Pb determinations are separated by commas.....	23
Table 2.4. Results from the stations occupied during the coastal cruise along transects off the coast of British Columbia and southern Alaska during August 2010. Depth is reported in meters (m), potential density (Sigma-0) and spiciness are in kg/m^3 and [Pb] is reported as pmol/kg . Multiple values for [Pb] separated by commas are replicate measurements as outlined in the methods section.....	29
Table 3.1. Comparison of certified or agreement values of reference materials and determination by ID-MS. Asterisk denote a certified value.....	46
Table 3.2. Results of Pb determinations in the Haida eddy along with relevant physical parameters. Latitude and longitude are presented as degrees north and west respectively, depth is in metres (m), potential density (Sigma-0) and spiciness are reported as kg/m^3 and [Pb] is in pmol/kg . [Pb] separated by commas are replicates from the same subsampled container. Values reported in brackets were prepared and analyzed a second time and replaced with the value of the second determination.....	48
Table 3.3. Results of Pb determinations in the Sitka and Yakutat eddy along with relevant physical parameters. Latitude and longitude are presented as degrees north and west respectively, depth is in metres (m), potential density (Sigma-0) and spiciness are reported as kg/m^3 and [Pb] is in pmol/kg . [Pb] separated by commas are replicates from the same subsampled container. [Pb] values with an asterisk are instrument replicates (same sample run on the instrument on consecutive days). Values reported in brackets were prepared and analyzed a second time and replaced with the value of the second determination.....	49
Table 4.1. Comparison of certified or agreement values of reference materials and determination by ID-MS. Asterisk denote a certified value.....	64
Table 4.2. Results of Pb determinations in the Canada Basin along with relevant physical parameters. Latitude and longitude are presented as degrees north and west respectively, depth is in metres (m), potential density (Sigma-0) is reported as kg/m^3 , salinity is reported in psu and [Pb] is in pmol/kg . [Pb] separated by commas are replicates from the same subsampled container.....	65
Table 5.1. The relative abundance of Pb isotopes in natural samples and the ^{207}Pb -enriched material used for isotope dilution.....	74
Table 5.2. Typical operating conditions for the Element 2 during analysis.....	75

List of Figures

Figure 1.1. A series of vertical profiles showing changes in [Pb] in the North Atlantic Ocean over time. Reprinted from <i>Analytica Chimica Acta</i> , 686(1-2), J.-M. Lee, E.A. Boyle, Y. Echegoyen-Sanz, J.N. Fitzsimmons, R. Zhang, R.A. Kayser, Analysis of trace metals (Cu, Cd, Pb, and Fe) in seawater using single batch nitrilotriacetate resin extraction and isotope dilution inductively coupled plasma mass spectrometry, pages 93-101, Copyright (2011), with permission from Elsevier.....	3
Figure 1.2. Map showing the bifurcation of the North Pacific Current (NPC) off the coast of North America. The northern stream becomes the Alaska Current and the southern stream becomes the California Current.....	5
Figure 1.3. Sample image showing near-realtime sea surface altimetry based on satellite measurements. The grey arrow shows an anticyclonic eddy (positive anomaly) off the coast of Haida Gwaii, Canada. Image is courtesy of Robert Leben, University of Colorado (http://www-ccar.colorado.edu/~realtime/welcome/).....	7
Figure 1.4. A sample vertical profile of temperature and salinity in the Canada Basin of the Arctic Ocean. Note the depth axis is on a logarithmic scale. Water masses identified are a near-surface temperature maximum (NSTM), the remnant of the previous winter's mixed layer (rWML), the summer and winter Pacific water masses (PSW and PWW, respectively) and the Atlantic and deep waters.....	9
Figure 2.1. Western coast of Canada and southwestern Alaska. Coastal samples were obtained from stations marked with a diamond and Line P samples from those stations labelled with a diamond. Black dots indicate CTD measurements but no trace-metal clean samples taken. The square at 48°N, 141°W is the location of “P12” used for historical comparison.....	20
Figure 2.2. Vertical profiles of dissolved Pb along Line P.	22
Figure 2.3. A cross-section of the surface waters of Line P. The coloured contouring represents transmissivity as a percentage of beam transmission. Lower transmissivity indicates greater turbidity. The black contour lines show chlorophyll a estimated from fluorescence in mg/L and coloured dots represent [Pb] in pmol/kg.....	23
Figure 2.4. Cross-section of data along Line P. The background colouring represents spiciness in kg/m ³ , black contours are isopycnal surfaces and coloured dots are [Pb] in pmol/kg. The three [Pb] data points at 127.6°W are from station G9, which coincidentally overlapped with the Line P transect.....	24
Figure 2.5. Property-property plot showing potential temperature against salinity for all 2010 NE Pacific samples from this study. [Pb] is shown as coloured dots in pmol/kg. The high [Pb] measurements in the warm/fresher waters were from the northernmost W-line.....	25
Figure 2.6. Cross-sections of hydrographic lines off the coast of Alaska and British Columbia. Colours and contours are as per Figure 2.4.....	28
Figure 2.7. Surface wind patterns at a buoy located 56.6°N, 136.1°W near Sitka, Alaska.....	28
Figure 2.8. Concentration of Pb in the outermost station of each coastal transect at a depth of 1500m, interpolated where necessary from nearest proximate data points.....	29

Figure 2.9. A series of vertical profiles acquired at or near P26 at the end of Line P. Data from “P12” and isotope ratios were published by Flegal et al (1986), the station was actually located south of Line P between the current P26 and P20. The remaining samples were collected by the Oriens laboratory and acidified until analysis in 2010.....30

Figure 3.1. Map of the northeast Pacific Ocean showing the region from which samples were taken. Vertical profiles to a depth of 800m were taken from stations with marked by large symbols which were chosen to provide a station outside the eddies (reference), one from the eddy edge and one through the core of the eddy. Two shallow samples (10m or 40m and 100m) were taken from each station marked by a white circle. Stations without trace metal sampling are shown as black dots. CTD measurements were taken from all stations.....37

Figure 3.2. Vertical profiles of dissolved [Pb] at the seven stations where full profiles were taken. A) is the reference, edge and centre stations of the Haida eddy and B) shows reference and edge stations in the Sitka eddy as well as a profile through the centre of each of the Sitka and Yakutat eddies.....39

Figure 3.3 a and b. [Pb] is plotted as a function of depth as coloured dots for the a) Haida eddy and b) Sitka and Yakutat eddies. The coloured shading of the background shows the spiciness calculated from temperature and salinity. Isopycnal surfaces are shown as black lines.....41

Figure 3.4. Vertical profile of [Pb] at the Haida eddy reference station collected in 2005 compared to Station P16 collected in 2010.....42

Figure 4.1. Depth profile of temperature and salinity at a representative station in the southern Canada Basin. Note the vertical axis is on a logarithmic scale.....49

Figure 4.2. Map of the southwestern Arctic Ocean showing the Canada Basin and the location of the six station sampled for this study.....51

Figure 4.3. All vertical profiles collected in this study. Arrows along the depth axis indicate method duplicates at that depth. The figure on the right is an expansion of the top 600 m.....53

Figure 4.4. The concentration of Pb in the sample closest to subsurface water masses in the Beaufort Gyre. Stations are listed in order sampled from left to right.....55

Figure 4.5. [Pb] against salinity for the four uncontaminated stations.....56

List of Abbreviations

BATS	Bermuda Atlantic Time Series
BC	British Columbia
BCE	before common era
C	celsius
CE	common era
E	east
CCGS	Canadian Coast Guard Ship
CTD	conductivity-temperature-depth
CUC	California Undercurrent
CUE	California Undercurrent Extension
DDI	Distilled deionised (water)
FiLTER	Fipke Laboratory for Trace Element Research
GoA	Gulf of Alaska
h	hour
HEPA	High-efficiency particulate air (filter)
HNLC	high-nutrient/low-chlorophyll
HOT	Hawai'i Ocean Time-series
ICP-MS	inductively-coupled plasma mass spectrometry
ID-MS	isotope-dilution mass spectrometry
kg	kilogram
km	kilometer
L	liter
m	meters
min	minute
ml	milliliter
MODIS	Moderate Resolution Imaging Spectroradiometer
ms	millisecond
N	north / normal
NPC	North Pacific Current
NSTM	Near-surface temperature maximum
NPIW	North Pacific Intermediate Water
OSP	Ocean Station Papa (50°N, 145°W)

pH	$-\log[H^+]$
pmol	picomole (10^{-12} mol)
PSW	Pacific Summer Water
PWW	Pacific Winter Water
RF	Radio frequency
R/V	Research Vessel
rWML	remnant of Winter Mixed Layer
S	salinity
v	volume
W	west / Watt

Acknowledgements

First and foremost I would like to thank Kristin Orians for her knowledge, patience and assistance in all aspects of this thesis from start to finish. I would like to acknowledge the help I've received from my committee, their insight into ocean and chemical dynamics has been invaluable. The committee consists of Susan Allen, Roger Francois and Dominique Weis. A big thank you to my labmates, Jason McAlister, Amy Cain, Nari Sim and Ania Posacka along with honorary labmate Francis Choi for making the process a bit more fun and for being good friends. A special mention goes to Alyssa Shiel for providing amazing advice and direction in this project and in the lab, and for providing moral support and helping me feel like everything was in its proper place when all felt lost. Kristina Brown assisted in getting me onto the *CCGS Louis S. St. Laurent* for which I will be forever grateful. Bert Mueller, from the Fipke Laboratory for Trace Element Research (FiLTER) at the UBC Okanagan campus provided assistance with sample analysis and instrument time, which was invaluable to the project. The Natural Science and Engineering Research Council provided funding in the form of a postgraduate scholarship.

Finally, I'd like to thank my family for being there when I needed it, and thanks to Yasha Podeswa and Trampus Goodman for good times shooting balls and pucks around when having fun was needed. Cathryn Clarke Murray was a great friend and along with her family gracious hosts for fine summer barbecues. Please don't feel slighted if you're not personally mentioned in this list, it is by no means exhaustive and I appreciate the help and friendship from everyone I've met along the way and those I've known for ages.

Dedication

For my family, nuclear and extended.

1. Introduction to Pb, the northeast Pacific and the southwestern Arctic Ocean.

1.1. Pb pollution and environmental behaviour

1.1.1. History of Pb pollution

With a current global population of roughly seven billion people, humans have greatly modified the distribution of various chemicals on the planet (Nriagu, 1996). Even during the civilizations of the Greek and Roman empires beginning about 500 B.C.E. and finally collapsing around 300 C.E., the quantities of Pb being released to the atmosphere were measurably higher than natural concentrations (Hong et al., 1994). In those times, ores were smelted on open fires to extract the metals of interest and the resulting smoke was a significant source of pre-industrial air pollution to those societies.

In the years leading up to the industrial revolution in the late 18th century and to an even greater extent in the years from then until the 1980s, the amount of Pb being released into the environment increased dramatically (Nriagu, 1996). Prior to the industrial revolution, emissions were primarily by-products of wood combustion and waste incineration and eventually as a by-product of large-scale ore smelting and iron and steel production in the early years of industry (Nriagu, 1979). Beginning in the 1920s, tetraethyl lead began being used as an anti-knock additive in fuel for internal combustion engines (Nriagu, 1990). At the time the compound was considered a “gift from God” because of its ability to improve the performance of engines in a growing society, but eventually the polluting nature of the added Pb was deemed too great to ignore and it was finally phased out of gasoline beginning in the mid-1970s. Along with Hg, Pb is one of the most anthropogenically disrupted elements on the planet.

The introduction to the work in this thesis will start by considering the upset of the natural Pb cycle as a result of anthropogenic activities, followed by the behavior of the element in seawater. An overview of the Northeast Pacific ocean and studies on Pb in the oceans will be given along with a brief description of the mesoscale eddies which form along the coast and move into the Gulf of Alaska. Finally we will cover the water masses of the Western Arctic Ocean and examine the work done on dissolved Pb in the remote Southern Ocean, which has comparably low atmospheric input and hostile conditions for biota as the Arctic.

1.1.2. Sources of Pb to the environment

According to estimates by Nriagu in 1979, there are about 24.5 million kilograms of Pb emitted to the atmosphere by natural sources annually. The main contributors to this total are wind-blown dusts (65% of total)

and volcanic particulates (26%). The remaining fraction comes from vegetation exudates, forest fires and sea-spray. At its peak in the late 1970's, human activities were responsible for the release of almost 450 million kilograms of Pb per year, an almost 20-fold increase over the natural releases as a global average. However, we must also consider that near point sources of Pb such as major cities, power plants and smelters, the anthropogenic emissions can be thousands of times higher than what would be released naturally. Once in the lower atmosphere, Pb generally will not cross from the northern to the southern hemisphere or vice-versa as a result of tropospheric circulation patterns. This, along with most major industrial centers being north of the equator, leads to the northern hemisphere being generally more polluted than the south (Wolff and Suttie, 1994; Nriagu, 1996).

In some instances, knowing only the concentration of Pb in a particular sample or reservoir is sufficient to determine the presence of contamination over natural background concentrations. For example, work done by (Murozumi et al., 1969) used the varying concentrations of Pb in Greenland ice cores, corrected for varying natural inputs, to deduce that anthropogenic contamination was occurring well before the industrial revolution. However, it is often useful to make determinations of the relative abundances of the four stable isotopes. This provides an isotopic “fingerprint” for the sample of interest, which can then be traced back to known source regions. Among many other uses, this method has been utilized for determining the Asian component of Pb in North American aerosols (Ewing et al., 2010).

1.1.3. Biogeochemical behaviour of Pb in seawater

One of the longest-studied stations in the ocean with regards to Pb is the Bermuda Atlantic Time Series (BATS), located about 90 km southwest of the island of Bermuda. Figure 1.1 shows a series of vertical profiles taken over a thirty year span from 1979 to 2008, measured by various researchers (Schaule and Patterson, 1983; Boyle et al., 1986; Wu and Boyle, 1997a; Lee et al., 2011). The decline in concentration after the phaseout of leaded gasolines in North America is drastic and appears to affect the ocean above a depth of about 2000m. In this region, the concentration of Pb in near-surface waters has shown a greater than three-fold decrease from greater than 150 pmol/kg for waters sampled in 1979 to well under 50 pmol/kg in 2008. Work by Kelly et al. (2009) in this same area examined the ratio of Pb to Ca in annually-banded corals and found that less Pb was being incorporated into the coral during the same time period.

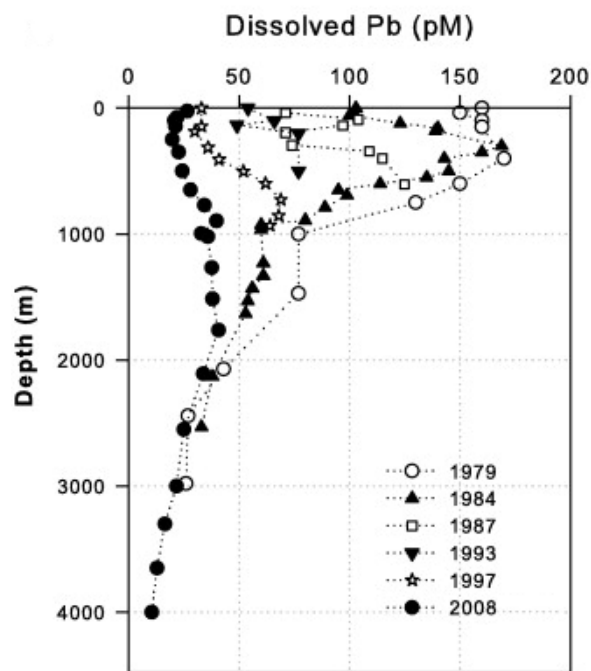


Figure 1.1. A series of vertical profiles showing changes in [Pb] in the North Atlantic Ocean over time. *Reprinted from Analytica Chimica Acta, 686(1-2), J.-M. Lee, E.A. Boyle, Y. Echegoyen-Sanz, J.N. Fitzsimmons, R. Zhang, R.A. Kayser, Analysis of trace metals (Cu, Cd, Pb, and Fe) in seawater using single batch nitrilotriacetate resin extraction and isotope dilution inductively coupled plasma mass spectrometry, pages 93-101, Copyright (2011), with permission from Elsevier.*

It was in 1974 that Patterson (1974) published a brief communication in *Science* that interlaboratory comparison of seawater samples was showing grossly inadequate results due to poor sampling and sample handling and that steps were needed to be taken to avoid contamination and provide accurate and precise results. Concentration measurements for Pb in seawater are therefore unfortunately not available prior to the mid 1970s. The concentration of Pb in seawater ranges from 1.2 pmol/L to about 80 pmol/L (0.3 to 16.6 ng/L) at present. These levels are easily contaminated during sample collection, preparation and storage. Thus, there are only a few decades worth of determinations available and prior observations of Pb are moot.

As a result, we still have much to learn of the biogeochemistry of Pb in seawater. The main source of Pb to the oceans comes from wet or dry deposition from atmospheric sources. During the middle of the 20th century, the main source of Pb to the atmosphere was combustion of leaded gasolines (Settle and Patterson, 1982; Flegal and Patterson, 1983; Schaule and Patterson, 1983; Patterson and Settle, 1987; Shen and Boyle, 1987; Kelly et al., 2009). The fraction from this source began to decline during the phaseout of these fuels in the late 1970s, with a greater fraction coming from other industrial processes such as coal combustion, which have increased in Asia in the last twenty years, especially in China (Ohara et al., 2007; Guberman, 2009). The main source of Pb to the North Pacific and North Atlantic Oceans are industrial aerosols from Asia and North

America, respectively. Work done in the Canadian Arctic has found that since the 1970s, anthropogenic lead from North America has become less predominant while Eurasian-source emissions appear to be becoming the major source (Shotyk et al., 2005) (see also (Osterberg et al., 2008)). It was possible to differentiate the atmospheric input (via aerosols) from these two regions by looking at seasonal differences in Pb concentrations – higher inputs were recorded in the winter months, when the Canadian arctic is dominated by air masses which originate in Asia.

Once dissolved in the ocean Pb exists primarily in complexes such as PbCO_3 , $\text{Pb}(\text{CO}_3)_2^{2-}$ and PbCl^+ , with only about 2% existing as the free Pb^{2+} cation (Powell et al., 2009). The distance between the source of an atmospheric aerosol and where it is finally deposited in the ocean appears to play a role in the solubility of Pb. Studies where aerosols were collected near a coast and subsequently leached using a seawater medium found that roughly 65% of the Pb was solubilized, whereas when aerosols were collected from a remote atoll roughly 90% of the total Pb was solubilized (Maring and Duce, 1990; Chester, 2003). In contrast, crustal aerosols (as opposed to anthropogenic) were effective at scavenging this Pb back out of solution and onto particle surfaces. Although considered to be quite particle-reactive, greater than 90% of Pb is found in the dissolved phase in seawater (Bacon et al., 1976).

The major removal mechanism of Pb from seawater is via sinking particles mainly of biological origin in (Michaels and Flegal, 1990). Although the majority of Pb^{2+} is likely adsorbed to cells with a high surface area-to-volume ratio (such as bacteria) at some point, it is known that the sinking export rate of radionuclides such as ^{210}Pb is related to the amount of new production in surface waters (Fisher et al., 1988). These fresh surfaces likely establish a dynamic equilibrium fairly quickly, which would slow the adsorption rate as particulate matter ages. Michaels and Flegal (1990) argue that the efficiency with which Pb is exported from the euphotic zone is a function of the surface area of phytoplankton, the efficiency of the formation of particles (e.g. fecal pellets) and the ease with which smaller particles can be aggregated into larger particles (see also (Luengen et al., 2007)). In a situation such as this, we would expect the concentrations to be lowest where the water has been away from the surface the longest in the deep North Pacific, since it would have more time for the Pb to be scavenged. However, it has recently been discovered that the lowest concentrations known in the oceans are in the South Pacific and increase into the North Pacific (Wu et al., 2010). This could be indicative of resolubilization of Pb from sinking particles which was hypothesized by Schaule and Patterson (1981), which will be discussed in greater detail in Chapter 3.

1.2. Lead in the Pacific Ocean

1.2.1. The subarctic northeast Pacific Ocean

The surface circulation of the NE Pacific Ocean is dominated by the cyclonic Alaska Gyre. To the south, the North Pacific Current (NPC) flows eastward, essentially separating the warm, saline waters of the subtropics from the cool, fresh waters of the subarctic (Dodimead et al., 1963). As it approaches the North American continent, this current bifurcates into northward (Alaska Current) and southward (California Current) branches (see Figure 1.2) (Kawabe and Fujio, 2010).

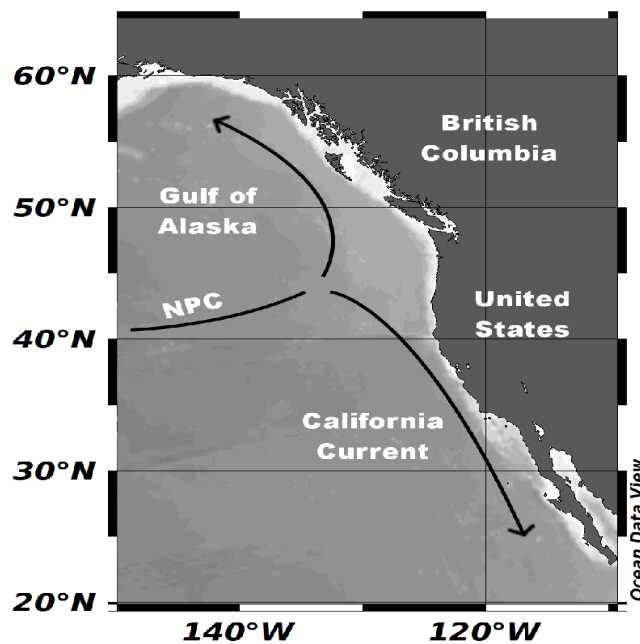


Figure 1.2. Map showing the bifurcation of the North Pacific Current (NPC) off the coast of North America. The northern stream becomes the Alaska Current and the southern stream becomes the California Current.

Line P is a series of oceanographic stations extending from the southern end of Vancouver Island, 1400 km west into the middle of the Gulf of Alaska (GoA). Ocean Station Papa (OSP, 50° N, 145° W) has been subject to sampling several times a year for over fifty years and counting, which makes it one of the oldest oceanic time series (Peña and Bograd, 2007). These stations cross from the nitrate-limited waters of the coast into the oligotrophic, iron-limited waters of the central gyre. (Whitney et al. (2007) divide the surface waters of this region into three zones: the oceanic, transition and coastal regions. The furthest from shore is the oceanic region, which is marked by low productivity and unused nutrients. Within 75km of shore is the coastal region, which

can have high productivity during periods of summer upwelling. Between these two zones is a transition region which is not directly affected by upwelling, but is also not iron-limited like the oceanic zone.

The growth of surface-dwelling autotrophic phytoplankton depends on the availability of various nutrient elements, previously thought to always be limited by nitrogen or phosphorus. In several vast expanses of ocean there exist high nutrient/low chlorophyll (HNLC) regions where there exists a surplus of both nitrate and phosphate where one would expect to find blooms of phytoplankton and yet there are none. In 1987, Martin and Fitzwater added nanomolar (10^{-9} mol/liter) concentrations of Fe to seawater collected from OSP and observed significantly higher levels of chlorophyll *a* being produced compared to control samples. As a result of this iron-limitation, the primary productivity of this region is generally low, and scavenging by biological particles would not be expected to play a large role in the distribution of lead in the central gyre (Martin and Fitzwater, 1988).

At intermediate depth (150-400 m) in this region we would expect to see the effects of North Pacific Intermediate Water (NPIW) along the σ_{θ} 26.8 isopycnal (You, 2005). The only known region where this water mass ventilates is around the Sea of Okhotsk on the western margin of the Pacific Ocean where a mixture of waters would sink in the cold winters and travel eastward toward the western stations of Line P (Ueno and Yasuda, 2003). It would be expected that if a Pb source were present to the surface waters of the Okhotsk Sea in winter when primary productivity is light-limited, this source may be able to advect below the mixed layer and provide a subsurface source of Pb to OSP.

1.2.2. Spiciness in the northeast Pacific

The density of a water parcel is dependent on its temperature and salinity. When plotting data on a temperature-salinity property-property plot isopycnals cover a range of temperature and salinity as seen in Figure 1.3. Munk (1981) referred to the difference between the points as “spice”, as the varying heat content (balanced by increased salinity) was responsible for this difference. Spiciness is defined as the field orthogonal to isopycnal surfaces, and in this manner can be used to condense the various combinations of potential temperature and salinity into a single conservative parameter similar to density, but which does not affect the flow balance (Dzieciuch et al., 2004). It was formally defined by Flament (2002) and has been used by others investigating the Northeast Pacific in its simplest form to describe potential temperature and salinity on a potential density surface (Davis et al., 2008). It should also be noted that although spice is conservative, solar radiation can significantly affect it near the ocean surface.

This variable was chosen in order to simplify the presentation of data while accenting the different water masses in the Northeast Pacific Region. Considering the data shown in Figure 1.3 the water present on the 26.5 potential density surface differs by over 1°C and about 0.25 practical salinity units, which could be indicative of

different sources. By contouring this data over depth and section distance (or any other unit of distance such as longitude) it is possible to get a visual interpretation of the various water masses of the region. Data on dissolved Pb concentration can then be plotted over the contour, which provides the information in the larger context of a dynamic oceanic system. Gay and Chereskin (2009) used a latitude-longitude plot of spiciness in the southern California Current System to investigate coastal processes in a manner similar to that used here, while Thomson and Krassovski (2010) used spiciness to determine the northern extent of the California Undercurrent Extension in the Gulf of Alaska. These studies provided the insight which resulted in the use of spiciness for the current application.

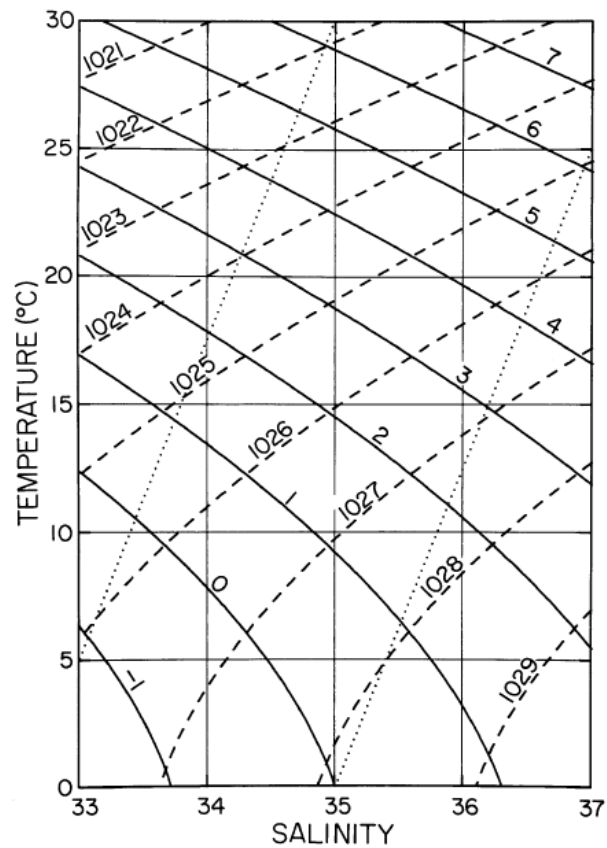


Figure 1.3. A temperature-salinity plot showing isopycnal surfaces as dashed lines in kg/m^3 , and spiciness isopleths as solid lines. Water parcels of a particular density can have a range of spiciness values depending on their temperature and salinity properties. *Reprinted from Progress in Oceanography, 54, Flament, P., A state variable for characterizing water masses and their diffusive stability: spiciness, 493-501, Copyright 2002, with permission from Elsevier.*

1.2.3. Mesoscale eddies in the Gulf of Alaska

There are numerous regions along the western coast of British Columbia and southern Alaska that spawn eddies that travel westward into the GoA, bringing with them anomalous water temperature and salinity signatures. The eddies form during the winter months as a result of the baroclinically unstable seasonal northward current before moving offshore, rotating anticyclonically with an average width of 80 to 200 km (Thomson and Gower, 1998; Di Lorenzo et al., 2005). The eddies are named based on their region of formation: Haida eddies form at Cape St. James off the southern tip of Haida Gwaii, Sitka eddies form near Baranof Island (near the town of Sitka, Alaska) in the Alexander Archipelago and Yakutat eddies form on the broad shelf near Yakutat, Alaska (Tabata, 1982; Melsom et al., 1999; Crawford, 2002; Ladd et al., 2009). Eddies can be discerned from surrounding waters by a positive sea surface height anomaly from satellite altimetry, which allows research vessels to be directed close to the core of the eddy for sampling (see Figure 1.4).

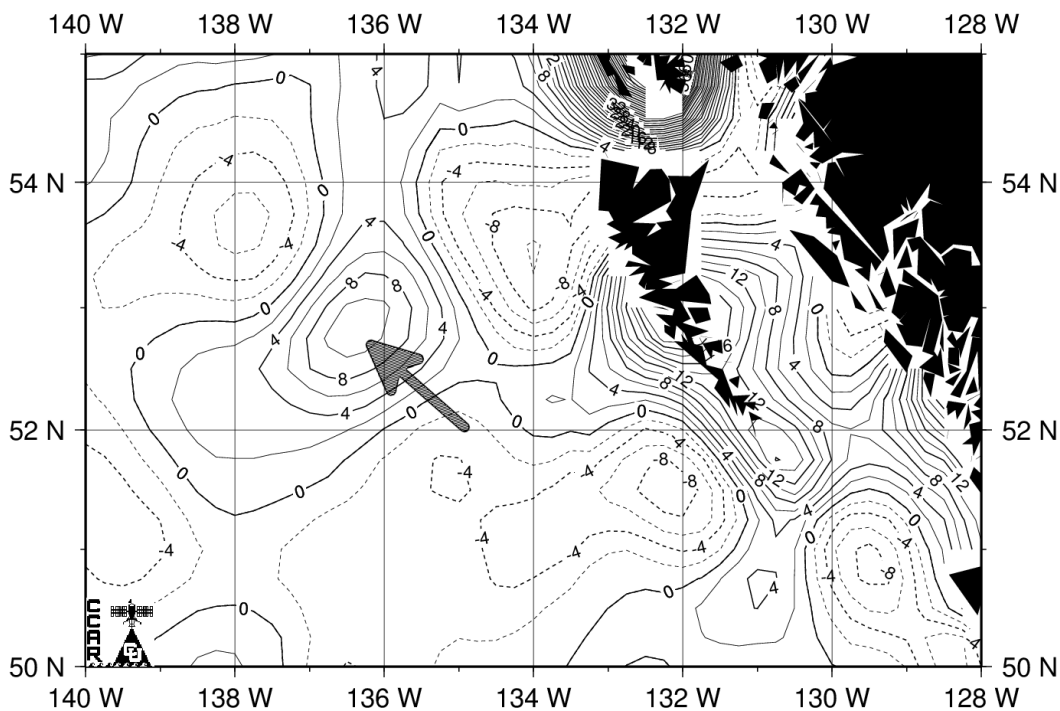


Figure 1.4. Sample image showing near-realtime sea surface altimetry based on satellite measurements. The grey arrow shows an anticyclonic eddy (positive anomaly) off the coast of Haida Gwaii, Canada. Image is courtesy of Robert Leben, University of Colorado (<http://www-ccar.colorado.edu/~realtime/welcome/>)

In the average winter, these eddies will transport an average of 50 km³ of fresh water into the open ocean (Crawford, 2005). These waters carry the physico-chemical parameters of the coastal waters from which they form, including temperature, salinity, nutrients and trace metals (e.g. Fe, Cu, Al, Mn and Cd) (Crawford, 2002;

Crispo, 2007). As these waters continue their transit to the west they slowly mix with the surrounding waters, losing energy and acquiring the same properties as their surroundings over the span of about two years.

To date, these eddies have been analyzed over several eddy-specific cruises such as Crispo (2007) and Johnson et al. (2005) from 2000-2001 as well as Ladd et al. in 2005 (published 2009) for Fe and several other trace elements (Cu, Al, Mn, Cd), but have yet to be analyzed for Pb. The samples analyzed for this work cover three young eddies, one each of Haida, Sitka and Yakutat.

1.2.4. Lead in the North Pacific Ocean

One of the earliest works concerning Pb in the Pacific Ocean measured a transect from 200km off the coast of California to the center of the north Pacific gyre. Values ranged from 75 pmol/kg in the surface at the center of the gyre to a fairly steady 5 pmol/kg at depth (Schaule and Patterson, 1981). Based on sediment Pb, it was calculated that the anthropogenic emissions at that time needed to be ten times the natural levels in order to maintain such high concentrations in the euphotic zone. They also found that concentrations were generally higher away from the coast and that the majority of Pb in seawater is in the dissolved phase (and due to uncertainty in measurement, the dissolved and total concentrations were indistinguishable).

The first use of fingerprinting using Pb isotopes with reasonable vertical resolution was a profile from station “P-12” (southwest of the present station P20 on Line P) in the northeast Pacific Ocean (Flegal et al., 1986). This research found that the high concentrations in the North Pacific were coming from both Asian and North American aerosols, but that it was likely the North American component was being advected isopycnally from closer to the coast. Samples were collected from five stations along a Line P cruise in the summer of 2010 to investigate the change over time in this area. Further, there are a number of archived seawater samples archived by our research group from cruises along Line P dating to 1992 and 2003 that can be used to fill in some temporal data gaps.

There are few studies of Pb in the open ocean North Pacific, but Pb was measured at the Hawai'i Ocean Time-series (HOT) station just north of the Hawai'ian islands in 1999 to compare with the values Schaule and Patterson found in 1976 (data published 1981) (Boyle et al., 2005). It was found that surface concentrations (<200m) had decreased from around 65 pmol/kg to 35 pmol/kg, while concentrations below this depth showed no change. This was reasonable because Pb is expected to have a residence time of about 15 years in the North Pacific and so should follow decreases in atmospheric emissions with only a short lag time (Nozaki et al., 1976). However, it is not known whether the lack of change at depth is the result of a lack of scavenging in the area or another source at intermediate depth.

A recent transect through the equatorial and subtropical eastern Pacific which almost overlapped both of

these stations found similar profiles at both locations and leaves unanswered the question of why the Pb is not being removed (Wu et al., 2010). The highest surface concentrations along the transect were found at the northernmost station at 30° N, 140° W with a value of 73 pmol/kg at 200m depth. Interestingly, this value is as high as those reported by Schaule and Patterson from samples collected three decades prior, with values slightly lower in shallower waters (on the order of 50-60 pmol/kg). The most likely explanation for these observations is that there is still a strong atmospheric input of Pb from Asia, an idea which is supported based on the isotopic data from Wu et al. (2010) and from the isotopic composition measured in corals off the coast of Japan (Inoue and Tanimizu, 2008). The residence time of Pb in the surface ocean is very short, on the order of several years, indicating that a constant supply is necessary to maintain these relatively high concentrations near the surface.

This is corroborated by a recent study by Gallon et al. (2012) which measured Pb in a series of surface samples from the Northwest Pacific collected in 2002. The concentration of Pb in these samples ranged from 32.7 to 103.5 pmol/kg with the highest concentrations offshore of China and Japan and lower concentrations in the open ocean and north near the Kamchatka Peninsula. This supports the ideas put forth by Schaule and Patterson (1981) that pollutant lead from Asia was likely the major source of Pb in the North Pacific. The authors expressed surprise at the consistency of measurements in surface waters over three decades, such as measurements at the Hawaii Ocean Time-Series (HOTS) which were statistically identical over a number of years.

The lowest known seawater concentrations, as low as 1.5 pmol/L were found in the deep equatorial Pacific transect studied by Wu et al. (2010). As previously mentioned, it was expected that the lowest concentrations would be found in the deep north Pacific where deep water is near the end of the meridional overturning circulation and has been isolated from the surface for longest. The fact that this was not the case has caused Wu et al. to conclude that some Pb is being resolubilized from sinking particles, thereby increasing concentration with northward transport of deep Pacific water. As Pb-laden particulate matter from the surface sinks into the abyssal ocean where [Pb] is lower, a new equilibrium is established which results in Pb desorbing from the surface of these particles, which results in an increase in Pb levels in these deeper waters. Since the more northern waters are generally older in the Pacific, this process has been occurring for a longer time period and thus concentrations increasing with distance to the north.

1.3. The polar seas

1.3.1. Hydrography of the western Arctic Ocean

Moving further north from the GoA, some Pacific water will pass through the Bering Strait into the

Western Arctic Ocean. The Arctic Ocean consists at the simplest level of three main water masses separated by strong halo- and/or thermoclines: a cold and quite fresh surface layer, a warmer and saltier intermediate layer and a cool, salty deep water mass (McLaughlin et al., 2005) (Figure 1.5). The potential temperatures (θ) in this ocean are so low and relatively consistent throughout the water column (range -1.8 to +1.1 °C) that density is dominated by salinity. A noteworthy feature of this ocean basin is the very large area occupied by continental shelves, which is on the order of 30%.

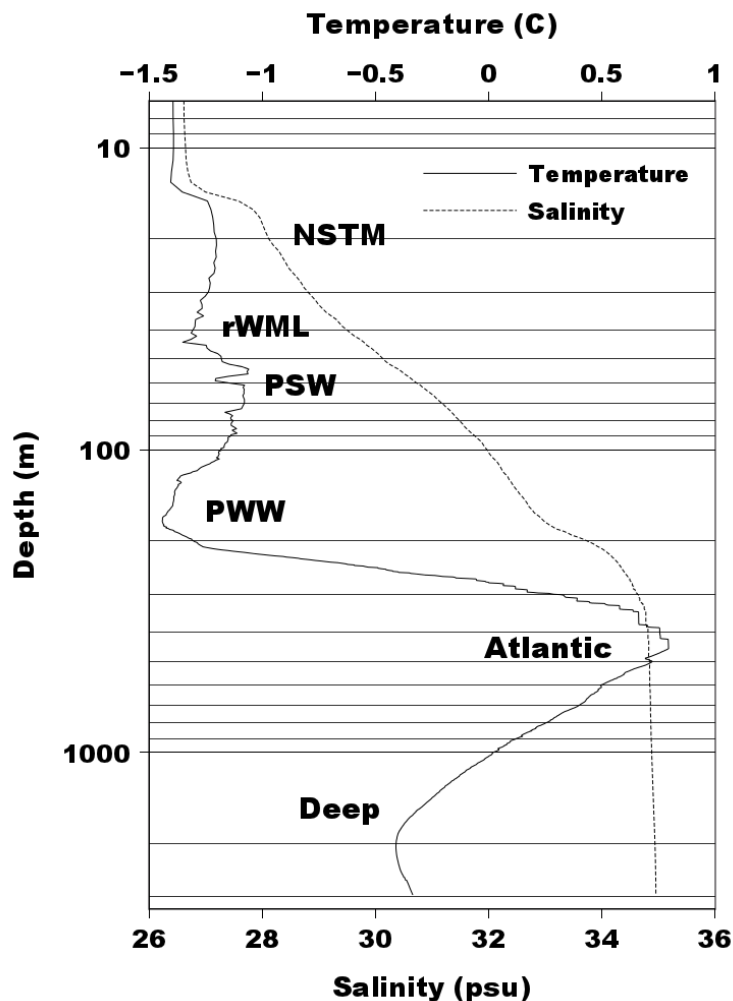


Figure 1.5. A sample vertical profile of temperature and salinity in the Canada Basin of the Arctic Ocean. Note the depth axis is on a logarithmic scale. Water masses identified are a near-surface temperature maximum (NSTM), the remnant of the previous winter's mixed layer (rWML), the summer and winter Pacific water masses (PSW and PWW, respectively) and the Atlantic and deep waters.

The upper layer is formed by fresher Pacific water entering the Arctic Ocean after passing through the Bering Strait (Coachman and Barnes, 1961; Coachman and Aagaard, 1966). As this water passes through the Bering and Chukchi seas, it is influenced by heat exchange, biological and benthic interactions to a greater or

lesser extent depending on the season (Coachman and Barnes, 1961; Nozaki et al., 1997). The Atlantic layer is separated from the Pacific waters by a halocline below 100m which leads to a temperature maximum at the core of the Atlantic water. This water forms in the North Atlantic and undergoes modifications through interactions with the shelf sediments before entering the Canada Basin, where the seawater for this thesis was collected (McLaughlin et al., 1996). The deep water in the basin has been dated using several methods which give an age of about 500 years (Macdonald and Carmack, 1991, 1993; Edmonds et al., 1998). The formation mechanism of these deep waters is still not known with certainty, but is thought to be a combination of exceptionally dense Atlantic water mixed with brine rejected during ice formation that is dense enough to reach these depths while entraining water from intermediate depths (Macdonald and Carmack, 1993; Jones et al., 1995).

Little work has been done on Pb in Arctic seawater, with no prior reported measurements in the western Arctic. Samples from the North Sea several decades ago found very high concentrations averaging 160 pmol/kg in the surface, similar to a station such as BATS during the same time period, with concentrations at depth on the order of 20 pmol/L (Brügmann et al., 1985). These waters could potentially be incorporated into the Atlantic layer of the Arctic Ocean. Dai and Martin (1995) reported that concentration in the “bottom waters” of the Kara Sea north of Russia had dissolved Pb concentrations from 11.4 to 35.6 pmol/L, which is consistent with subsurface waters of other regions.

Other work on Pb in the Arctic has found that aerosols from the eastern side of the Canadian archipelago appear to consist primarily of Pb of anthropogenic origin (Shotyk et al., 2005). However, the low absolute mass of Pb delivered to the Arctic has resulted in lichens on Baffin Island having some of the lowest Pb concentrations in any mosses or lichens known (France and Coquery, 1996). As such, it is expected that atmospheric sources will be a minor pathway of Pb, and most of the element will be a remnant of the Pacific or Atlantic source waters for the surface and intermediate waters, respectively.

1.3.2. Lead trends in the Southern Ocean

It is also worth considering Pb in the Southern Ocean, as the area surrounding Antarctica is far from any major point sources of anthropogenic pollution. Further, as a result of less continental landmass in the southern hemisphere, models have shown that the natural abundance of Pb should be an order of magnitude lower than the northern hemisphere (Henderson and Maier-Reimer, 2002). Although the first concentration profiles analyzed for Pb in the region found no evidence of anthropogenic contamination, the first analyses of isotopes in this region on samples collected in 1987 and 1988 found that anthropogenic contamination appeared to be present in surface waters of what the authors called “the most remote region of the Earth” (Westerlund and Öhman, 1991; Flegal et al., 1993). This was in spite of the fact that concentrations of the surface waters were

found to be very low compared to other oceans – ranging from 4 to 37 pmol/L.

1.4. Aims of thesis

This thesis aims to provide greater understanding of the biogeochemistry of Pb in the Northeast Pacific. The work in mesoscale eddies will complement similar work on this topic such as the work done by Crispo (2007). The sampling resolution in the surface waters of Line P is greater than any previous work in this region, which may give better insight into processes which are often simply glazed over in published literature. It will also provide an update on the concentration of Pb in the region, which has not been done in decades. As the Asian continent develops economically and more of their population moves into the middle class the pollution may travel into the North Pacific on prevailing winds, or travel with NPIW to become a source at depth (see Chapter 4).

Further, I have investigated whether anthropogenic lead exists in the Canada Basin of the Arctic Ocean. Sediment cores in the Canada Basin appear to be affected very little, if at all, by anthropogenic lead (Gobeil et al., 2001). It was determined based on ^{210}Pb in the sediment that particles were actively being removed from the water column, but that contaminant Pb from the Atlantic simply never reaches the Canada Basin. This is in contrast to North Atlantic water which flows to the south and becomes North Atlantic Deep Water which has been transported further south than Bermuda (Véron et al., 1999). It is possible that over the shallow shelf areas of the Eurasian Arctic a large proportion of Pb is stripped out during periods of intense primary productivity or interaction with sediments. However, there has never been a determination of Pb in the Western Arctic Ocean to my knowledge, so it may be possible to infer a pollution source from elevated concentrations alone.

2. Distribution of Pb in the upper waters of the subarctic northeast Pacific Ocean.

2.1. Introduction

Anthropogenic Pb emissions during the combustion of fossil fuels has elevated atmospheric concentrations ten-fold higher than natural levels over the past century (Osterberg et al., 2008). Ice cores taken from various icefields in the northern hemisphere have shown that while the North Atlantic and Arctic have experienced less deposition of Pb since the phaseout of leaded gasoline in the 1970s the North Pacific has shown an opposite trend, with concentrations increasing between the 1970s and the end of the study in 1998. Oceanic concentrations of Pb have shown a similar trend with near-surface concentrations in the Atlantic declining from over 150 pmol/kg to about 25 pmol/kg between 1979 and 2011 whereas there does not seem to be a significant change in Northeast Pacific concentrations which remain steady around 70 pmol/kg in the subsurface waters (Schaule and Patterson, 1981, 1983; Boyle et al., 1986; Flegal et al., 1986; Wu et al., 2010; Lee et al., 2011).

Recent research along a meridional transect of the Pacific Ocean has shown a gradient with higher concentrations at all depths with increasing latitude as a result of desorption of Pb from sinking particles and the older age of more northerly waters (Wu et al., 2010). Although vertical profiles of Pb have been determined at various locations in the Northeast Pacific in the past, there lacks any information on zonal distribution of Pb in this region (Schaule and Patterson, 1981; Flegal et al., 1986). The current study was undertaken to acquire some understanding of Pb biogeochemical behaviour in this region which may shed light on how the system will respond to future changes in Pb pollution.

Most recent work involving Pb in seawater has utilized isotopic information to make inferences on anthropogenic pollution (for example, Wu et al., (2010)). Other work has shown great temporal resolution of [Pb] albeit with no spatial variability (Boyle et al., 2005). The most recent publication investigating biogeochemical cycling in-depth in the Northeast Pacific was also one of the earliest works in the field by Schaule and Patterson (1981) consisting of two vertical profiles and a surface transect. The present work aims to build on this foundation with emphasis on the upper water masses in the subarctic Northeast Pacific. See Chapter 1.2.1 for more information on the Line P time series.

The main source of lead to the oceans is via atmospheric deposition, which in the North Pacific is of Asian origin (Osterberg et al., 2008; Ewing et al., 2010). An estimated 65-90% of this Pb dissolves, with generally greater than 90% of seawater Pb existing in the dissolved phase (Bacon et al., 1976; Maring and Duce,

1990; Chester et al., 1993). The major removal mechanism for Pb from seawater is via scavenging by biogenic particles (Michaels and Flegal, 1990). Although the majority of Pb²⁺ is likely adsorbed to bacteria at some point, it is known that the sinking export rate of radionuclides such as ²¹⁰Pb is related to the amount of new production in surface waters (Fisher et al., 1988). Michaels and Flegal (1990) argue that the efficiency with which Pb is exported from the euphotic zone is a function of the surface area of phytoplankton, the efficiency of the formation of particles (e.g. fecal pellets) and the ease with which smaller particles can be aggregated into larger particles (see also Luengen et al. (2007)).

Wu et al. (2010) deduced from isotopic data that Pb in the upper 400 m of the subtropical Northeast Pacific is predominantly of Asian origin, which conflicted with conclusions that Pb in waters of intermediate depth (400m) was of North American origin drawn earlier by Flegal et al. (1986) of the subarctic Northeast Pacific, though the difference was chalked up to samples being taken from different geographic locations. The current study is in close proximity with the stations occupied by Flegal et al. (1986) in 1980 and it is hoped that greater sampling resolution may clarify the reason a difference is seen between these locations. Archived samples from cruises between the time of that study and the present were also available to provide a sense of temporal variability in the subarctic Northeast Pacific.

2.2. Methods

Samples were collected from a number of hydrographic lines extending offshore of British Columbia, Canada and Washington and Alaska, USA aboard the *CCGS John P. Tully* during August and September of 2010 (Figure 2.4). Five of the hydrographic lines extend about 100-200 km from shore, while the Line P transect extends over 1400 km into the subarctic gyre of the Pacific Ocean. Samples from the coastal hydrographic lines were collected using a trace-metal clean rosette on Kevlar line. GO-Flo bottles were used on Kevlar line on Line P. A normal rosette cannot be used in order to avoid in-situ trace metal contamination. Subsampling from the rosette and GO-Flo bottles was done in a container on deck (coastal cruise) or the ship wet lab (Line P). Samples were collected into 500 or 1000 ml acid-leached low-density polyethylene bottles and acidified in laminar flow hoods to pH ~1.8 until analysis using Seastar Chemicals Baseline HCl. On both cruises, CTD casts were done at stations from which trace metal samples were not taken. The physico-chemical data from these casts were used to fill in data gaps between the stations from which trace metal samples were taken.

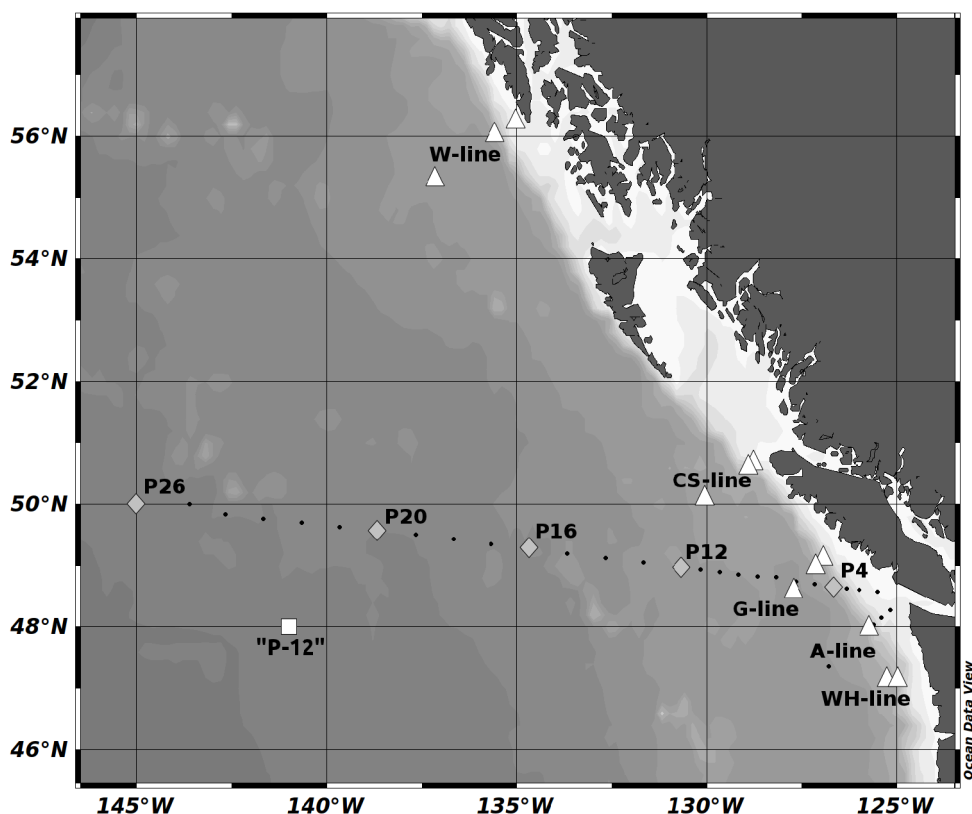


Figure 2.1. Western coast of Canada and southwestern Alaska. Coastal samples were obtained from stations marked with a triangle and Line P samples from those stations labelled with a diamond. Black dots indicate CTD measurements but no trace-metal samples taken. The square at 48°N, 141°W is the location of “P12” used for historical comparison.

The analysis method used was a modified version of the magnesium-induced coprecipitation technique introduced for Pb analysis by Wu and Boyle (1997b). Briefly, 13 ml of acidified seawater was transferred to a 15 ml acid-cleaned centrifuge tube and spiked with 50 µl of a ²⁰⁷Pb-enriched standard (see Appendix I for detailed method). After sitting for greater than 1h to allow isotopic equilibration, 175 µl of Seastar Chemicals concentrated NH₄OH (11 N) was added and shaken to mix. This solution was allowed to react and precipitate for five minutes before centrifuging. The supernatant was decanted and recentrifuged to remove as much liquid as possible. The remaining Mg(OH)₂ pellet was dissolved in 1-2 ml of 1% HNO₃ for analysis.

Determinations were performed using a Thermo Scientific Element XR high-resolution ICP-MS at the Fipke Laboratory for Trace Element Research (FiLTER) at the Okanagan Campus of the University of British Columbia. Blanks were analyzed every ten samples, one sample out of 20 was prepared and analyzed in duplicate and one sample out of 20 was prepared and analyzed in triplicate which resulted in replicate measurements on greater than one in every 10 samples. Typical operating conditions used during analysis can be

seen in Table 2.1.

Table 2.1. Typical operating conditions during ICP-MS analysis.

Parameter	Setting
Forward Power	1100 W
Reflected RF Power	3 W
Cooling Gas	16.0 L/min
Auxiliary Gas	0.9 L/min
Sample Gas	1.125 L/min
Isotopes detected	²⁰⁷ Pb, ²⁰⁸ Pb
Dwell time /isotope	50 ms
Passes per run	120
Number of runs	5
Scan mode	Electric sector

The isotope-dilution mass spectrometric (ID-MS) method used here was found to be quick and robust in the determination of Pb in seawater. The results of replicate measurements on certified or interlaboratory materials can be found in Table 2.2. The SAFe samples were originally collected for interlaboratory validation of Fe concentrations, and the GEOTRACES Surface (GSI) and deep (GDI) are samples being compiled for intercomparison of laboratories participating in the GEOTRACES program (Johnson, 2007; Sohrin and Bruland, 2011). The expected concentration range normally seen in seawater ranges from 10 to 150 pmol/kg, thus this method is suitable to accurately determine the [Pb] of a particular sample. It should be acknowledged that the measurements in our laboratory are on the lower end of the consensus values, although our determinations were in agreement with individual measurements reported by other laboratories to develop the mean value. If the difference between our values and consensus values were random, it would be expected that some of our values would be higher than the mean rather than consistently lower. This indicates some sort of systematic bias which we were unable to isolate and remove from the method, or it could be that the samples received by our lab were slightly more free of any possible contamination than those received by other labs. There was no correction made for mass bias within the ICP-MS, as this effect should be negated as a result of performing the initial reverse-isotope dilution of the known standard. The uncertainty in concentration determination is about 10% at 8 pmol/kg and decreases to 2% at 30 pmol/kg.

Table 2.2. Comparison of certified or agreement values of reference materials determined by ID-MS in pmol/kg. Asterisk denotes a certified value. Error for all values except CASS-4 is 1 standard deviation, error for CASS-4 is 95% confidence interval.

	SAFe S	SAFe D1	SAFe D2	CASS-4*
Consensus	47.0 ± 3.4	26.0 ± 1.5	27.6 ± 1.9	47 ± 17
Measured	43.6 ± 0.4	25.4 ± 4.3	25.7 ± 0.3	36.9 ± 0.4
<i>n</i> =	5	5	5	4

2.3. Results and discussion

Vertical profiles from each of the five stations along Line P can be seen in Figure 2.2. The maximum sample depth reflects the deepest the sample bottles were able to go based on a relatively short length of Kevlar line (~800m). The bottom depth ranged from 1300m at P4 to > 4300m at P26 and is thus only considered in the nearshore stations. The general trend in [Pb] at all stations is similar: a surface minimum which rises fairly rapidly to a subsurface maximum around 150m before slowly decreasing in concentration with depth. This type of profile closely matches that acquired by Wu et al. (2010) at a station 1800 km south of P26. Numerical values as well as potential density and spiciness can be found for Line P in Table A2.1 of Appendix II.

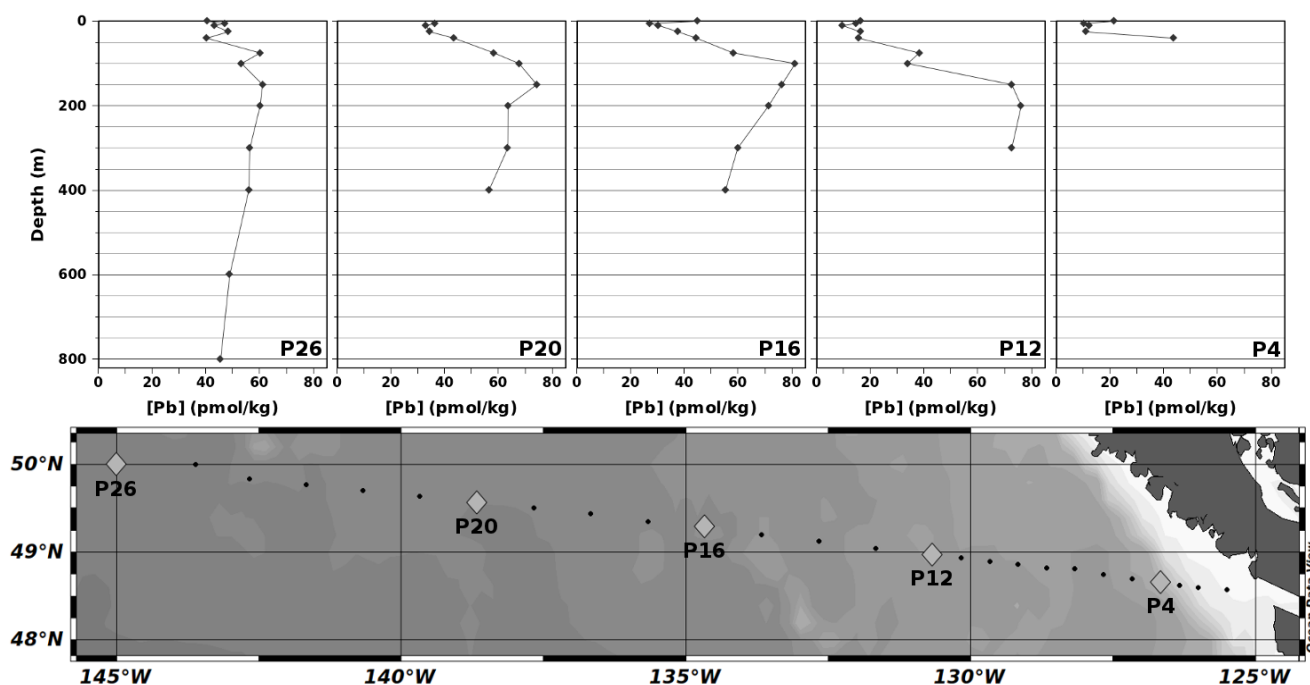


Figure 2.2. Vertical profiles of dissolved Pb along Line P.

The waters of the surface mixed layer (from the surface to σ_t approximately 25) show a strong positive correlation between [Pb] and longitude west ($R^2 = 0.71$, $p < 0.001$) as we might expect when moving closer to the atmospheric source. Figure 2.3 shows the top 100m of the water column along the Line P transect, showing optical transmissivity which is a measure of the turbidity of the water, and CTD fluorescence, which can be used as an estimate of chlorophyll *a* abundance. Since the major removal mechanism of Pb from the water column is

via sorption to particulate matter, linear regressions were performed for [Pb] against transmissivity and against fluorescence in order to determine the impact of these variables on Pb distribution. [Pb] and fluorescence (as a proxy for chlorophyll *a*) were found to be weakly positively correlated ($R^2 = 0.21$, $p < 0.01$), indicating that as chlorophyll *a* concentrations increase, so do those of [Pb]. It was expected that regions of higher chlorophyll would have lower [Pb] as a result of scavenging by biogenic particles, though this does not seem to be fully substantiated here. The density pattern suggests coastal upwelling is occurring, where Ekman pumping would be pushing surface waters offshore (see Figure 2.4). This could advect water from the P4 region further from the coast, where it would have had been subjected to measurement after the phytoplankton have begun to sink and be degraded and thus not fluoresce. [Pb] and transmissivity show a positive correlation ($R^2 = 0.30$, $p < 0.001$) as expected, waters with higher transmissivity (less particulate matter) having higher [Pb]. So although these seems to be much complexity in the upper waters, longitude (source proximity) and turbidity of the water seem to be the major factors controlling Pb distribution.

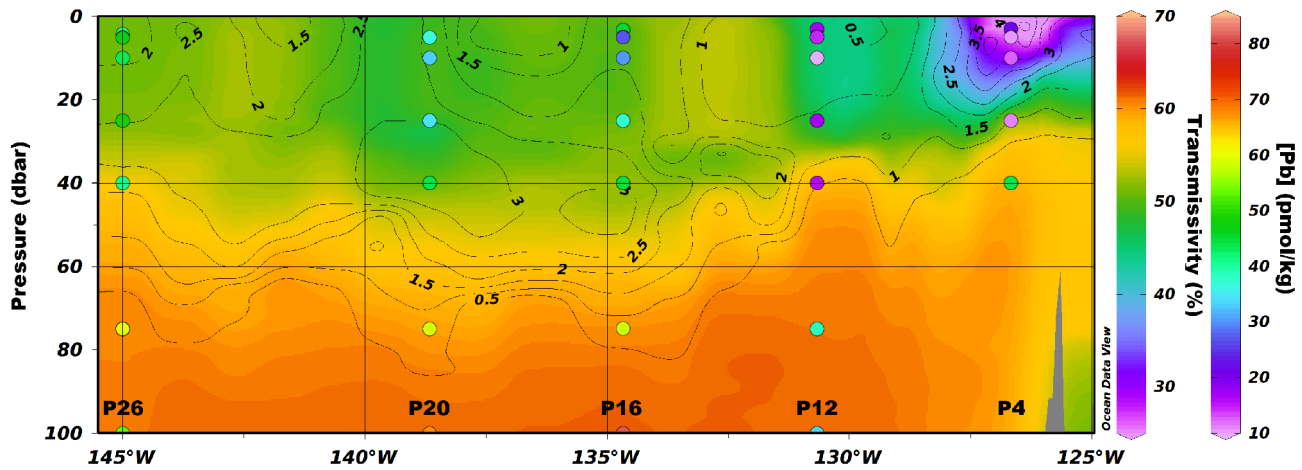


Figure 2.3. A cross-section of the surface waters of Line P. The coloured contouring represents transmissivity as a percentage of beam transmission. Lower transmissivity indicates greater turbidity. The black contour lines show chlorophyll *a* estimated from fluorescence in mg/L and coloured dots represent [Pb] in pmol/kg.

If the main source of Pb to these waters is Asian aerosols, there could be a balance between aerosol input and particle-removal output which would likely not be in a steady-state. This is indicated by looking at the surface value for each profile (which was not collected at station P20). Most stations show an increase in the surface sample which decreases rapidly by 10m depth. The only station where this is not seen is at OSP, where a high input and low phytoplankton abundance (due to being in an HNLC region) lead to the highest mixed layer concentrations of Pb.

It is worth noting as well that there is a large increase in transmissivity and decrease in chlorophyll

concentration at the base of the seasonal thermocline between roughly 40 and 70m in Figure 2.3. Due to the stratification of waters at this interface, conditions in the lower layer are inhospitable to phytoplankton growth. As a result, the region between the surface mixed layer and above the permanent pycnocline shows higher Pb concentration which would likely correspond to the concentration in the winter mixed layer, which would be exempt to scavenging associated with spring and summer phytoplankton blooms.

In order to get a more complete picture of what is occurring in the subsurface waters of this region, it is useful to consider the state variable “spiciness” (Flament, 2002). Water has a particular potential density as a result of the temperature and salinity of the water parcel in question, but the density does not provide information on whether the water is relatively cool and fresh or warm and salty for a particular density. Determining the spiciness of a parcel of water can provide this information, with water high in spiciness being relatively warm and salty compared to cooler, fresher lower spiciness water. A cross-section of Line P spiciness can be seen in Figure 2.4, with black density contours plotted over spiciness, and coloured dots representing point-measurements of [Pb]. The temperature and salinity data required to calculate spiciness and density was collected continuously during CTD casts at all stations, whereas the samples collected for Pb determination were more sparse. As such, it makes sense to contour the spiciness data while providing coloured dots to convey [Pb] as this should remove the “smearing” effect caused by interpolating sparse data.

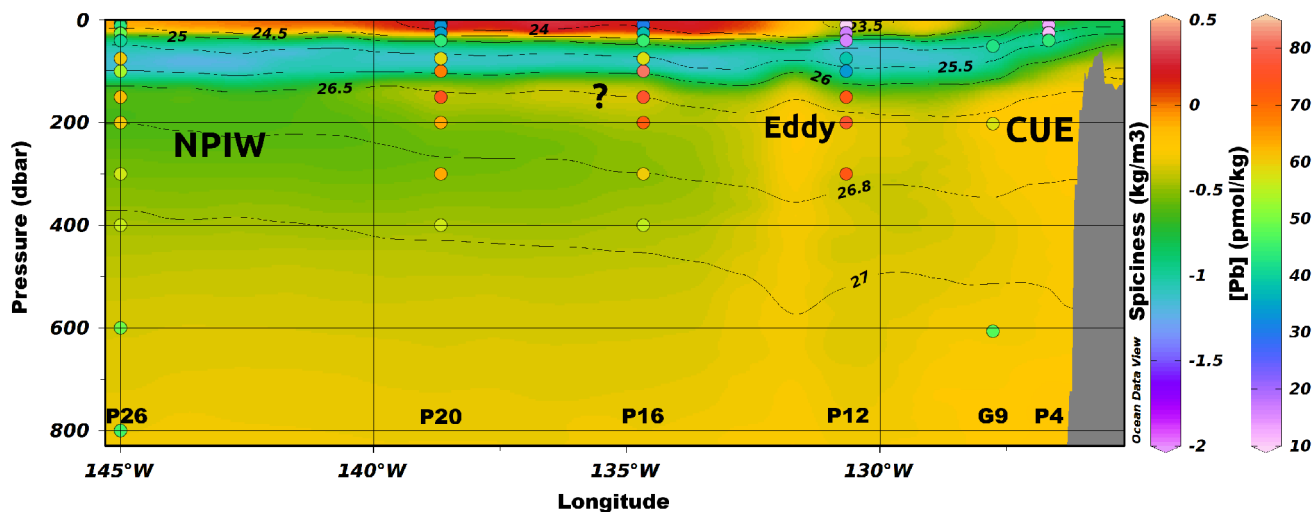


Figure 2.4. Cross-section of data along Line P. The background colouring represents spiciness in kg/m^3 , black contours are isopycnal surfaces and coloured dots are [Pb] in pmol/kg . The three [Pb] data points at 127.6°W are from station G9, which coincidentally overlapped with the Line P transect.

Contouring the spiciness variable provides valuable information regarding the top 800m of the waters of Line P. Immediately noticeable is the presence of the seasonal and permanent pycnoclines in the top 150m of the transect. During the cold winters of the subarctic Pacific, the summer thermocline deteriorates and strong winter

storms are capable of mixing the surface layer to a depth of around 150m. As solar radiation increases during the summer months, a seasonal thermocline forms in the surface waters, seen in Figure 2.4 as high-spiciness water above depths of roughly 50m. The turquoise band below this depth ($\sigma_T \approx 25$ -26) is the colder water which was ventilated during the previous winter. In the remnant of the winter mixed layer, a trend showing increasing [Pb] with distance from shore can be seen. This trend likely exists for the same reason as that seen in the seasonal mixed layer: more input of Asian aerosol Pb as a result of being closer to the source along with greater scavenging in the coastal region.

Isopycnal surfaces were plotted in these figures after it was noted that with few exceptions (being the W-line stations at the northern end of the study area) the highest concentrations of Pb for a given station were between the waters with a potential density of 26.4 and 26.9 (Figure 2.5). We can then pay closer attention to this region in Figure 2.4 to attempt to explain the acquired distribution of Pb.

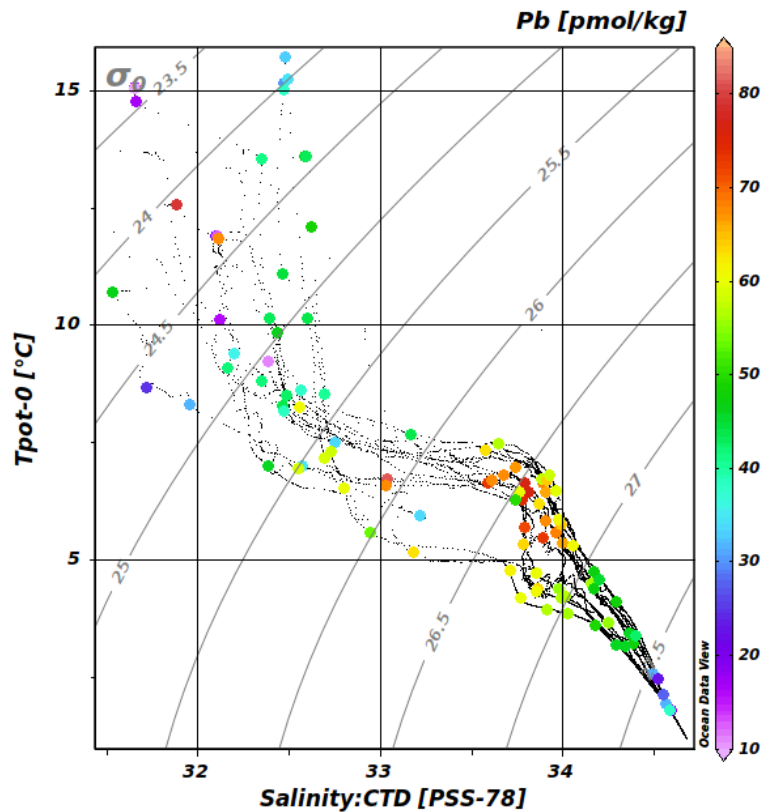


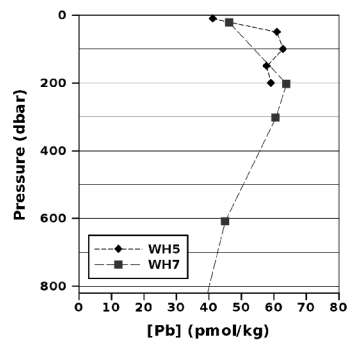
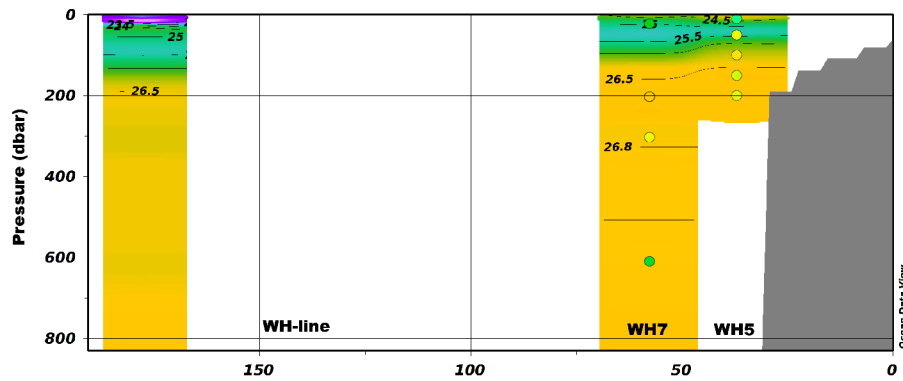
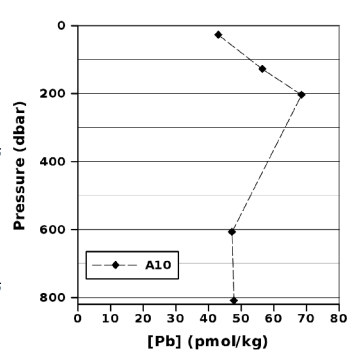
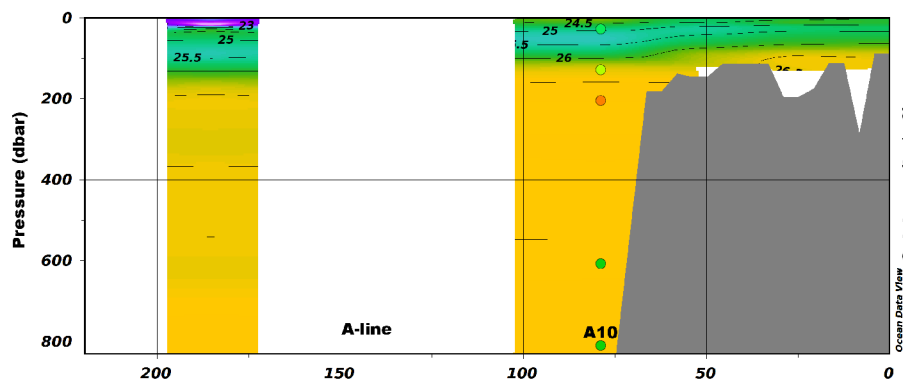
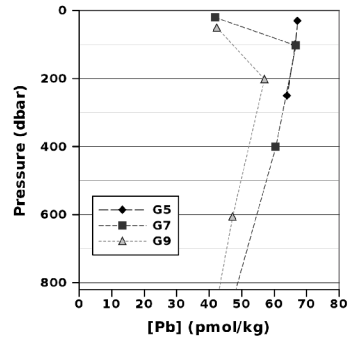
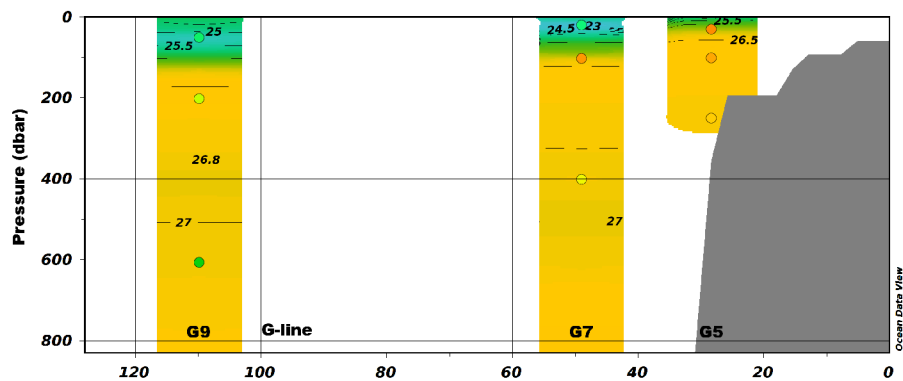
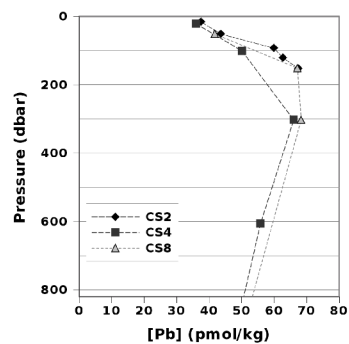
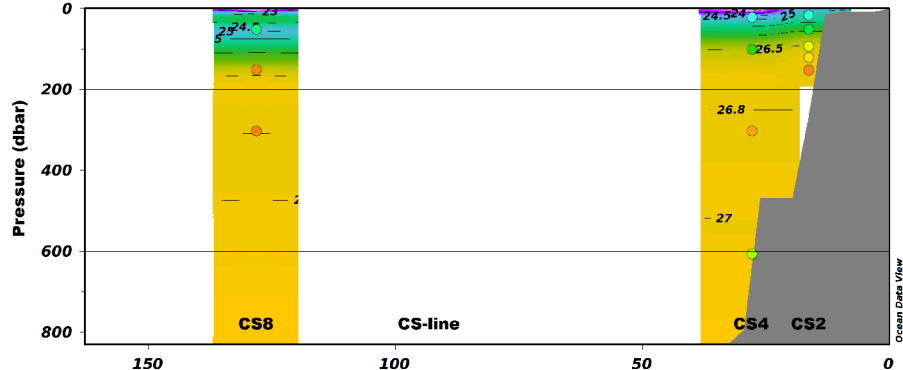
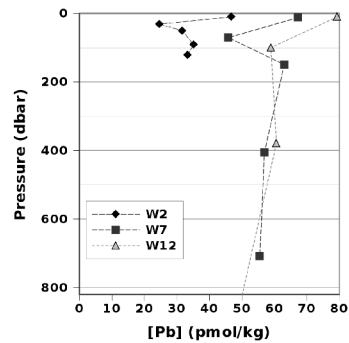
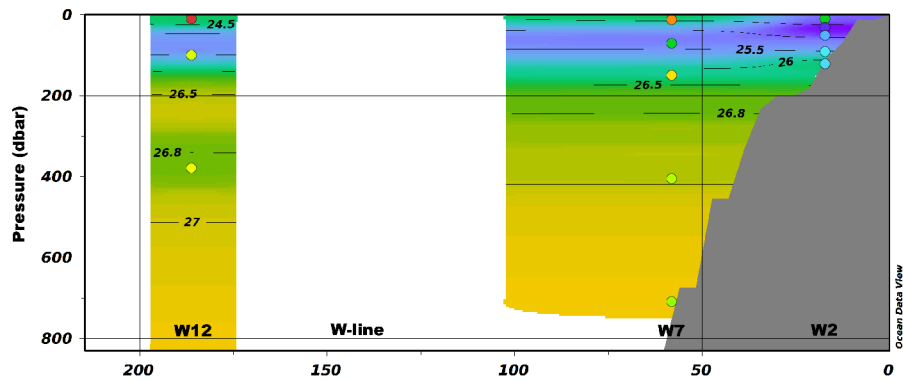
Figure 2.5. Property-property plot showing potential temperature against salinity for all 2010 NE Pacific samples from this study. [Pb] is shown as coloured dots in pmol/kg. The high [Pb] measurements in the warm/fresher waters were from the northernmost W-line.

The σ_θ 26.5 surface lies immediately below the permanent pycnocline in the west, and sinks to more than

30m below it as this surface nears the coast. From west to east along this surface, there is an intrusion of relatively cool and fresh water from the west, a pocket of slightly spicier water around the centre of the transect, a decrease in depth and jump in spiciness as the line crosses a Haida eddy (at 131 to 133°W) and finally some higher-spice water near the coast.

The colder, fresher water coming in from the west along this surface is likely North Pacific Intermediate Water (NPIW), a water mass which is thought to form during the winter as water cools and mixes in the Sea of Okhotsk near Japan which leads to an increase in density via cabelling (Inoue et al., 2006). This water mass brings with it Pb concentrations of 60-65 pmol/kg, which are relatively high but lower than those seen in the higher-spiciness waters above it at roughly 140°W. A transect in the western Pacific in 1991 included a profile at 27.8 °N 175 °W which had [Pb] between 58.8 and 70.6 pmol/kg through the water column from surface to 500m, which would likely also be NPIW and corroborate with the idea of this water mass being seen in the western end of the Line P transect (Orlans and Yang, 1994). Gallon et al. (2012) measured Pb in surface water in the summer of 2002 in the Northwest Pacific Ocean, including stations near the Sea of Okhotsk. It is difficult to make comparisons with these surface waters and NPIW since the latter is formed during the winter months, but the surface waters nearest the Sea of Okhotsk had [Pb] of about 73 pmol/kg, which isn't a great deal higher than the concentrations found in NPIW.

A water mass which appears to be an offshoot of the California Undercurrent Extension (CUE) waters can be seen as a spiciness maximum centred around 200m against the continental slope. The [Pb] in the waters of the CUE are not known based on the data collected from the Line P cruise, but this poleward current was sampled weeks earlier during the coastal cruise and [Pb] was found to have a maximum value of 68.5 pmol/kg at station A10, located southeast of P4 (Figure 2.1). If there were CUE waters meandering into the open ocean and mixing with NPIW, we would expect concentrations below 68.5 pmol/kg, yet all measurements in this water mass are greater than 70 pmol/kg. This indicates that this water likely has a different source than the CUE since this source contains insufficient concentrations of Pb to provide the distribution seen here. This is backed up by considering the NO signature across the transect ($NO = 9.2[NO_3] + [O_2]$) (Whitney et al., 2007). The CUE has lower NO (406 μ mol/kg) as a result of denitrification along the coastal shelf, but the region of high-Pb waters of interest here has a much higher value of 439 μ mol/kg which indicates the entrained Pb is probably not of shelf origin. Similarly high concentrations of Pb (72.7 - 74.5 pmol/kg) were reported at 150-200m depth at a station at 30°N, 140°W by Wu et al. (2010). This maximum in their profile was attributed to isopycnal advection from ventilated tropical waters, which could possibly be entrained during the bifurcation of the North Pacific Current. Presently the exact source of Pb is unknown and it is hoped that isotopic analysis may some day provide more insight.



Section Distance (km)

Figure 2.6. Cross-sections of hydrographic lines off the coast of Alaska and British Columbia, moving north to south from top to bottom. Colours and contours are as per Figure 2.4.

The series of transects along the coast are much shorter longitudinally, but cover a similar distance zonally. Numeric results from the coastal cruise can be found in Table A2.2 in Appendix II. The CUE can be seen to decrease in spiciness with increasing latitude, eventually being replaced by the cooler, fresher NPIW (Figure 2.6). Many of the samples collected within the CUE have [Pb] between 60 and 70 pmol/kg. A sample taken from the core of the NPIW at station W12 was found to contain 60.6 pmol/kg Pb, very similar to the values found in this water mass at P26 indicating that this water mass is stable with respect to Pb concentrations. Higher concentrations of Pb at station CS8 may also indicate that the high-Pb water mass previously mentioned could be present at higher latitudes as well. The highest concentration of Pb in the coastal samples was actually found at a depth of 10m in the most northwesterly station (W12), which was found to contain 79.3 pmol/kg. The two other stations along this transect also had elevated concentrations in their uppermost sample depth, decreasing to 67.3 pmol/kg and 46.7 pmol/kg for stations W7 and W2, respectively. This is a reminder of the sometimes patchy nature of aeolian-source elements, as these elevated concentrations were likely caused by an improbable and small-scale event. It is considered that in this sparsely-inhabited region, winds blowing offshore may have carried smoke or ash from forest fires into the region where it was deposited to the surface. However, wind data from a buoy located in close proximity to these stations between June and September of 2010 show that winds are predominantly blowing from the northwest and southeast, parallel with the shore and sometimes onshore from the southwest. Crusius et al. (2011) describe a phenomenon where scoured glacial flour is blown into the GoA during October and November with some regularity. If these types of events were to happen on a smaller scale earlier in the year, it could possibly transfer Pb into the region. Once more, the isotopic distribution of Pb would be helpful in determining where this “extra” Pb originated.

Several determinations were made on samples collected from greater depths than shown in previous figures (ie. deeper than 800m). The extensive latitudinal gradient of these coastal transects show a similar feature first noted by Wu et al. (2010) in their work along a transect from 7°S to 30°N. A general increase in Pb with increasing latitude was noted, which was credited to the larger quantity of anthropogenic Pb in the northern hemisphere as well as the proximity to Asian Pb blown to sea by prevailing westerlies (Schaule and Patterson, 1981). In this study we also observed that waters below the quite dynamic upper layers (> 800m) increase in concentration with increasing latitude as seen in Figure 2.7. The concentrations seen in this figure are either taken from data points in close proximity to 1500m, or interpolated from the data points above and below this depth. The four more southerly points are quite linear, while the northernmost station shows a plateau. When we instead plot [Pb] against the spiciness of the water in which it originated, we get a negative linear relationship with a fairly strong correlation. Although it is possible that the region may experience an augmentation of Pb as

reversible exchange with particles, the linear relationship with the change in spiciness indicates that this is more likely a result of the simple mixing of water masses. We must then consider why the more northerly waters would have more than double the [Pb] than those in the south, whether it is the product of reversible particle exchange/remineralization at depth or a more complex mechanism.

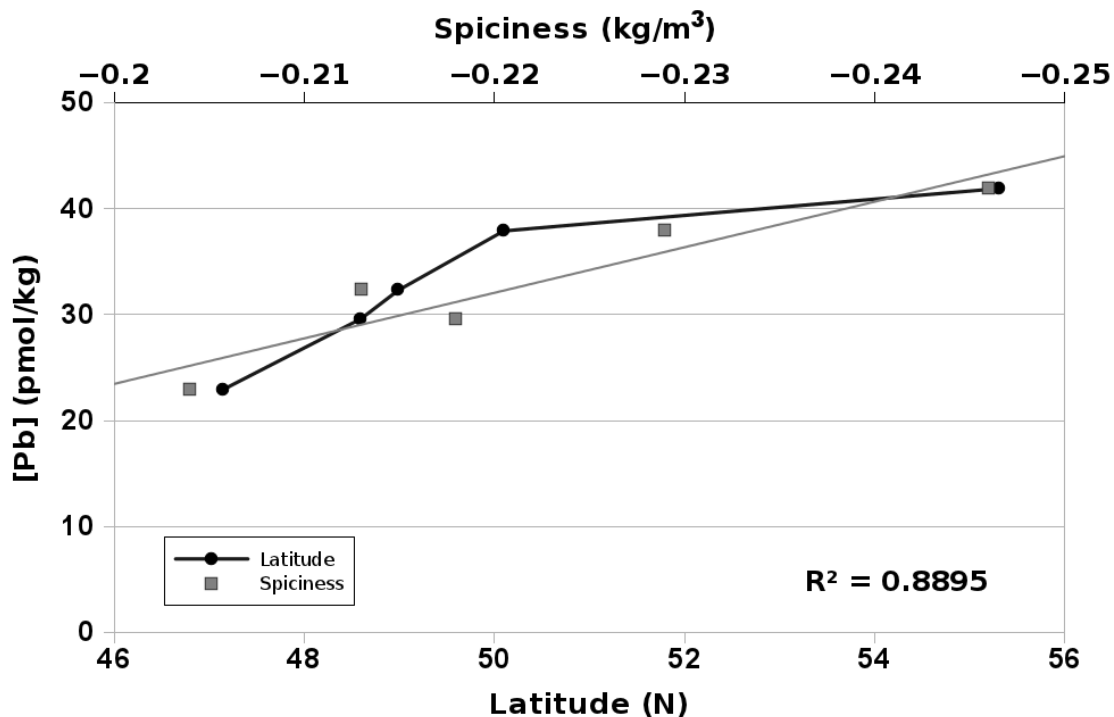


Figure 2.7. Concentration of Pb in the outermost station of each coastal transect at a depth of 1500m, interpolated where necessary from nearest proximate data points.

Once familiar with the spiciness variable, it can also be visualized on a simple T-S diagram as in Figure 2.5. Spiciness isolines run orthogonally to isopycnals (shown in light grey). If we consider, for example the σ_0 27 isopycnal surface, less spicy waters would be lower on the figure (ie. lower on the temperature scale) with more spicy waters having warmer temperatures. With this in mind, it can be seen in this figure that near this particular isopycnal, waters with less spiciness have higher Pb concentration. Similarly, between the 26.5 and 26.7 isopycnals, we can see that the highest [Pb] is of intermediate spice, bordered by higher- and lower-spiciness waters of lower [Pb]. This intermediate water could not be the result of mixing of the higher- and lower-spiciness waters around it, which is evidence that the source of Pb in this water mass is likely different, discounting the possibility it has the same origin as CUE.

Comparison with historic data

There are no published data with which to make a direct comparison with those from the current study, but those published by Flegal et al. (1986) were collected 370 km to the southeast of P26, close enough to make a good comparison. The archived samples from 1992 and 2003 were stored in controlled conditions and appear to provide a reasonable data set with which to derive the temporal evolution of Pb at this location (Figure 2.8).

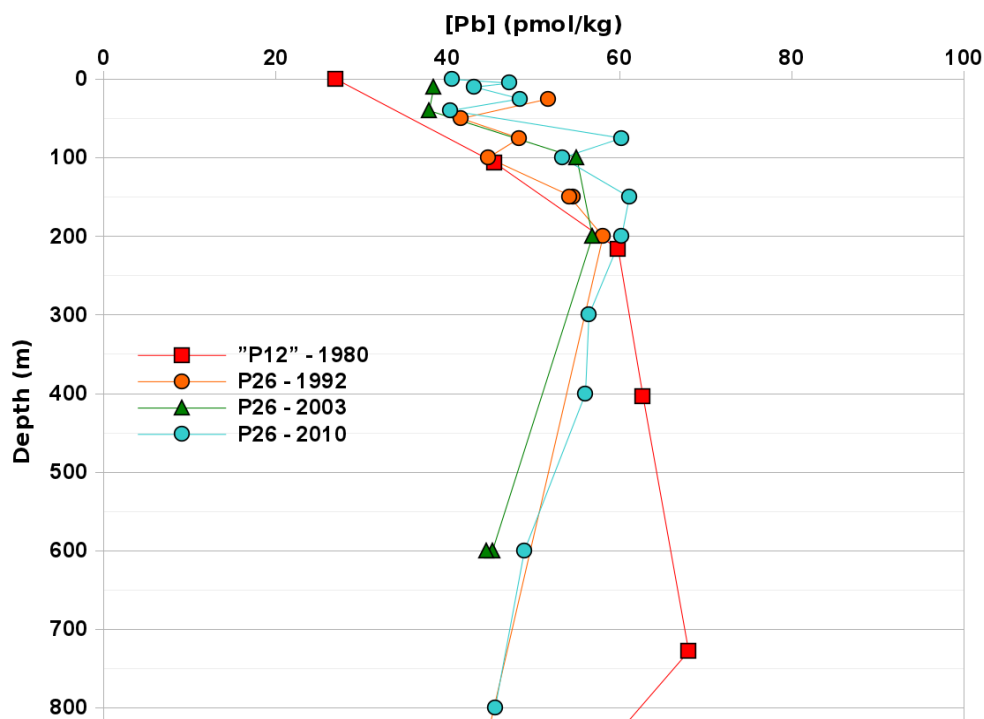


Figure 2.8. A series of vertical profiles acquired at or near P26 at the end of Line P. Data from “P12” and isotope ratios were published by Flegal et al. (1986), the station was actually located south of Line P between the current P26 and P20. The remaining samples were collected by the Orians laboratory and acidified until analysis in 2010.

Although there has been a remarkable decline in the surface concentrations of lead in the North Atlantic Ocean, there is an almost equally remarkable lack thereof in the Northeast Pacific (Lee et al., 2011). In the surface mixed layers, it appears as though [Pb] rose between 1980 and 1992 before plateauing at levels similar to those seen presently. Below the permanent mixed layer at 200m, the values converge to a range between 56.8 and 60.2 pmol/kg, which is very narrow considering that the samples were taken over a time span of three decades. The complication in this observation is that coal use and anthropogenic pollution are on the rise in China and the rest Asia, so if this water mass was forming just north of Japan it might even be expected that this would result in an increase in Pb concentration (see, for example (Ohara et al., 2007). One possibility is that this water mass forms to the north of Japan where the population density is lower than many other regions further

south. During the winter months the dominant climatological feature of the subarctic North Pacific is the Aleutian Low, which would bring in air from the remote Aleutian Island chain and Bering Sea while flushing Asian pollutant aerosols away from the formation region. This low pressure system is also associated with a large amount of wet deposition, which would scavenge any North American aerosol Pb from the troposphere before making it to the western edge of the Pacific. As previously stated, recent Pb measurements in the Northwest Pacific near the sea of Okhotsk were not especially high compared to the concentrations in NPIW, and the spatial distribution of Pb place the Sea of Okhotsk further north than the main plume of Asian pollutant Pb (Gallon et al., 2012).

The residence time of Pb should also play a role in the stability of the Pb concentration in NPIW over time. If the residence time were variable, as expected in the surface mixed layer and especially close to shore where fluctuations in nutrient concentrations lead to relatively sporadic phytoplankton blooms, we would expect more volatility in the measured concentrations. Since the NPIW is thought to form and subduct below the thermocline in winter, this variability could be largely ruled out. Studies on the residence time in the Pacific Ocean have found very short residence times of 1.7 years in the surface water, which increased to well over one hundred years in the intermediate and deep Pacific (Nozaki et al, 1976, 1980). As partially seen in Figure 2.3, the turbidity of the water decreases markedly below the seasonal thermocline, and more so below the permanent halocline. Since the main removal mechanism of Pb is via scavenging, we can infer that clearer water results in a longer residence time. It has been calculated that NPIW reaches OSP in about 5-7 years from the time of formation in the western Pacific (Ueno and Yasuda, 2003). From this we can determine that Pb must have a residence time in this water mass of well over 5-7 years, and is likely on the order of a number of decades and consistent over time. As a result, it appears that NPIW is able to maintain a very steady concentration of Pb over time.

Below 200m, the results from the present study diverge from those from 1980. There are two possible explanations for this: first, that there has been some type of change in the intermediate water mass entering the region; or second, the earlier samples may have been contaminated in some way during processing and analysis. The latter idea is only put forth due to the more recent samples showing a somewhat consistent pattern of decline with depth and over time, though there is no reason to discount the earlier data.

There is also an inconsistency between the isotopic composition of samples from 1980 and some of the theories proposed in the current study. The isotopic ratio of $^{206}\text{Pb}:$ ^{207}Pb (not shown) suggest that surface samples were rich in Asian Pb, congruent with the evidence presented here. At a depth of 400m, the ratio increased such that it was suggested that North American Pb was polluting the region. As stated by the authors of that publication, it was unfortunate that insufficient data was collected to determine Pb inputs at this location.

Potential densities of greater than 26.7 are not ventilated in the eastern North Pacific (Mecking et al., 2006). The potential density at P26 within a month of the samples being taken at “P12” was 27.0 and as such the Pb could not have been mixed to that depth unless it was transferred by diapycnal mixing, which is unlikely. Unfortunately for the current study, there does not presently exist any isotopic evidence to the contrary and thus the origin of Pb at this depth remains unknown. It is probable that this Pb was brought to the region via the meridional overturning circulation, in which case there is little chance that the Pb is anthropogenic. One further point which bears mention is that the ratio seen at 400m is similar to ratios found in sediment and manganese nodules, indicating that this measurement may actually simply be natural Pb (Chow and Patterson, 1962; O’Nions et al., 1998; Jones et al., 2000).

2.4. Conclusions

The results presented here have greatly increased the number of dissolved Pb concentration measurements in the northeastern Pacific, and represent an important contribution to the understanding of Pb biogeochemical cycling across a coastal to open-ocean transect. The surface mixed layer concentration increases with distance from shore as expected, but the subsurface waters (centred around the 26.8 isopycnal) show more complexity than originally thought. There appear to be at least three distinct water masses along this surface through the transect consisting of the California Undercurrent Extension close to shore, an unknown water mass with the highest [Pb] in the transect and North Pacific Intermediate Water most prominent at OSP which seems to extend as far east as P16. Future studies would be useful in determining whether the elevated concentrations in the unknown water mass are an ephemeral condition or whether this is a relatively static feature.

The coastal cruise provided more data on a meridional transect within a couple of hundred kilometers from shore. Many of these profiles showed very similar Pb profiles to those collected along Line P, with a maximum value at or about a potential density of 26.8, with generally lower values in the surface and decreasing to the lowest values in the water column at depth. At 1500m (and more generally, at depths > 800m), the concentration was found to correlate quite well with latitude, an observation originally seen in the deep Pacific by Wu et al. (2010). These profiles also differed from Line P profiles in that several of the transects seemed to show elevated [Pb] closer to shore, which may be indicative of more complex energetic processes occurring near shore which would require greater sampling resolution to resolve. An unknown aeolian source also appeared to deposit Pb in the most northern transect, where the highest [Pb] in this study were found.

Contrary to findings in the Atlantic Ocean, a series of profiles taken in close proximity between 1992 and 2010 in the Northeast Pacific show little change in [Pb] in the upper 800m of the water column. It is expected that this is a result of the dominant water mass in the upper waters here (NPIW) being formed during

the winter while aeolian sources would be less anthropogenically-dominated than other times of year, along with a consistent residence time once the water mass submerges below the permanent thermocline. A profile consisting of the isotopic distribution of Pb exists from 1980, which could be compared to more recent values in order to determine whether the source of Pb has changed over time, and what that source may be.

Acquisition of more data in this region would provide or detract support to the arguments put forth here which would be beneficial to others studying this element in the ocean. The data is of interest because it demonstrates the difficulty of using information acquired in one region (such as the central North Atlantic) and expecting similar results in a different region (the North Pacific) for a reactive element with complex sources. The data from the deeper samples collected also provide further evidence for the possibility of reversible particle exchange leading to elevated [Pb] in the deep Pacific as discussed by Wu et al. (2010). As a whole, this dataset has been utilized to garner a greater understanding of Pb distribution in the Northeast Pacific and the processes leading to this distribution.

3. A synoptic survey of Pb in three eddies in the Gulf of Alaska.

3.1. Introduction

Mesoscale anticyclonic eddies form each winter in the Gulf of Alaska (GoA), located in the northeastern Pacific Ocean. Their sizes range from 80 km to about 200 km in diameter and can transport up to 6000 km³ of coastal water into the open ocean (Tabata, 1982; Whitney and Robert, 2002). These high-nutrient coastal waters are known to impact productivity in the GoA by providing high-nutrient/low-chlorophyll (HNLC) waters with iron, a trace nutrient necessary for phytoplankton growth (Martin and Fitzwater, 1988; Martin et al., 1991; Crawford, 2005; Johnson et al., 2005; Law et al., 2006). In the eastern GoA, there exists three formation regions near Haida Gwaii (Queen Charlotte Islands), British Columbia, Sitka, Alaska and Yakutat, Alaska after which the eddies are named Haida, Sitka and Yakutat eddies, respectively (Gower, 1989; Gower and Tabata, 1993; Okkonen et al., 2001). These three types of eddies have been studied individually over time, and were studied synoptically for the first time in 2005 (Ladd et al., 2009).

Eddies in the GoA are responsible for transporting anomalous water properties such as temperature, salinity and nutrients into the open ocean. Along with these properties, anomalous concentrations of trace metals similar to iron are present in these eddies, although little work has been done to date. The most studied trace element in these eddies has been Fe as a result of its direct impact on the productivity of the region (Crawford, 2005; Johnson et al., 2005; Xiu et al., 2011). Only four other elements have been studied in these eddies: Al, Cu, Cd and Mn were analyzed from a series of cruises through a Haida eddy on eddies formed in 2000 and 2001 (Crispo, 2007). As the eddies aged, the concentrations of Al and Mn decreased as a result of mixing and scavenging, while the concentrations of Cu and Cd increased over time as a result of mixing with surrounding waters with higher concentrations of these elements. Other studies have investigated the effects of a Haida eddy by chance along Line P, such as the elevated offshore concentrations of Ag seen by Kramer et al. (2011). It is expected that Pb will behave similarly to Al, which also has a primary aeolian source and removal by scavenging.

Pb is of interest because it is likely the most anthropogenically perturbed element in the environment, with atmospheric levels about ten times natural concentrations (Osterberg et al., 2008). Although locations around the Atlantic Ocean received less Pb input from atmospheric sources as a result of the phaseout of leaded gasolines in the 1970s, sites in the eastern Pacific have actually seen an increase in Pb deposition since that time. As a result, seawater concentrations of Pb in the north Atlantic have dropped roughly 6-fold between 1979 and 2008, while those in the Pacific showed very little change between 1977 and 2005 (Schaule and Patterson, 1981,

1983; Boyle et al., 1986; Flegal et al., 1986; Wu et al., 2010; Lee et al., 2011). Below the surface mixed layer in the North Pacific, the dominant water mass at intermediate depth is formed in the Sea of Okhotsk in the winter (Ueno and Yasuda, 2003), when Asian pollution is being pushed south by the Aleutian Low. This results in a water mass being formed which has consistent concentrations at intermediate depth which can be seen as a subsurface maximum if the Pb in the above-laying water has been heavily scavenged by particulate matter such as phytoplankton.

At present, there is only one known report of [Pb] in an eddy. This occurred coincidentally while sampling transects in the southern East China Sea where the analyzed concentrations were an order of magnitude greater than those seen in the open Pacific Ocean (Lin et al., 2000). The authors believed that the eddy brought higher-[Pb] offshore water closer to the coast. In the northeast Pacific, eddies generally move westward (offshore) as a result of planetary β -effects which will carry coastal water out to sea (Nof, 1981; Cushman-Roisin et al., 1990). Pb concentrations were determined in a fjord just northeast of Haida Gwaii in the early 1980s (Stukas et al., 1999). The concentrations found in this fjord were very low, with average concentration at the mouth of the Nass river being 70.8 pmol/kg (14.5 ng/kg) dropping rapidly through the estuary to an average of 16.4 pmol/kg (3.4 ng/kg) between the surface and 440m depth. It was found that concentrations were low in the seawater mixing into the estuary, estimated at 2.4 pmol/kg (0.5 ng/kg) in water advected up from the deep shelf. This is several orders of magnitude lower than those reported in the East China Sea, which could be an indicator of the strong effect of local pollution sources on [Pb] in the East China Sea. The region around Haida Gwaii is relatively remote, and the low values reported in the fjord were attributed to in-situ scavenging during chemical precipitation as the Nass River reached the estuary.

The current study is the first to investigate Pb distribution through eddies in the GoA in order to clarify some of the biogeochemical processes which affect this element as the eddies move toward the sea. By studying the eddies synoptically, it may be possible to determine the similarity of these processes between eddies and make inferences regarding any differences.

3.2. Methods

The samples for this study were collected aboard the *R/V Thomas G. Thompson* in late April to early May of 2005. The cruise was undertaken specifically to study eddies in the Gulf of Alaska and used satellite data and satellite-tracked drifters to determine as accurately as possible the centre of the eddies (see Ladd et al. (2009) for more cruise information). These eddies are named for their region of formation, with Haida eddies forming off the southern tip of Haida Gwaii, British Columbia and Sitka and Yakutat eddies forming offshore off

the towns of Sitka and Yakutat, Alaska, respectively. Samples from two transects collected using trace-metal clean techniques to 800m were collected through three eddies, one through a Haida eddy and the other passing through Sitka and Yakutat eddies in close proximity (Figure 3.1). A total of seven full profiles (to 800m) were taken, two outside of the eddies in regions with low chlorophyll abundance to serve as reference stations, one station on the edge of both the Haida and Sitka eddy and one profile through the centre of each of the three eddies (Figure 3.1). Nine other stations had two samples taken from the upper waters at 10m and either 40m or 100m. Altogether this resulted in a total of 102 discrete sample depths.

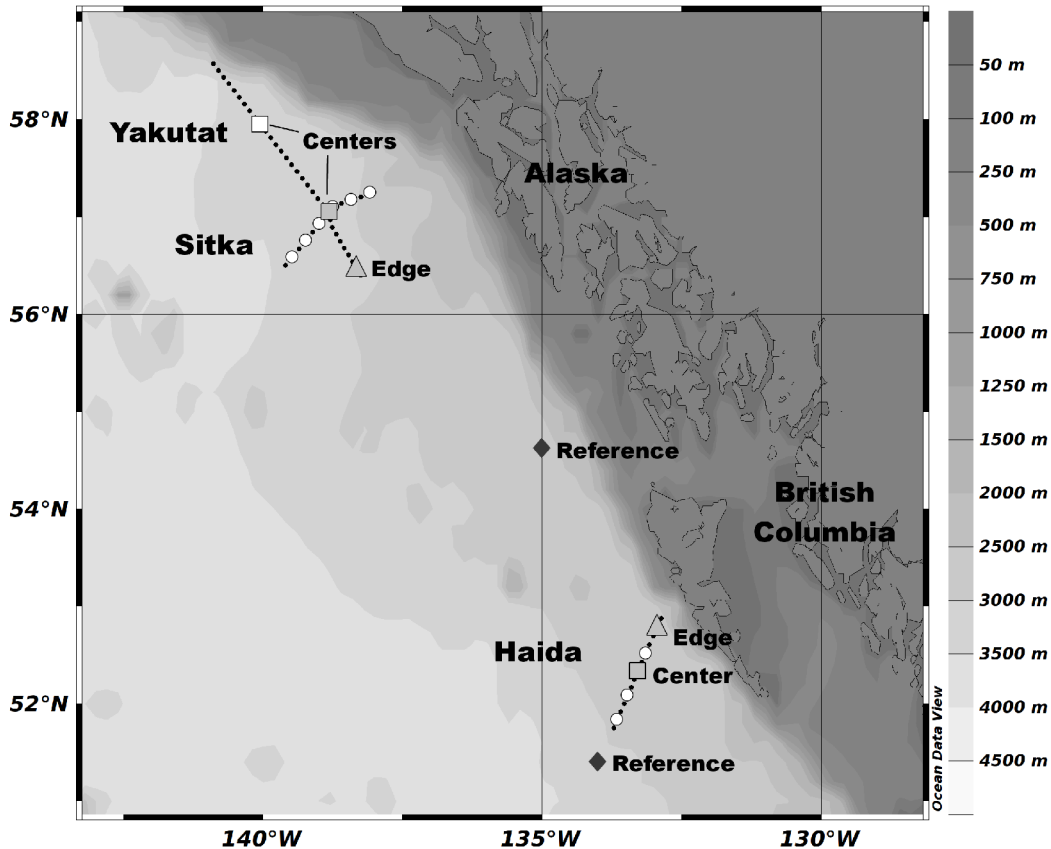


Figure 3.1. Map of the northeast Pacific Ocean showing the region from which samples were taken. Vertical profiles to a depth of 800m were taken from stations with marked by large symbols which were chosen to provide a station outside the eddies (reference), one from the eddy edge and one through the core of the eddy. Two shallow samples (10m or 40m and 100m) were taken from each station marked by a white circle. Stations without trace metal sampling are shown as black dots. CTD measurements were taken from all stations.

Seawater was collected in 30-, 12- or 10-L Go-Flo bottles attached to a metal-free rosette on Kevlar-coated conducting wire. These bottles were subsampled in the ship's laboratory using bell jar dust covers and filtered using 0.22 μm Opticap cartridges. Samples above 40m were collected using a bellows-driven, all-plastic/Teflon pump and Teflon-lined tubing and collected within a HEPA filtered flow hood. Other

oceanographic parameters such as CTD, nutrient and iron data were collected as described elsewhere (Johnson et al., 2005; Ladd et al., 2009).

The analysis method used was a modified version of the magnesium-induced coprecipitation technique introduced for Pb analysis by Wu and Boyle (1997b). Briefly, 13 ml of acidified seawater was transferred to a 15 ml acid-cleaned centrifuge tube and spiked with 50 μl of a ^{207}Pb -enriched standard. After sitting for greater than 1h to allow isotopic equilibration, 175 μl of Seastar Chemicals concentrated NH_4OH (11 N) was added and shaken to mix. This solution was allowed to react and precipitate for five minutes before centrifuging. The supernatant was decanted and recentrifuged to remove as much liquid as possible. The remaining $\text{Mg}(\text{OH})_2$ pellet was dissolved in 1-2 ml of 1% HNO_3 for analysis. More detail is available in Chapter 2.

Determinations were performed using a Thermo Scientific Element XR high-resolution ICP-MS at the Fipke Laboratory for Trace Element Research (FiLTER) at the Okanagan Campus of the University of British Columbia. Blanks were analyzed every ten samples, one sample out of 20 was prepared and analyzed in duplicate and one sample out of 20 was prepared and analyzed in triplicate which resulted in replicate measurements on greater than one in every 10 samples.

The ID-MS method used here was found to be quick and reliable in the determination of Pb in seawater. The results of replicate measurements on certified or interlaboratory materials can be found in Figure 2.1. The expected concentration range normally seen in seawater ranges from 10 to 150 pmol/kg, thus this method seems suitable to accurately determine the [Pb] of a particular sample.

3.3. Results

The results of the determinations performed on the seven full vertical profiles to 800m can be seen in Figure 3.2. These profiles, especially those of the reference stations, are similar to others seen in the northeast Pacific (Schaule and Patterson, 1981; Flegal et al., 1986; this thesis, Chapter 2). They feature fairly low concentrations in the surface as a result of a dynamic equilibrium between input by atmospheric deposition and scavenging by phytoplankton and other particulates, with a subsurface maximum. The strong correlation between the Sitka and Yakutat central profiles provide confidence in the sample collection, storage and analysis since they were in close proximity geographically when sampled and likely exposed to many of the same processes prior to being sampled.

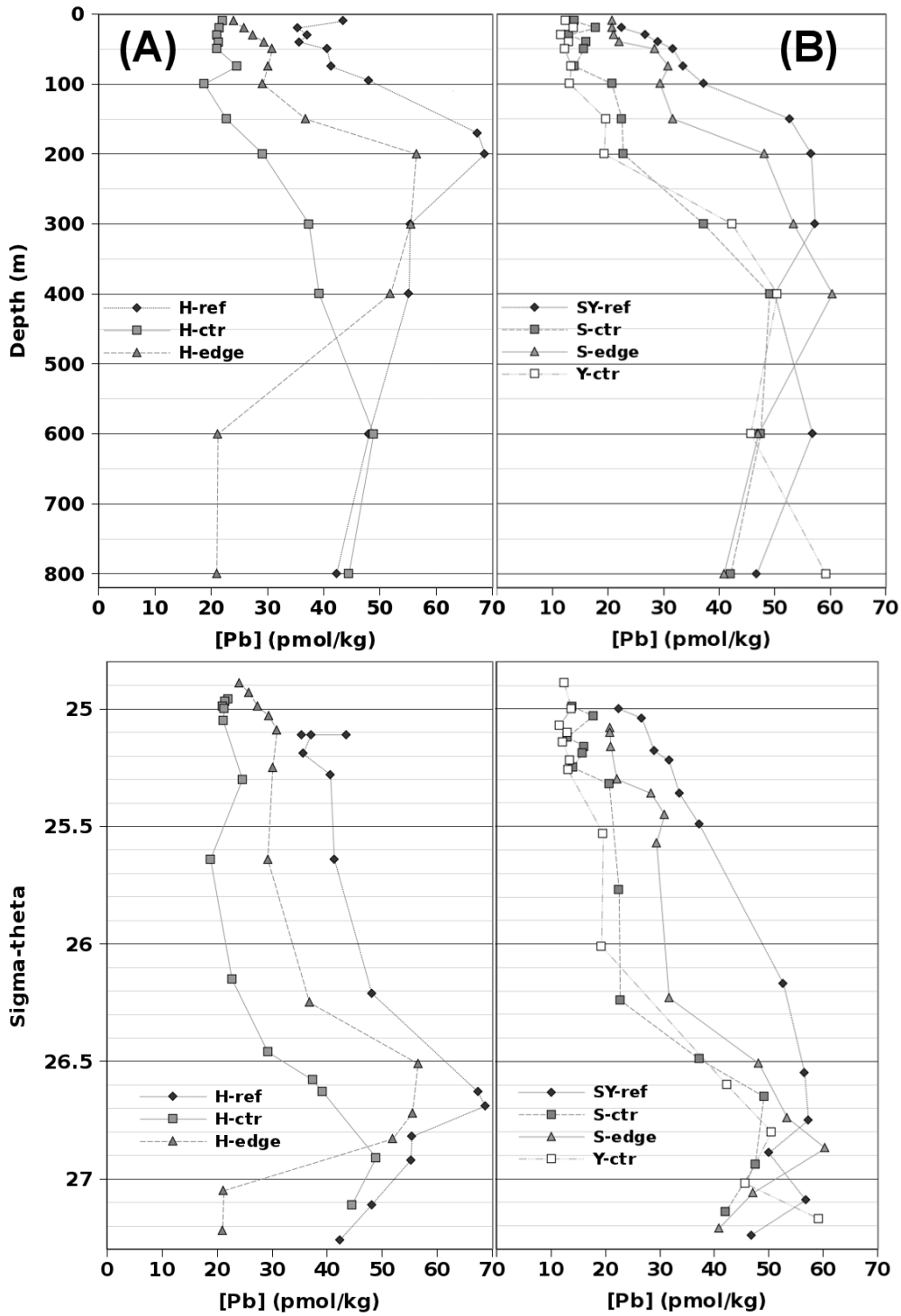


Figure 3.2. Vertical profiles of dissolved [Pb] at the seven stations where full profiles were taken. A) is the reference, edge and centre stations of the Haida eddy and B) shows reference and edge stations in the Sitka eddy as well as a profile through the centre of each of the Sitka and Yakutat eddies.

As a general trend, the concentrations of dissolved Pb were lowest in the eddy core and highest at the

reference station outside the influence of the eddy, with intermediate concentrations at edge stations. The maximum concentration within the eddy was lower than those at the reference or edge stations and was several hundred meters lower in the water column. This effect was much more pronounced in the Haida eddy.

A number of other oceanographic parameters were utilized in order to get a more complete idea of the processes involved which leads to the Pb distribution we see here. Many of these parameters have been discussed previously elsewhere (see Ladd et al, (2009)), the spiciness variable will be used here to develop a better understanding of the water masses involved (Flament, 2002). Density is controlled by the temperature and salinity of the water and spiciness is useful in differentiating cold, fresher water from warmer, saltier water masses. Isolines of spiciness are orthogonal to isopycnals on a temperature-salinity diagram. Numerical data for all Pb determinations can be seen in Tables A2.3 and A2.4 of Appendix II.

3.4. Discussion

This is the first time Pb has been studied in the eddies of the eastern GoA, and thus there does not exist other data with which the current results can be compared. The concentrations determined in this study ranged from 11.5 to 68.7 pmol/kg, which are very consistent with other measurements in the northeastern Pacific (Schaule and Patterson, 1981; Flegal et al., 1986; Boyle et al., 2005; Wu et al., 2010; this thesis, Chapter 2). The general structure of a vertical profile of Pb is expected to have high concentration in the surface as a result of surface deposition, with concentration decreasing with depth below this maximum. Over time it has become clear that the biogeochemical cycling of Pb in the ocean is more dynamic, with Pb often being removed from the surface by sorbing to phytoplankton cells and being scavenged from the water column. The purpose of this study is to investigate the distribution of Pb in and around three mesoscale anticyclonic eddies, which are common yet anomalous features in the GoA.

The spiciness variable is quite useful in the GoA to discern different water masses as seen in Figure 3.3. Although two water masses may exist on the same isopycnal surface, spiciness allows differentiation of two water masses based on their temperature and salinity characteristics, which together define density. A warmer, saltier water masses appears in these figures towards the red end of the spectrum, while a colder and fresher water mass appears blue or violet. The colour scale depicted in this Chapter is the same as those for spiciness in Chapter 2, allowing direct comparison of this property if desired. The Haida eddy shows surface waters very similar to those surrounding the eddy in terms of spiciness, while below the thermocline it is seen as a large region of high-spiciness water, which was also observed in a 2010 eddy which crossed routine sampling along Line P in the northeast Pacific (Figure 2.4). Such a mass of high-spiciness water is absent below the pycnocline in both the Sitka and Yakutat eddies, indicative of differing temperatures in the source waters of these eddies.

The cold, fresh water which is thought to be highly influenced by river inputs in the Sitka and Yakutat eddies can be seen as lighter purple regions in the surface mixed layer (Ladd et al., 2009).

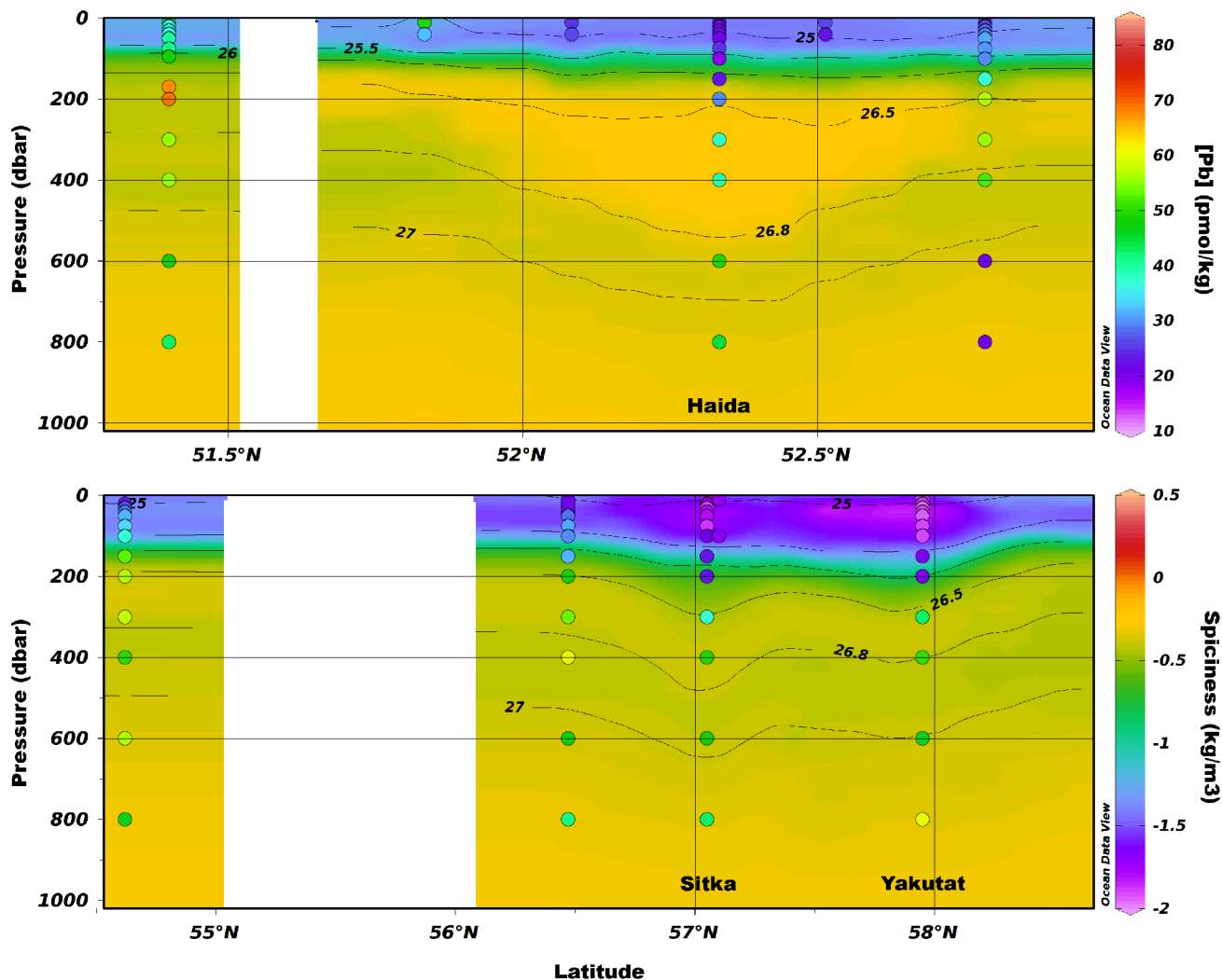


Figure 3.3 a and b. [Pb] is plotted as a function of pressure as coloured dots for the a) Haida eddy and b) Sitka and Yakutat eddies. The coloured shading of the background shows the spiciness calculated from temperature and salinity. Isopycnal surfaces are shown as black lines.

3.4.1. Haida eddy

The Haida eddy reference station was 240km NNE of Line P's Station P16. Figure 3.4 shows a comparison of the samples collected in April 2005 compared with those collected August 2010 (see Chapter 2). The samples from the cruise in 2005 were collected, acidified and stored for several years before being analyzed within several months of the 2010 Line P samples. Having converging values at depths from 200-400m (which also showed very similar σ_θ values) indicate that the storage conditions likely introduced negligible change to Pb

concentration. The concentrations in shallower waters are more prone to seasonal effects and short-term fluctuations, hence the decrease in correlation above 200m.

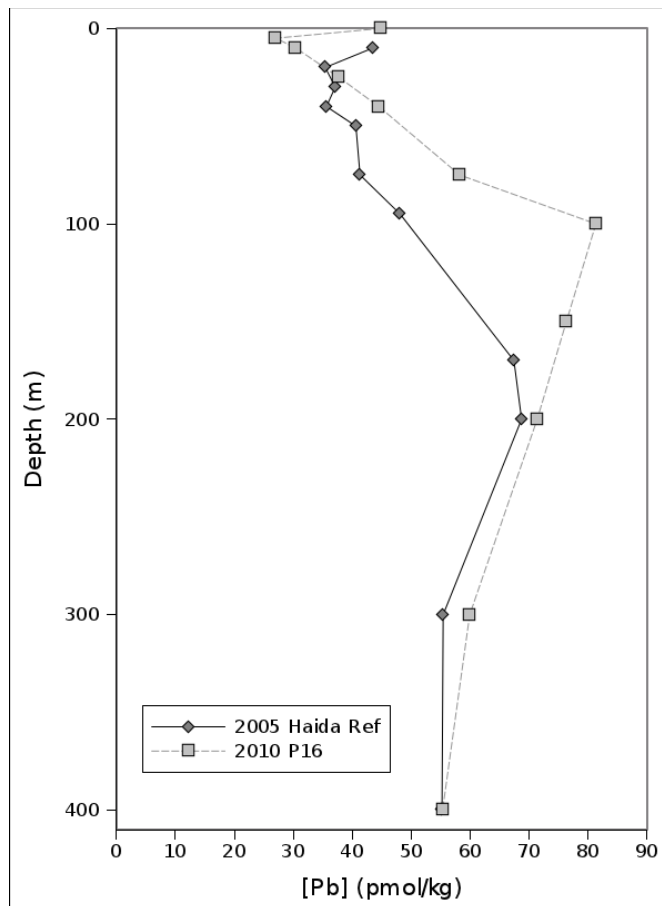


Figure 3.4. Vertical profile of [Pb] at the Haida eddy reference station (51°24' N, 134°00' W) collected in 2005 compared to Station P16 (49°17' N, 134°40' W) collected in 2010.

The core of the Haida eddy extends to potential density of 26.8, below which isopycnal surfaces are still depressed, but have similar properties to water outside of the eddy's influence. From the surface to the bottom of the eddy core, Pb concentration is consistently lower at the centre of the eddy relative to the edge and the reference station due to the coastal origin of this water (Figure 3.2). Other studies of [Pb] in the northeast Pacific appear to show removal of Pb by sorption to phytoplankton to be the major reason surface Pb concentrations are lower than those at depth (Schaule and Patterson, 1981); this thesis). However, availability of light and shallow mixed layers constrain phytoplankton growth to the upper 50-100m of the water column. Above this depth in the Haida eddy, nutrient drawdown has occurred, indicating that a spring phytoplankton bloom had occurred by the time sampling was undertaken. This was further evidenced by a band of high-Chlorophyll *a* water drawn around the eddy as seen by MODIS satellite data (Ladd et al., 2009).

The data presented here show that the lower [Pb] in the eddy centre is consistent throughout the profile to a depth of 800m. The edge station shows a drop in concentration below a depth of 400m which is expected to be related to processes related to the continental shelf, but otherwise shows a similar trend. This can not be explained entirely as a result of scavenging by phytoplankton. Instead, it is thought that the mesothermal waters of the eddy core consist of waters with about 39 pmol/kg Pb. The core waters of the eddy likely mix with the higher [Pb] waters surrounding the eddy, which produces the intermediate concentrations seen at the edge station. The high-spiciness and low NO ($\text{NO} = [\text{O}_2] + 9.2[\text{NO}_3]$ (Broecker, 1974)) of this water indicates that the subsurface eddy core waters may be strongly influenced by waters of the California Undercurrent along the continental slope (Ladd et al., 2009). The conflict with this proposal in terms of [Pb] is that the concentrations in the eddy core are much lower than those measured in the CUC in samples collected in August 2010 which were determined to be on the order of 65 pmol/kg. It is likely that this simply represents the influence of source water from Hecate Strait and/or Queen Charlotte Sound which seems to have quite low concentrations of Pb (Stukas et al., 1999).

3.4.2. Sitka and Yakutat eddies

Relative to the Haida eddy, both the Sitka and Yakutat eddies show greater surface depletion above the σ_θ 25.3, which marks the top of the subsurface core waters of the eddies. This density is found at 89m in the Sitka eddy and 110m in the Yakutat eddy. The average [Pb] from the surface to this depth are 15.1 ± 1.8 pmol/kg (± 1 std. dev.) and 12.8 ± 0.8 pmol/kg for the Sitka and Yakutat eddies, respectively. Although not statistically different, the Yakutat eddy was found to have the lowest measured [Pb] in this study at 11.5 pmol/kg. The spiciness minimum was lower in the Yakutat eddy, which indicates that there is greater river water influence in the surface water of this eddy.

Based on concentrations of nutrients and Fe in these eddies, it was determined that a bloom had likely occurred in the Sitka eddy, while a lack of nutrient drawdown is indicative that the Yakutat eddy had yet to experience a spring bloom (Ladd et al., 2009). When low concentrations of Pb are found near the surface, it can generally be considered that scavenging by phytoplankton has occurred and/or the region is far from atmospheric sources. In the current case, the eddies were sampled while being only several months old. The surface water is derived from coastal water which is strongly influenced by rivers, which are enriched in Pb relative to oceans.

Past research has found that as freshwater enters an estuary, iron and manganese show a strong tendency to flocculate and precipitate (Sholkovitz, 1978). Several years prior to that, it was found that essentially 100% of Pb^{2+} was stripped from solution when exposed to freshly precipitated iron and manganese oxy-hydroxides at a

relevant pH (Gadde and Laitinen, 1973). This is in agreement with other studies which have shown Pb to be strongly scavenged in estuaries in many different estuarine systems (e.g. Pope and Langston, (2011); Tang et al, (2002)). The concentration of [Pb] in river water would vary depending on a number of factors, such as river flow volume and the underlying substrate. The work by Stukas et al. (1999) found that Pb appeared to be scavenged from the water column during transit through a fjordal estuary in southern Alaska, near the formation region of the northern eddies. It was also found that the seawater being advected into the estuary at depth was very low in dissolved Pb. It is thus expected that these eddies do not necessarily have the Pb scavenged from the water column by biotic processes as expected to be the primary mechanism for Pb removal in the Haida eddy, but rather they simply transport low-Pb water from the coast out into the open ocean. Further testing in the coastal GoA waters, especially winter sampling in the region surrounding Haida Gwaii, would provide evidence as to whether this is an accurate portrayal of the actual process or not.

3.5. Conclusions

The results presented here are the first known detailed analysis of Pb in eddies of the GoA and appear to be the first to study the biogeochemistry of Pb in any marine eddies. In the waters ranging from the surface to the bottom of the eddy core waters, [Pb] was found to be lowest in the centre stations and highest at the reference stations outside the eddies, with the edge stations showing intermediate values. Waters below subsurface core waters became more uniform for the most part, indicating a more common source of waters below the eddies in spite of isopycnal depression associated with the eddy.

It was also found that there may be more than scavenging by phytoplankton controlling the surface concentrations of Pb. In two profiles from different times of year (May, 1995 and September, 2010), surface concentrations were found to have similar near-surface [Pb], likely controlled by phytoplankton. In the northern eddies, the Sitka was expected to have experienced a phytoplankton bloom while the Yakutat eddy did not appear to have the same nutrient drawdown although conditions seemed suitable for phytoplankton growth. As a result, the influence of estuarine systems was considered which may play a role in the very low concentrations of Pb seen in the centre of those eddies. This could be the result of strong scavenging of Pb to the freshly precipitated iron and manganese oxy-hydroxides, which have been shown to scavenge Pb from solution almost quantitatively. Indeed, it is a similar precipitation that was used to separate Pb almost quantitatively from the seawater matrix in the method introduced by Wu and Boyle (1997b).

Other metals have been shown to be concentrated in eddies, which then act as a source of these metals into the oceanic GoA. The current study has found that Pb is depleted in these eddies, which may eventually act

as a diluent of Pb in the upper waters of the GoA.

4. A first look at dissolved Pb in the Canada Basin of the western Arctic Ocean.

4.1. Introduction

The Arctic Ocean is a mediterranean system which receives seawater inputs from the Atlantic and Pacific Oceans, and freshwater input from precipitation and rivers (e.g. Carmack and McLaughlin, (2011)). The region is relatively remote and hazardous for oceanographic research, requiring vessels with ice-breaking capabilities which are even then only capable of operating for several summer months each year. The GEOTRACES program was developed with the intention of providing baseline measurements of trace elements and their isotopes (TEI) on a global scale (SCOR Working Group, 2007; Sohrin and Bruland, 2011). This provided an opportunity through the Canadian IPY GEOTRACES program to obtain samples using trace metal-clean techniques from the Canada Basin region of the Western Arctic Ocean.

Pacific water enters the system through the Bering Strait, which is only 150 km wide and 50m deep (Coachman and Aagaard, 1966). This water is fresher than that coming from the Atlantic sector owing to moisture from the Atlantic advecting over the isthmus of Panama and being rained into the Pacific Ocean. The water from the Atlantic Ocean enters the Arctic Ocean via the cold Nordic seas and sinks below the Pacific water as it circulates through the ocean before eventually returning to the Atlantic via Fram Strait (Coachman and Aagaard, 1974).

The upper waters of the Canada Basin are undergoing rapid change as a result of the decrease in sea ice extent and thickness, which affects surface waters (Serreze et al., 2007). The water closest to the surface in the Canada Basin in summer is a relatively fresh mixed layer formed by the melting of the previous winters' sea ice, and although historically found to be as deep as 30-50m, this mixed layer is only 16m deep in summer (see Figure 4.1) (McLaughlin et al., 2004; Toole et al., 2010). Below this mixed layer is found a near-surface temperature maximum (NSTM), formed by solar radiation being trapped below the halocline at the base of the surface mixed layer (Jackson et al., 2010a). Below this is a local temperature minimum which indicates the remnants of the previous winters' mixed layer (rWML) which is saltier than the surface layer as a result of brine rejection during sea ice formation, which also mixes the surface layer downward via convection. A temperature minimum and maximum found below the rWML are of Pacific origin, with the warmer water entering the region during the summer months while the lower temperatures were modified in the Bering and Chukchi seas during the cold winter months (Coachman and Barnes, 1961).

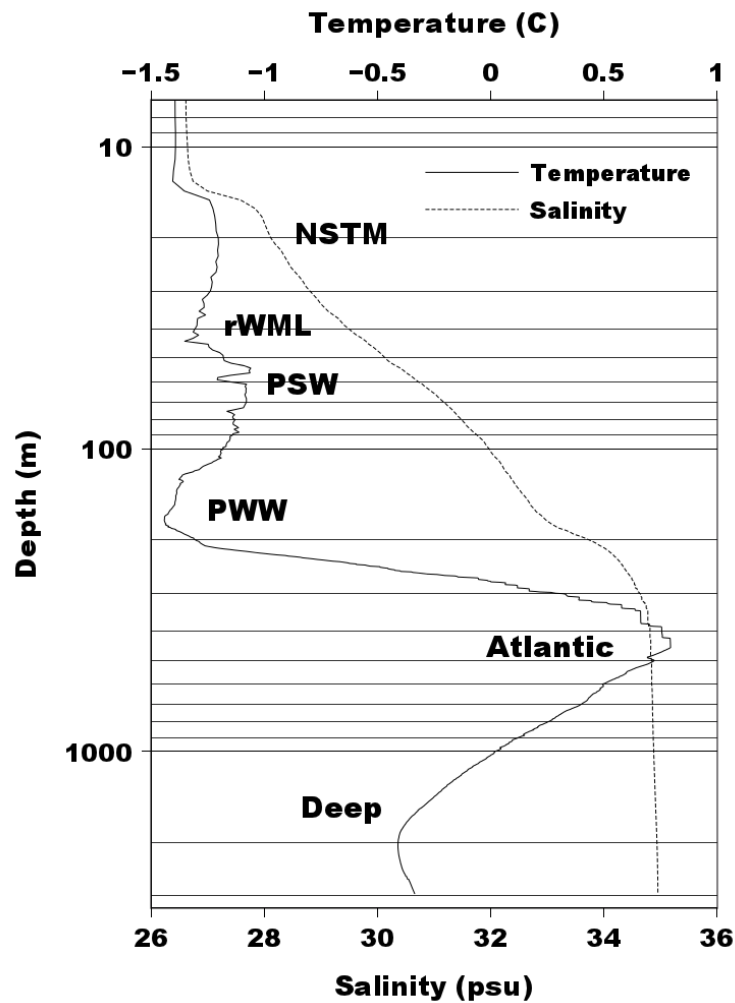


Figure 4.1. Depth profile of temperature and salinity at a representative station in the southern Canada Basin. Note the vertical axis is on a logarithmic scale.

The Atlantic water subducts below the Pacific water layers and can be seen as a clear temperature maximum above 0 °C and $S \approx 34.8$. The haline stratification is a feature of β -oceans (as opposed to α -oceans, which are stratified by temperature) which occur predominantly at high-latitudes and where temperature differences in the water column are small (Carmack, 2007). The Atlantic water passes through Fram Strait and the Barents Sea before making its way through the basins of the Arctic Ocean, entering the Canada Basin last before being flushed through the Canadian Archipelago to be returned to the north Atlantic (McLaughlin et al., 2005). The deep water in the basin has been dated using several methods which give an age of about 500 years (Macdonald and Carmack, 1991, 1993; Edmonds et al., 1998). The formation mechanism of these deep waters is still not known with certainty, but is thought to be a combination of exceptionally dense Atlantic water mixed with brine rejected during ice formation that is dense enough to reach these depths while entraining water from

intermediate depths (Macdonald and Carmack, 1993; Jones et al., 1995). The deepest waters below roughly 2,750m are isolated by the Alpha-Mendeleev ridge and have not been renewed for about 500 years (Schlosser et al., 1997; Timmermans and Garrett, 2006).

Generally speaking, the Arctic Ocean is vastly undersampled for most trace elements, including Pb. The outflow of the Ob and Yenisey rivers in the north of Russia were analyzed for dissolved Pb, along with Kara Sea bottom water (Dai and Martin, 1995). The river waters had Pb concentrations of 19.4 – 35.3 pmol/L and the bottom of the Kara Sea was 12.3 pmol/L which suggests as discussed by Dai and Martin that Pb is removed by particulate material during estuarine mixing (see Chapter 3). Other studies have determined that major removal mechanisms of Pb from seawater are via biogenic particulate matter and adsorption to fresh mineral phases precipitated during estuarine processes (Michaels and Flegal, 1990; Tanguy et al., 2011). Jackson et al. (2010b) observed the distribution of particulate matter in the Canada Basin between 2003 and 2008 and found that close to the shelf of the eastern Beaufort Sea, surface waters had the highest beam attenuation (highest turbidity), while waters about 15-25m and at a latitude of 70°N had the highest concentrations of chlorophyll, with subsurface chlorophyll showing a maximum at 55-60m. With very low aeolian flux to this region, these regions of elevated particulate are expected to have depleted [Pb].

4.2. Methods

Seawater samples were collected aboard *CCGS Amundsen* between 27 August and 12 September, 2009 using a metal-free rosette on a Kevlar-wrapped conducting wire. Six stations were sampled to bottom depths of 279 to 2957 m at stations S4 and L2, respectively (see Figure 4.2). The deeper L3 station was only sampled to mid-depth. Subsampling from the rosette was done in class 100 fume hoods in a container on deck. Samples were filtered through 0.22 µm Opticap filters and collected into 500 ml, 1000 ml or 4000 ml acid-leached low-density polyethylene bottles and acidified to pH ~1.8 until analysis using Seastar Chemicals Baseline HCl. Physicochemical parameters such as conductivity, temperature and oxygen content were collected from the rosette during each cast. Samples from each bottle were analyzed for nutrients using standard shipboard colourimetric methods.

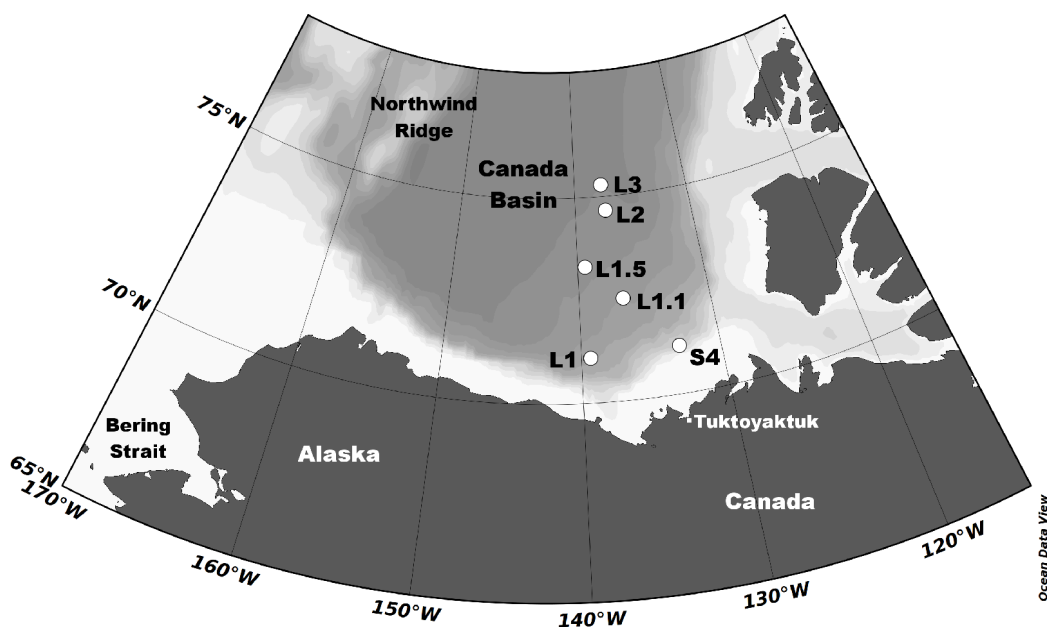


Figure 4.2. Map of the southwestern Arctic Ocean showing the Canada Basin and the location of the six station sampled for this study.

The analysis method used was a modified version of the magnesium-induced coprecipitation technique introduced for Pb analysis by Wu and Boyle (1997). Briefly, 13 ml of acidified seawater was transferred to a 15 ml acid-cleaned centrifuge tube and spiked with 50 μl of a ^{207}Pb -enriched standard. After sitting for greater than 1h to allow isotopic equilibration, 175 μl of Seastar Chemicals concentrated NH_4OH (11 N) was added and shaken to mix. This solution was allowed to react and precipitate for five minutes before centrifuging. The supernatant was decanted and recentrifuged to remove as much liquid as possible. The remaining $\text{Mg}(\text{OH})_2$ pellet was dissolved in 1-2 ml of 1% HNO_3 for analysis. More detail is available in Chapter 2.

Determinations were performed using a Thermo Scientific Element XR high resolution ICP-MS at the Fipke Laboratory for Trace Element Research (FiLTER) at the Okanagan Campus of the University of British Columbia. Blanks were analyzed every ten samples, one sample out of 20 was prepared and analyzed in duplicate and one sample out of 20 was prepared and analyzed in triplicate which resulted in replicate measurements on greater than one in every 10 samples.

The ID-MS method used here was found to be quick and reliable in the determination of Pb in seawater. The results of replicate measurements on certified or interlaboratory materials can be found in Figure 2.1. The expected concentration range normally seen in seawater ranges from 10 to 150 pmol/kg, thus this method seems suitable to accurately determine the [Pb] of a particular sample.

4.3. Results

Figure 4.3 shows the vertical Pb distribution in the Arctic Ocean, which is generally low and scattered relative to many other profiles seen in the open oceans (Wu et al., 2010; Lee et al., 2011). Numerical data is presented in Table A2.5 of Appendix II. It was considered that the scatter may have arisen due to problems during sampling or preparatory protocol, but this does not seem to be the case. The same procedures were used for these samples as for seawater samples analyzed for Pb from the Northeast Pacific, which showed very oceanographically consistent results (see Chapters 2 and 3). The same rosette was used to collect samples which were analyzed shipboard for Fe(II) with good results (Ramirez and Cullen, 2010), which does not necessarily verify the bottles were not Pb-contaminated but combined with a lack of consistency between the bottle from which a sample was taken and the [Pb] of the sample, this seems doubtful. Finally, the bottles used to collect and store samples were thoroughly cleaned by proven methods and showed no signs of contamination in other studies. As a result the concentrations determined here are considered to be accurate within the confines of the analytical method used.

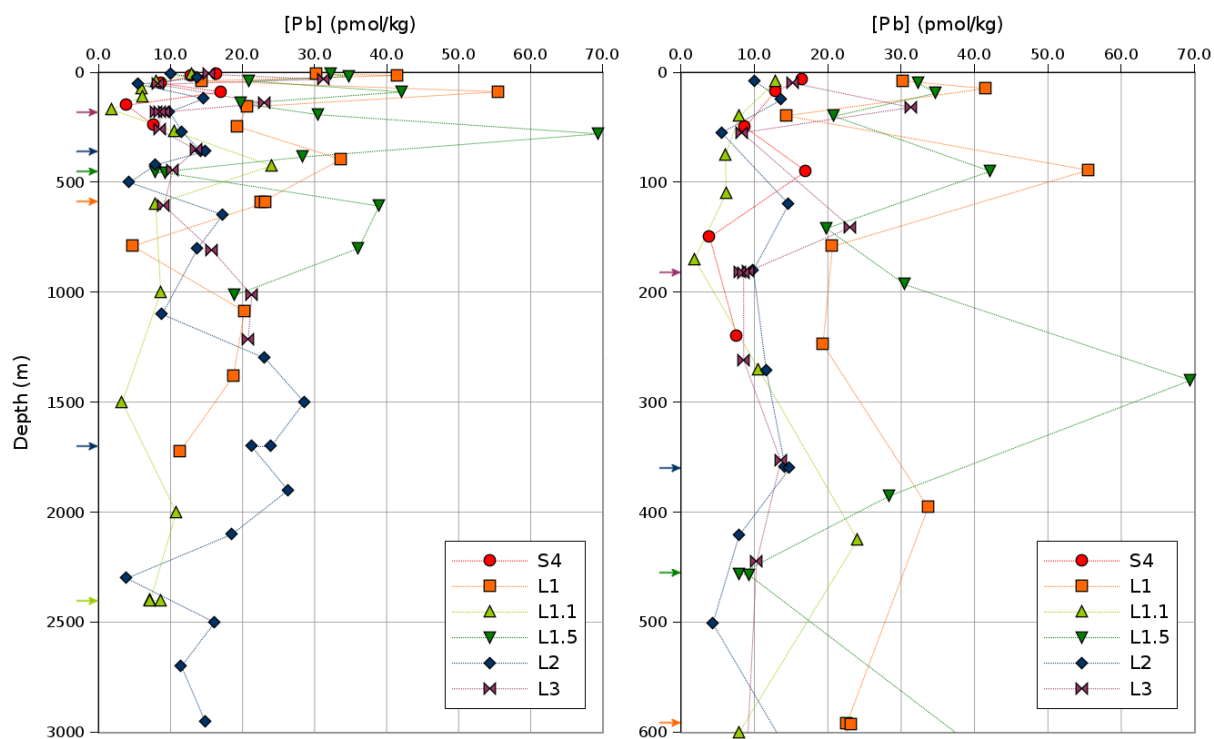


Figure 4.3. All vertical profiles collected in this study. Arrows along the depth axis indicate method duplicates at that depth. The figure on the right is an expansion of the top 600 m. The order of the station in the legend is in order from closest to shore to furthest from shore.

One point was rejected from this data set and is not shown in figures; a sample collected at 900 m at Station L2 was repeatedly analyzed to be 100 to 105 pmol/kg and is considered to be an outlier. The data point at

280 m from Station L1.5 was determined to be 69.5 pmol/kg, which was much higher than the other data from that profile. This data point seemed reasonable from an oceanographic standpoint and was thus left as part of the dataset but is considered suspect. The lowest concentration measured in this study was 1.8 pmol/kg at 170 m at Station L1.1, which is only marginally higher than the 1.2 pmol/kg measured by Wu et al. (2010) in the deep South Pacific.

Two of the six stations (L1.1 and S4) were found to have vertical profiles of [Pb] which were predominantly below 20 pmol/kg, with only a single measurement from Station L1.1 being above this at 24.1 pmol/kg. Station L3 had only a single measurement which exceeded 30 pmol/kg and every sample from station L2 was below 30 pmol/kg. So out of these four stations, only a single measurement was found to exceed 30 pmol/kg. The troubling aspect is that there does not seem to be a logical reason for Stations L1 and L1.5 to have higher [Pb] than the other stations, considering that Station L1.1 is located between them and would therefore be expected to have similar concentrations. Concentrations well over 30 pmol/kg occur to depths of 800m, which therefore cannot be attributed to possible patchy surface processes. Further, as a result of the complex stratification pattern of the Arctic Ocean, this scatter in the data exists across water masses which originated in completely different ocean basins. If this scatter were real, it would be expected to occur in specific water masses rather than being seen in a vertical profile. That is to say, scatter constrained to the Atlantic water mass in samples from different stations would be more expected than scatter from different depths at a single station. As a result, the data from Stations L1 and L1.5 are being treated as suspect until more evidence is gathered that may support or refute the claim that these measurements reflect actual concentrations at these depths at these locations.

4.4. Discussion

The data presented here are similar to those determined in the Southern Ocean, which ranged in concentration from 10 to 30 pmol/kg with no correlation with other parameters (temperature, salinity, nutrients, oxygen, NO), with surface concentrations reaching higher levels due to direct inputs of both anthropogenic and natural Pb (Flegal et al., 1993; Ellwood, 2008). The Beaufort Gyre of the Arctic Ocean has a very different stratification than the Southern Ocean and so direct comparisons cannot necessarily be made of the two, save from implying that the low concentration of Pb are likely a result of the remoteness of these oceans from point sources of anthropogenic pollution. Although Flegal (1993) found similarly high concentrations as our rejected data point (around 100 pmol/kg), his value was found in a surface sample where concentrations are more patchy as a result of atmospheric deposition and having been subjected to small amounts of scavenging. The 103 pmol/kg rejected data point from our dataset came from a depth of 900m where the water mass would be expected to have mixed sufficiently with surrounding waters to have significantly decreased such a high

concentration, and is likely therefore an artifact of contamination rather than elevated Pb.

Further to this, it is expected that the rosette used to collect the trace metal samples may itself have provided some contamination to the present samples. The stations were not sampled in ascending numerical order, but first L1 and L1.5, before occupying L2 and L3 and returning to land via L1.1 and S4. Figure 4.4 shows [Pb] from the sample nearest to the PSW, PWW and Atlantic water masses at each station except for S4 which was not deep enough to reach the temperature maximum of the Atlantic layer. The concentration from Stations L1 and L1.5 are higher than all but one of the concentrations from these water masses at the remaining stations. Station L2 was sampled in higher resolution as a series of two casts, the deeper of which was performed first. It appears in Figure 3 that the shallow cast at Station L2 appears to be more oceanographically consistent and will thus remain within the dataset but the deeper cast will remain suspect. It is suggested that the Pb data acquired from Stations L1 and L1.5 be flagged in the dataset as possibly contaminated.

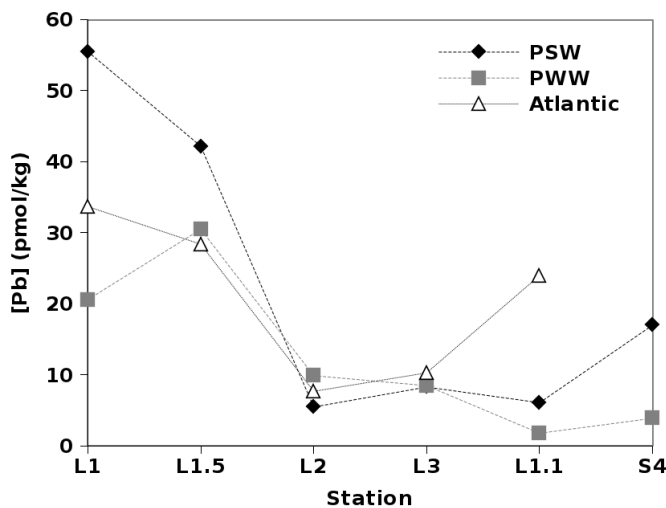


Figure 4.4. The concentration of Pb in the sample closest to subsurface water masses in the Beaufort Gyre. Stations are listed in order sampled from left to right.

Considering the samples which remain after excluding those which are expected to be contaminated yields a dataset containing 4 stations, with [Pb] ranging from 1.8 to 31.3 pmol/kg, which are in line with those found during the winter in the Southern Ocean, a similarly remote environment (Ellwood, 2008). The highest concentration was found at Station L3 in the rWML, which may have been exposed to some sediment-laden ice, since the concentrations found in other regions in the water masses are generally much lower. With the exclusion of a few elevated points, the concentration of Pb in the surface and Pacific waters seem to show a slight decreasing trend with depth, consistent with a scavenged-type element (Figure 4.5). Salinity is being used in place of depth, which serves almost the same function as density except that it is conservative, and can be used to compare results among stations. Salinity of 32 corresponds with the very bottom of the PSW in these samples

where there is a spike in concentration among three of the four stations, which could be indicative of sediment interactions in the deepest of the PSW during formation. It does not appear that this would be the result of any interaction with PWW, since the samples were taken from the PSW end-member of a mixing line between these two water masses on a temperature-salinity diagram (not shown). The core of PWW is at $S = 32.9$ which has the lowest [Pb] at both L1.1 and S4 and slightly higher concentrations at the offshore station. This may be the result of freshly precipitated iron and manganese oxy-hydroxides forming fresh mineral phases after being precipitated from the outflow of the Mackenzie River and scavenging Pb from the water column near Station S4 (Dai and Martin, 1995; Tanguy et al., 2011) or sediment interactions during the formation of PWW and its transit across the shallow shelves into the basin.

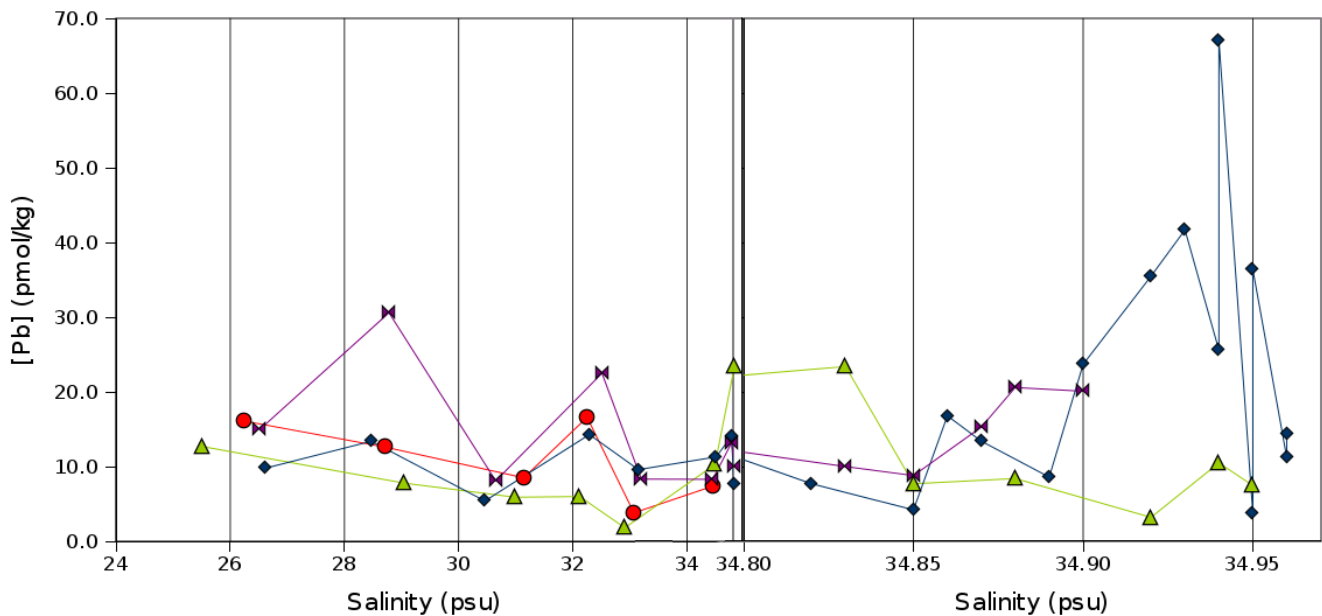


Figure 4.5. [Pb] against salinity for the four uncontaminated stations. Note the change of scale at a salinity of 34.8 in order to clearly show the deeper values.

At salinities higher than 34, Figure 4.5 appears to show a maximum in the Atlantic core water, which is simply an artifact of the deep waters being compressed into a small amount of space. Most of the values in this range belong to L2, which are being considered suspect and thus will not be expanded upon. Station L1.1 has a concentration of 24.0 pmol/kg at the core of the Atlantic water, while [Pb] in this same core water at L2 and L3 were below 15 pmol/kg. The two more northern stations (L2 and L3) had a higher temperature, and could indicate slightly different waters than were found at L1.1 which could account for the difference in [Pb]. The two samples taken from L3 below the Atlantic core showed elevated concentration of Pb which is inconsistent with the concentration seen at similar depths at L2 and may be the result of contamination.

Most samples in this region were below 20 pmol/kg, which is considered quite depleted in many regions

of the ocean in close proximity to anthropogenic pollution. Although it is possible to attempt to interpret this data, the risk of contamination in the samples that are considered clean here remains present. Although small amounts of anthropogenic contamination is expected to be present in the Arctic atmosphere and could therefore be deposited to the ocean surface, it does not appear that these waters are heavily contaminated (France and Coquery, 1996; Macdonald et al., 2000, 2005; Vinogradova, 2000). Wu et al. (2010) were able to use isotopic distribution of stable Pb isotopes to infer anthropogenic pollution via reversible particle exchange in the deep Pacific, a similar method could be useful in the present case. Isotopic distribution has already been determined for sediment samples throughout the Arctic Ocean, which indicate that the Canada Basin may not be contaminated with anthropogenic Pb (Gobeil et al., 2001).

4.5. Conclusions

Based on results from four uncontaminated stations in the Beaufort Sea, there appears to be little impact from anthropogenic pollution in this region. It is difficult to make such a statement, as others have used isotope ratios to demonstrate anthropogenic pollution where Pb concentrations are as low as those in this study (Wu et al., 2010). Concentration was generally low and quasi-conservative through the region, with what appear to be minima in the profiles coincident with the PWW. A lack of clear correlation between [Pb] and any available parameters limit the usefulness of Pb as a tracer of any processes in the Beaufort Sea. Since Pb concentration has not previously been determined in this region prior to the present study, these measurements should prove valuable as a baseline to which future changes (or lack thereof) can be compared.

5. Conclusion

The past three chapters provide one of the largest single collections of dissolved Pb data in seawater to date. This study has shown that the magnesium-induced coprecipitation method originally presented by Wu and Boyle (1997b) is a quick, accurate and precise way to acquire data on dissolved Pb. However, the data from the Arctic are a reminder that even using trace metal clean sampling techniques and working to reduce the possibility of contamination that these concentrations are so low that even slight contamination can put data into question.

The use of the spiciness variable was useful in visualizing different water masses in the Northeast Pacific Ocean, and allowed a more cohesive presentation of [Pb] data. In the Arctic Ocean, the temperature differences relative to those in salinity are so small that the spiciness variable is more or less useless. Eddies are easily visible in a transect based on the bowing up and down of isopycnal surfaces, and this is aided by the spiciness variable by emphasizing regions of anomalously cold/fresh or warm/salty water which these eddies may be transporting offshore. This data is all available by plotting the data series in a temperature-salinity diagram, but by presenting the data as a function of pressure and distance (such as latitude or longitude) it is much simpler to interpret the information as a result of biogeochemical processes occurring in the natural environment.

As expected, much of the scavenging along Line P occurred closest to shore where there was high water turbidity and abundant phytoplankton (based on high chlorophyll *a* fluorescence). Concentrations were elevated in the uppermost sample across the transect, consistent with an aeolian source. The subsurface maximum seen at all stations along Line P was unexpected, with Pb being delivered from the west and south in North Pacific Intermediate Water and the California Undercurrent Extension, respectively, and from another as-of-yet unknown source which contained some of the highest levels of dissolved Pb seen in this study. Elevated values were seen below the surface in all of the profiles sampled in the Northeast Pacific, including those from within the eddies from different formation regions. The upper waters of the Yakutat eddy did not appear to have been affected by a spring bloom by the time sampling was done, though the upper waters still showed low concentrations of Pb, similar to those at P4 in the autumn where there was an abundance of phytoplankton. It is expected that this decrease was caused by scavenging by freshly formed mineral phases precipitating from fresh water undergoing estuarine processes near river mouths (Stukas et al., 1999; Pope and Langston, 2011). As a result the eddies actually transport Pb-poor surface waters into the Pacific.

Overall, the work done in this study is considered successful and a useful addition to the growing spatial and temporal Pb dataset in the oceans. The downside to the rather sparse data currently available in the Northeast Pacific and Western Arctic is that there are few other data with which these results can be compared. However, it

has been shown that samples can be acidified and stored for years before being prepared for analysis if the proper methods are used, which may allow for a much larger amount of data to be collected in the coming years. The small sample requirement (13 mL) means that large volumes of water need not be collected, facilitating logistics when many groups aboard a ship may be competing for a limited supply of water. It will also serve as a reasonable starting point for future work as Line P is sampled for trace metals somewhat frequently, a time series could be constructed relatively easily which could improve upon the observations made in this thesis. On the same vein, this work has provided the first reports of dissolved Pb in the Western Arctic Ocean, which can serve as a baseline with which future data can be compared, in the event that climate change indeed allows for greater commercialization and population of the Arctic, bringing with it the pollution which has affected most of the rest of the planet.

A shortcoming of this work is in the limited amount of information available from only having concentration data available, lacking isotopic information. This would have offered more insight into the source of Pb which would offer more information of the movement of this element, such as a more insightful explanation of the high surface values of the W-line from the coastal cruise. Work is being undertaken in our lab group to be able to provide this information in the near future. A lack of easily available instrumentation also limited the possibility of rerunning some samples to ensure accurate measurement, such as the highest measurement in the Line P data set at station P16 which seemed to be out of place (occurring in the mixed layer as opposed to the high-Pb water mass as would be expected) which could clarify a few data points. This does not imply that the value as measured is necessarily incorrect, simply that it does not fit the expected pattern.

Future work can go in several directions. As previously mentioned, a time-series along Line P would improve our understanding of this element along a transect over time, which has only really been done in single profiles before (such as Lee et al. (2011)). While researching for this thesis it became clear that the ocean is vastly undersampled for Pb and many other trace elements, so simply expanding the regions where such measurements are available would be an improvement. Focus could also be put on some of the more detailed aspects of work covered here, such as the establishment of equilibria between various particulate phases (mineral surfaces or phytoplankton) which would influence the removal of Pb from seawater. Isotopic data in the Arctic should provide greater insight into the possibility of anthropogenic Pb already existing in the region or not. Although sediment profiles have not provided evidence of this, anthropogenic Pb has been found to be present in the North Pacific water, which having been away from the surface for the greatest amount of time would be expected to be pristine (Gobeil et al., 2001; Wu et al., 2010). A series of transects such as those presented by Middag et al. (2009) for Al who analyzed a total of 666 samples throughout the Eurasian Arctic Ocean would provide a large leap forward in the understanding of the global biogeochemistry of Pb. The problem with such a plan is of course that ship time is expensive and in short supply, with difficult logistics. At present, the GEOTRACES IPY cruise which allowed for the data presented here was useful in setting a benchmark to which

future excursions may be compared.

As it stands, the work presented in this thesis is a useful update on the present distribution of Pb in the Northeast Pacific, which had previously been analyzed three decades prior. It also presents the distribution of Pb through three eddies, which provide more insight into the cycling of the element in the Gulf of Alaska. It also fills a data gap in the high latitude ocean, as the Western Arctic had heretofore lacked any data whatsoever. As with any scientific pursuit there remains a great deal of work to be done, but this work has added an important piece to the puzzle.

References

- Bacon M.P., Spencer D.W. and Brewer P.G. (1976) $^{210}\text{Pb}/^{226}\text{Ra}$ and $^{210}\text{Po}/^{210}\text{Pb}$ disequilibria in seawater and suspended particulate matter. *Earth Planet. Sci. Lett.* **32**, 277–296, doi:10.1016/0012-821X(76)90068-6.
- Boyle E.A., Chapnick S.D., Shen G.T. and Bacon M.P. (1986) Temporal variability of lead in the western North Atlantic. *J. Geophys. Res.* **91**, 8573–8593, doi:10.1029/JC091iC07p08573.
- Boyle E.A., Bergquist B.A., Kayser R.A. and Mahowald N. (2005) Iron, manganese, and lead at Hawaii Ocean Time-series station ALOHA: Temporal variability and an intermediate water hydrothermal plume. *Geochim. Cosmochim. Acta* **69**, 933–952, doi:16/j.gca.2004.07.034.
- Broecker W.S. (1974) “NO”, a conservative water-mass tracer. *Earth Planet. Sci. Lett.* **23**, 100–107, doi:10.1016/0012-821X(74)90036-3.
- Brügmann L., Danielsson L.-G., Magnusson B. and Westerlund S. (1985) Lead in the North Sea and the north east Atlantic Ocean. *Mar. Chem.* **16**, 47–60, doi:10.1016/0304-4203(85)90027-1.
- Carmack E. and McLaughlin F. (2011) Towards recognition of physical and geochemical change in Subarctic and Arctic Seas. *Prog. Oceanogr.* **90**, 90–104, doi:10.1016/j.pocean.2011.02.007.
- Carmack E.C. (2007) The alpha/beta ocean distinction: A perspective on freshwater fluxes, convection, nutrients and productivity in high-latitude seas. *Deep Sea Res. Part II* **54**, 2578–2598, doi:10.1016/j.dsr2.2007.08.018.
- Chester R. (2003) *Marine Geochemistry*, Wiley-Blackwell, New York.
- Chester R., Murphy K.J.T., Lin F.J., Berry A.S., Bradshaw G.A. and Corcoran P.A. (1993) Factors controlling the solubilities of trace metals from non-remote aerosols deposited to the sea surface by the “dry” deposition mode. *Mar. Chem.* **42**, 107–126, doi:10.1016/0304-4203(93)90241-F.
- Chow T.J. and Patterson C.C. (1962) The occurrence and significance of lead isotopes in pelagic sediments. *Geochim. Cosmochim. Acta* **26**, 263–308, doi:10.1016/0016-7037(62)90016-9.
- Coachman L. and Barnes C. (1961) The Contribution of Bering Sea Water to the Arctic Ocean. *Arctic* **14**, 147–161.
- Coachman L.K. and Aagaard K. (1966) On the Water Exchange Through Bering Strait. *Limnol. Oceanogr.* **11**, 44–59, doi:10.4319/lo.1966.11.1.0044.
- Coachman L.K. and Aagaard K. (1974) Physical oceanography of arctic and subarctic seas, in *Marine Geology and Oceanography of the Arctic Seas*, edited by Y. Herman, pp. 1–81, Springer-Verlag, New York.
- Crawford W. (2002) Physical characteristics of Haida Eddies. *J. Oceanogr.* **58**, 703–713, doi:10.1023/A:1022898424333.
- Crawford W.R. (2005) Heat and fresh water transport by eddies into the Gulf of Alaska. *Deep Sea Res. Part II* **52**, 893–908, doi:16/j.dsr2.2005.02.003.

- Crispo S.M. (2007) Studies on trace metal dynamics in mesoscale anticyclonic eddies in the Gulf of Alaska, PhD. thesis, University of British Columbia, Vancouver, Canada.
- Crusius J., Schroth A.W., Gassó S., Moy C.M., Levy R.C. and Gatica M. (2011) Glacial flour dust storms in the Gulf of Alaska: Hydrologic and meteorological controls and their importance as a source of bioavailable iron. *Geophys. Res. Lett.* **38**, 5 PP., doi:201110.1029/2010GL046573.
- Cushman-Roisin B., Tang B. and Chassignet E.P. (1990) Westward Motion of Mesoscale Eddies. *J. Phys. Oceanogr.* **20**, 758–768, doi:10.1175/1520-0485(1990)020<0758:WMOME>2.0.CO;2.
- Dai M.-H. and Martin J.-M. (1995) First data on trace metal level and behaviour in two major Arctic river-estuarine systems (Ob and Yenisey) and in the adjacent Kara Sea, Russia. *Earth Planet. Sci. Lett.* **131**, 127–141, doi:10.1016/0012-821X(95)00021-4.
- Davis R.E., Ohman M.D., Rudnick D.L., Sherman J.T. and Hodges B. (2008) Glider surveillance of physics and biology in the southern California Current System. *Limnology and Oceanography* **53**, 2151–2168, doi:10.4319/lo.2008.53.5_part_2.2151.
- Dodimead A.J., Favorite F., Hirano T. and Commission I.N.P.F. (1963) *Salmon of the North Pacific Ocean: Review of oceanography of the subarctic Pacific region*, International North Pacific Fisheries Commission.
- Dzieciuch M., Munk W. and Rudnick D.L. (2004) Propagation of sound through a spicy ocean, the SOFAR overture. *The Journal of the Acoustical Society of America* **116**, 1447–1462, doi:10.1121/1.1772397.
- Edmonds H.N., Moran S.B., Hoff J.A., Smith J.N. and Edwards R.L. (1998) Protactinium-231 and Thorium-230 Abundances and High Scavenging Rates in the Western Arctic Ocean. *Science* **280**, 405–407, doi:10.1126/science.280.5362.405.
- Ellwood M.J. (2008) Wintertime trace metal (Zn, Cu, Ni, Cd, Pb and Co) and nutrient distributions in the Subantarctic Zone between 40–52°S; 155–160°E. *Mar. Chem.* **112**, 107–117, doi:10.1016/j.marchem.2008.07.008.
- Ewing S.A., Christensen J.N., Brown S.T., Vancuren R.A., Cliff S.S. and Depaolo D.J. (2010) Pb Isotopes as an Indicator of the Asian Contribution to Particulate Air Pollution in Urban California. *Environ. Sci. Technol.* **44**, 8911–8916, doi:10.1021/es101450t.
- Fisher N.S., Cochran J.K., Krishnaswami S. and Livingston H.D. (1988) Predicting the oceanic flux of radionuclides on sinking biogenic debris. *Nature* **335**, 622–625, doi:10.1038/335622a0.
- Flament P. (2002) A state variable for characterizing water masses and their diffusive stability: spiciness. *Prog. Oceanogr.* **54**, 493–501, doi:10.1016/S0079-6611(02)00065-4.
- Flegal A.R. and Patterson C.C. (1983) Vertical concentration profiles of lead in the Central Pacific at 15°N and 20°S. *Earth Planet. Sci. Lett.* **64**, 19–32, doi:10.1016/0012-821X(83)90049-3.
- Flegal A.R., Itoh K., Patterson C.C. and Wong C.S. (1986) Vertical profile of lead isotopic compositions in the north-east Pacific. *Nature* **321**, 689–690, doi:10.1038/321689a0.
- Flegal A.R., Maring H. and Niemeyer S. (1993) Anthropogenic lead in Antarctic sea water. *Nature* **365**, 242–244, doi:10.1038/365242a0.

- France R. and Coquery M. (1996) Lead concentrations in lichens from the Canadian high arctic in relation to the latitudinal pollution gradient. *Water Air. Soil Pollut.* **90**, 469–474, doi:10.1007/BF00282662.
- Gadde R.R. and Laitinen H.A. (1973) Study of the Sorption of Lead by Hydrous Ferric Oxide. *Environ. Lett.* **5**, 223–235, doi:10.1080/00139307309435531.
- Gay P.S. and Chereskin T.K. (2009) Mean structure and seasonal variability of the poleward undercurrent off southern California. *J. Geophys. Res.* **114**, C02007, doi:10.1029/2008JC004886.
- Gobeil C., Macdonald R.W., Smith J.N. and Beaudin L. (2001) Atlantic Water Flow Pathways Revealed by Lead Contamination in Arctic Basin Sediments. *Science* **293**, 1301–1304, doi:10.1126/science.1062167.
- Gower J.F.R. (1989) Geosat altimeter observations of the distribution and movement of sea-surface height anomalies in the north-east Pacific, in *Oceans 89: The Global Ocean*, pp. 977–981, Institute of Electricity and Electrical Engineering, Seattle.
- Gower J.F.R. and Tabata S. (1993) Measurement of eddy motion in the north-east Pacific using the Geosat altimeter, in *Satellite Remote Sensing of the Oceanic Environment*, edited by I. S. F. Jones, Y. Sugimori, and R. W. Stewart, pp. 375–382, Seibutsu Kenkyusa, Tokyo.
- Guberman D.E. (2009) Lead, in *2009 Minerals Yearbook*, U.S. Government Printing Office.
- Henderson G.M. and Maier-Reimer E. (2002) Advection and removal of ²¹⁰Pb and stable Pb isotopes in the oceans: a general circulation model study. *Geochim. Cosmochim. Acta* **66**, 257–272, doi:10.1016/S0016-7037(01)00779-7.
- Heumann K.G. (1988) *Inorganic mass spectrometry*, Wiley, New York.
- Hong S., Candelone J.-P., Patterson C.C. and Boutron C.F. (1994) Greenland Ice Evidence of Hemispheric Lead Pollution Two Millennia Ago by Greek and Roman Civilizations. *Science* **265**, 1841–1843, doi:10.1126/science.265.5180.1841.
- Inoue M. and Tanimizu M. (2008) Anthropogenic lead inputs to the western Pacific during the 20th century. *Sci. Total Environ.* **406**, 123–130, doi:10.1016/j.scitotenv.2008.07.032.
- Inoue M., Hata A., Suzuki A., Nohara M., Shikazono N., Yim W.W.-S., Hantoro W.S., Donghuai S. and Kawahata H. (2006) Distribution and temporal changes of lead in the surface seawater in the western Pacific and adjacent seas derived from coral skeletons. *Environ. Pollut.* **144**, 1045–1052, doi:10.1016/j.envpol.2005.11.048.
- Jackson J.M., Carmack E.C., McLaughlin F.A., Allen S.E. and Ingram R.G. (2010a) Identification, characterization, and change of the near-surface temperature maximum in the Canada Basin, 1993–2008. *J. Geophys. Res.* **115**, 16 PP., doi:10.1029/2009JC005265.
- Jackson J.M., Allen S.E., Carmack E.C. and McLaughlin F.A. (2010b) Suspended particles in the Canada Basin from optical and bottle data, 2003–2008. *Ocean Sci.* **6**, 799–813, doi:10.5194/os-6-799-2010.
- Johnson K.W., Miller L.A., Sutherland N.E. and Wong C.S. (2005) Iron transport by mesoscale Haida eddies in the Gulf of Alaska. *Deep Sea Res. Part II* **52**, 933–953, doi:10.1016/j.dsr2.2004.08.017.
- Johnson W.K. (2007) Developing standards for dissolved iron in seawater. *EOS* **88**, 131–132.

- Jones C.E., Halliday A.N., Rea D.K. and Owen R.M. (2000) Eolian inputs of lead to the North Pacific. *Geochim. Cosmochim. Acta* **64**, 1405–1416, doi:10.1016/S0016-7037(99)00439-1.
- Jones E.P., Rudels B. and Anderson L.G. (1995) Deep waters of the Arctic Ocean: origins and circulation. *Deep Sea Res. Part I* **42**, 737–760, doi:16/0967-0637(95)00013-V.
- Kawabe M. and Fujio S. (2010) Pacific ocean circulation based on observation. *J. Oceanogr.* **66**, 389–403, doi:10.1007/s10872-010-0034-8.
- Kelly A.E., Reuer M.K., Goodkin N.F. and Boyle E.A. (2009) Lead concentrations and isotopes in corals and water near Bermuda, 1780-2000. *Earth Planet. Sci. Lett.* **283**, 93–100, doi:10.1016/j.epsl.2009.03.045.
- Kramer D., Cullen J.T., Christian J.R., Johnson W.K. and Pedersen T.F. (2011) Silver in the subarctic northeast Pacific Ocean: Explaining the basin scale distribution of silver. *Mar. Chem.* **123**, 133–142, doi:16/j.marchem.2010.11.002.
- Ladd C., Crawford W.R., Harpold C.E., Johnson W.K., Kachel N.B., Stabeno P.J. and Whitney F. (2009) A synoptic survey of young mesoscale eddies in the Eastern Gulf of Alaska. *Deep Sea Res. Part II* **56**, 2460–2473, doi:16/j.dsr2.2009.02.007.
- Law C.S. et al. (2006) Patch evolution and the biogeochemical impact of entrainment during an iron fertilisation experiment in the sub-Arctic Pacific. *Deep Sea Res. Part II* **53**, 2012–2033, doi:10.1016/j.dsr2.2006.05.028.
- Lee J., Boyle E., Echegoyen-Sanz Y., Fitzsimmons J., Zhang R. and Kayser R. (2011) Analysis of trace metals (Cu, Cd, Pb, and Fe) in seawater using single batch nitrilotriacetate resin extraction and isotope dilution inductively coupled plasma mass spectrometry. *Anal. Chim. Acta* **686**, 93–101, doi:10.1016/j.aca.2010.11.052.
- Lin F.-J., Hsu S.-C. and Jeng W.-L. (2000) Lead in the southern East China Sea. *Mar. Environ. Res.* **49**, 329–342, doi:10.1016/S0141-1136(99)00076-8.
- Di Lorenzo E., Foreman M.G.G. and Crawford W.R. (2005) Modelling the generation of Haida Eddies. *Deep Sea Research Part II: Topical Studies in Oceanography* **52**, 853–873, doi:10.1016/j.dsr2.2005.02.007.
- Luengen A.C., Raimondi P.T. and Flegal A.R. (2007) Contrasting biogeochemistry of six trace metals during the rise and decay of a spring phytoplankton bloom in San Francisco Bay. *Limnol. Oceanogr.* **52**, 1112–1130, doi:10.4319/lo.2007.52.3.1112.
- Macdonald R.W. and Carmack E.C. (1991) Age of Canada Basin Deep Waters: A Way to Estimate Primary Production for the Arctic Ocean. *Science* **254**, 1348–1350, doi:10.1126/science.254.5036.1348.
- Macdonald R.W. and Carmack E.C. (1993) Tritium and Radiocarbon Dating of Canada Basin Deep Waters. *Science* **259**, 103–104, doi:10.1126/science.259.5091.103.
- Macdonald R.W. et al. (2000) Contaminants in the Canadian Arctic: 5 years of progress in understanding sources, occurrence and pathways. *Sci. Total Environ.* **254**, 93–234, doi:10.1016/S0048-9697(00)00434-4.
- Macdonald R.W., Harner T. and Fyfe J. (2005) Recent climate change in the Arctic and its impact on contaminant pathways and interpretation of temporal trend data. *Sci. Total Environ.* **342**, 5–86, doi:10.1016/j.scitotenv.2004.12.059.

- Maring H.B. and Duce R.A. (1990) The Impact of Atmospheric Aerosols on Trace Metal Chemistry In Open Ocean Surface Seawater 3. Lead. *J. Geophys. Res.* **95**, 5341–5347, doi:10.1029/JC095iC04p05341.
- Martin J.H. and Fitzwater S.E. (1988) Iron deficiency limits phytoplankton growth in the north-east Pacific subarctic. *Nature* **331**, 341–343, doi:10.1038/331341a0.
- Martin J.H., Fitzwater S.E. and Gordon R.M. (1991) We Still Say Iron Deficiency Limits Phytoplankton Growth in the Subarctic Pacific. *J. Geophys. Res.* **96**, PP. 20,699–20,700, doi:199110.1029/91JC01935.
- McLaughlin F., Shimada K., Carmack E., Itoh M. and Nishino S. (2005) The hydrography of the southern Canada Basin, 2002. *Polar Biol.* **28**, 182–189, doi:10.1007/s00300-004-0701-6.
- McLaughlin F., Carmack E., Macdonald R., Melling H., Swift J., Wheeler P., Sherr B. and Sherr E. (2004) The joint roles of Pacific and Atlantic-origin waters in the Canada Basin, 1997–1998. *Deep Sea Res. Part I* **51**, 107–128, doi:10.1016/j.dsr.2003.09.010.
- McLaughlin F.A., Carmack E.C., Macdonald R.W. and Bishop J.K.B. (1996) Physical and geochemical properties across the Atlantic/Pacific water mass front in the southern Canadian Basin. *J. Geophys. Res.* **101**, 1183–1197, doi:10.1029/95JC02634.
- Mecking S., Warner M.J. and Bullister J.L. (2006) Temporal changes in pCFC-12 ages and AOU along two hydrographic sections in the eastern subtropical North Pacific. *Deep Sea Res. Part I* **53**, 169–187, doi:10.1016/j.dsr.2005.06.018.
- Melsom A., Meyers S.D., O'Brien J.J., Hurlburt H.E. and Metzger J.E. (1999) ENSO Effects on Gulf of Alaska Eddies. *Earth Interact.* **3**, 1–30, doi:10.1175/1087-3562(1999)003<0001:EEOGOA>2.3.CO;2.
- Michaels A.F. and Flegal A.R. (1990) Lead in Marine Planktonic Organisms and Pelagic Food Webs. *Limnol. Oceanogr.* **35**, 287–295, doi:10.4319/lo.1990.35.2.0287.
- Middag R., de Baar H.J.W., Laan P. and Bakker K. (2009) Dissolved aluminium and the silicon cycle in the Arctic Ocean. *Marine Chemistry* **115**, 176–195, doi:10.1016/j.marchem.2009.08.002.
- Munk W. (1981) Internal Waves and small-scale processes, in *Evolution of Physical Oceanography—Scientific Surveys in Honor of Henry Stommel*, edited by B. Warren and C. Wunsch, pp. 264–291, MIT, Boston.
- Murozumi M., Chow T. and Patterson C. (1969) Chemical concentrations of pollutant lead aerosols, terrestrial dusts and sea salts in Greenland and Antarctic snow strata. *Geochim. Cosmochim. Acta* **33**, 1247–1294, doi:10.1016/0016-7037(69)90045-3.
- Nof D. (1981) On the β -Induced Movement of Isolated Baroclinic Eddies. *J. Phys. Oceanogr.* **11**, 1662–1672, doi:10.1175/1520-0485(1981)011<1662:OTIMOI>2.0.CO;2.
- Nozaki Y., Thomson J. and Turekian K.K. (1976) The distribution of ^{210}Pb and ^{210}Po in the surface waters of the Pacific Ocean. *Earth Planet. Sci. Lett.* **32**, 304–312, doi:10.1016/0012-821X(76)90070-4.
- Nozaki Y., Zhang J. and Takeda A. (1997) ^{210}Pb and ^{210}Po in the equatorial Pacific and the Bering Sea: the effects of biological productivity and boundary scavenging. *Deep Sea Res. Part II* **44**, 2203–2220, doi:10.1016/S0967-0645(97)00024-6.
- Nriagu J.O. (1979) Global inventory of natural and anthropogenic emissions of trace metals to the atmosphere. *Nature* **279**, 409–411, doi:10.1038/279409a0.

- Nriagu J.O. (1990) The rise and fall of leaded gasoline. *Sci. Total Environ.* **92**, 13–28, doi:10.1016/0048-9697(90)90318-O.
- Nriagu J.O. (1996) A history of global metal pollution. *Science* **272**, 223–224, doi:10.1126/science.272.5259.223.
- Ohara T., Akimoto H., Kurokawa J., Horii N., Yamaji K., Yan X. and Hayasaka T. (2007) An Asian emission inventory of anthropogenic emission sources for the period 1980–2020. *Atmos. Chem. Phys.* **7**, 4419–4444, doi:10.5194/acp-7-4419-2007.
- Okkonen S.R., Jacobs G.A., Joseph Metzger E., Hurlburt H.E. and Shriver J.F. (2001) Mesoscale variability in the boundary currents of the Alaska Gyre. *Cont. Shelf Res.* **21**, 1219–1236, doi:10.1016/S0278-4343(00)00085-6.
- O’Nions R., Frank M., von Blanckenburg F. and Ling H.-F. (1998) Secular variation of Nd and Pb isotopes in ferromanganese crusts from the Atlantic, Indian and Pacific Oceans. *Earth Planet. Sci. Lett.* **155**, 15–28, doi:10.1016/S0012-821X(97)00207-0.
- Orians K.J. and Yang L. (1994) Cadmium, zinc, nickel, copper, lead, manganese and cobalt in the Western North Pacific, in *Data and results from R.V. Aleksandr Vinogradov cruises 91-AV-19/1, North Pacific Hydrochemistry Transect; 91-AV-19/2, North Equatorial Pacific Karin Ridge Fe-Mn crust studies; and 91-AV-19/4, Northwest Pacific and Bering Sea sediment geochemistry and paleoceanographic studies*, edited by J. R. Hein, A. S. Bychkov, and A. E. Gibbs, pp. 19–38, United States Geological Survey.
- Osterberg E. et al. (2008) Ice core record of rising lead pollution in the North Pacific atmosphere. *Geophys. Res. Lett.* **35**, 4 PP., doi:200810.1029/2007GL032680.
- Patterson C.C. (1974) Lead in seawater. *Science* **183**, 553–554, doi:10.1126/science.183.4124.553.
- Patterson C.C. and Settle D.M. (1987) Review of data on eolian fluxes of industrial and natural lead to the lands and seas in remote regions on a global scale. *Mar. Chem.* **22**, 137–162, doi:10.1016/0304-4203(87)90005-3.
- Peña M.A. and Bograd S.J. (2007) Time series of the northeast Pacific. *Prog. Oceanogr.* **75**, 115–119, doi:10.1016/j.pocean.2007.08.008.
- Pope N.D. and Langston W.J. (2011) Sources, distribution and temporal variability of trace metals in the Thames Estuary. *Hydrobiologia* **672**, 49–68, doi:10.1007/s10750-011-0758-5.
- Powell K., Brown P., Byrne R., Gajda T., Hefter G., Leuz A., Sjöberg S. and Wanner H. (2009) Chemical speciation of environmentally significant metals with inorganic ligands. Part 3: The Pb²⁺ + OH⁻, Cl⁻, CO₃²⁻, SO₄²⁻, and PO₄³⁻ systems (IUPAC Technical Report). *Pure Appl. Chem.* **81**, 2425–2476, doi:10.1351/PAC-REP-09-03-05.
- Ramirez R.E. and Cullen J.T. (2010) Iron(II) in seawater of the Arctic Ocean: Observations from the GEOTRACES IPY Expedition in the Beaufort Sea, in *2010 AGU Fall Meeting*, San Francisco, USA.
- Schaule B.K. and Patterson C.C. (1981) Lead concentrations in the northeast Pacific: evidence for global anthropogenic perturbations. *Earth Planet. Sci. Lett.* **54**, 97–116, doi:10.1016/0012-821X(81)90072-8.
- Schaule B.K. and Patterson C.C. (1983) Perturbations of the natural lead depth profile in the Sargasso Sea by industrial lead., in *Trace Metals in Sea Water*, edited by C. S. Wong, E. Boyle, and K. W. Bruland, pp.

487–504, Plenum Press, New York.

- Schlosser P., Kromer B., Ekwurzel B., Bönisch G., McNichol A., Schneider R., von Reden K., Östlund H.G. and Swift J.H. (1997) The first trans-Arctic ^{14}C section: comparison of the mean ages of the deep waters in the Eurasian and Canadian basins of the Arctic Ocean. *Nucl. Instrum. Methods Phys. Res., Sect. B* **123**, 431–437, doi:10.1016/S0168-583X(96)00677-5.
- SCOR Working Group (2007) GEOTRACES – An international study of the global marine biogeochemical cycles of trace elements and their isotopes. *Chem. Erde* **67**, 85–131, doi:10.1016/j.chemer.2007.02.001.
- Serreze M.C., Holland M.M. and Stroeve J. (2007) Perspectives on the Arctic's Shrinking Sea-Ice Cover. *Science* **315**, 1533–1536, doi:10.1126/science.1139426.
- Settle D.M. and Patterson C.C. (1982) Magnitudes and sources of precipitation and dry deposition fluxes of industrial and natural leads to the North Pacific at Enewetak. *J. Geophys. Res.* **87**, PP. 8857–8869, doi:10.1029/JC087iC11p08857.
- Shen G. and Boyle E. (1987) Lead in corals - reconstruction of historical industrial fluxes to the surface ocean. *Earth Planet. Sci. Lett.* **82**, 289–304, doi:10.1016/0012-821X(87)90203-2.
- Sholkovitz E.R. (1978) The flocculation of dissolved Fe, Mn, Al, Cu, Ni, Co and Cd during estuarine mixing. *Earth Planet. Sci. Lett.* **41**, 77–86, doi:10.1016/0012-821X(78)90043-2.
- Shotyk W., Zheng J., Krachler M., Zdanowicz C., Koerner R. and Fisher D. (2005) Predominance of industrial Pb in recent snow (1994–2004) and ice (1842–1996) from Devon Island, Arctic Canada. *Geophys. Res. Lett.* **32**, 4 PP., doi:200510.1029/2005GL023860.
- Sohrin Y. and Bruland K.W. (2011) Global status of trace elements in the ocean. *TrAC, Trends Anal. Chem.* **30**, 1291–1307, doi:10.1016/j.trac.2011.03.006.
- Stukas V., Wong C. and Johnson W. (1999) Sub-part per trillion levels of lead and isotopic profiles in a fjord, using an ultra-clean pumping system. *Mar. Chem.* **68**, 133–143, doi:10.1016/S0304-4203(99)00070-5.
- Tabata S. (1982) The Anticyclonic, Baroclinic Eddy off Sitka, Alaska, in the Northeast Pacific Ocean. *J. Phys. Oceanogr.* **12**, 1260–1282, doi:10.1175/1520-0485(1982)012<1260:TABEOS>2.0.CO;2.
- Tang D., Warnken K.W. and Santschi P.H. (2002) Distribution and partitioning of trace metals (Cd, Cu, Ni, Pb, Zn) in Galveston Bay waters. *Mar. Chem.* **78**, 29–45, doi:10.1016/S0304-4203(02)00007-5.
- Tanguy V., Waeles M., Gigault J., Cabon J.-Y., Quentel F. and Riso R.D. (2011) The removal of colloidal lead during estuarine mixing: seasonal variations and importance of iron oxides and humic substances. *Mar. Freshwater Res.* **62**, 329–341, doi:10.1071/MF10220.
- Thomson R. and Krassovski M. (2010) Poleward reach of the California Undercurrent extension. *Journal of Geophysical Research - Oceans* **115**, doi:10.1029/2010JC006280.
- Thomson R.E. and Gower J.F.R. (1998) A basin-scale oceanic instability event in the Gulf of Alaska. *J. Geophys. Res.* **103**, PP. 3033–3040, doi:199810.1029/97JC03220.
- Timmermans M.-L. and Garrett C. (2006) Evolution of the Deep Water in the Canadian Basin in the Arctic Ocean. *J. Phys. Oceanogr.* **36**, 866–874, doi:10.1175/JPO2906.1.

- Toole J.M., Timmermans M.-L., Perovich D.K., Krishfield R.A., Proshutinsky A. and Richter-Menge J.A. (2010) Influences of the ocean surface mixed layer and thermohaline stratification on Arctic Sea ice in the central Canada Basin. *J. Geophys. Res.* **115**, 14 PP., doi:201010.1029/2009JC005660.
- Ueno H. and Yasuda I. (2003) Intermediate water circulation in the North Pacific subarctic and northern subtropical regions. *J. Geophys. Res.* **108**, 14 PP., doi:200310.1029/2002JC001372.
- Véron A., Church T., Rivera-Duarte I. and Flegal A. (1999) Stable lead isotopic ratios trace thermohaline circulation in the subarctic North Atlantic. *Deep Sea Res. Part II* **46**, 919–935, doi:10.1016/S0967-0645(99)00009-0.
- Vinogradova A.A. (2000) Anthropogenic pollutants in the Russian Arctic atmosphere: sources and sinks in spring and summer. *Atmos. Environ.* **34**, 5151–5160, doi:10.1016/S1352-2310(00)00352-6.
- Westerlund S. and Öhman P. (1991) Cadmium, copper, cobalt, nickel, lead, and zinc in the water column of the Weddell Sea, Antarctica. *Geochim. Cosmochim. Acta* **55**, 2127–2146, doi:10.1016/0016-7037(91)90092-J.
- Whitney F.A. and Robert M. (2002) Structure of Haida eddies and their transport of nutrient from coastal margins into the NE Pacific Ocean. *J. Oceanogr.* **58**, 715–723, doi:10.1023/A:1022850508403.
- Whitney F.A., Freeland H.J. and Robert M. (2007) Persistently declining oxygen levels in the interior waters of the eastern subarctic Pacific. *Prog. Oceanogr.* **75**, 179–199, doi:10.1016/j.pocean.2007.08.007.
- Wolff E.W. and Suttie E.D. (1994) Antarctic snow record of southern hemisphere lead pollution. *Geophys. Res. Lett.* **21**, 781–784, doi:199410.1029/94GL00656.
- Wu J. and Boyle E. (1997a) Lead in the western North Atlantic Ocean: Completed response to leaded gasoline phaseout. *Geochim. Cosmochim. Acta* **61**, 3279–3283.
- Wu J. and Boyle E.A. (1997b) Low Blank Preconcentration Technique for the Determination of Lead, Copper, and Cadmium in Small-Volume Seawater Samples by Isotope Dilution ICPMS. *Anal. Chem.* **69**, 2464–2470, doi:10.1021/ac961204u.
- Wu J., Rember R., Jin M., Boyle E. and Flegal A. (2010) Isotopic evidence for the source of lead in the North Pacific abyssal water. *Geochim. Cosmochim. Acta* **74**, 4629–4638, doi:10.1016/j.gca.2010.05.017.
- Xiu P., Palacz A.P., Chai F., Roy E.G. and Wells M.L. (2011) Iron flux induced by Haida eddies in the Gulf of Alaska. *Geophys. Res. Lett.* **38**, doi:10.1029/2011GL047946.
- You Y. (2005) Unveiling the mystery of North Pacific intermediate water formation. *Eos Trans. AGU* **86**, 65, doi:10.1029/2005EO070002.

Appendix I

Isotope dilution mass spectrometry method

All plasticware including centrifuge tubes, pipette tips and reagent containers should be cleaned thoroughly by acid leaching of trace metals before use. The first cleaning step is a 3% v/v Extran detergent solution, allowed to soak for greater than 24h. Second, 6N HCl is allowed to soak for seven days and finally soaking in 0.7 N HNO₃ for at least seven days. A vented oven can be used to speed up the process, in which case the seven day soakings can be reduced to 24h at 60 °C. Between each step, plasticware should be rinsed with ultrapure water (≥ 18.2 MΩ, DDI) at least 5 times for the acids and 10 times for the detergent solution. After rinsing the bottles following the HCl soak, the transfer of HNO₃ was performed in a clean room in order to minimize possible contaminants. The bottles were kept in autoclave bags while soaking in the oven, also to prevent contamination. Bottles used for sample storage were cleaned more thoroughly, spending at least a week in the oven for each of the acid stages, or for a month at each stage at room temperature. Before leaving the cleanroom, bottles were double-bagged and only reopened in a cleanroom or the cleanest possible condition shipboard.

The ²⁰⁷Pb spike was prepared by dissolving roughly 0.42 mg of ²⁰⁷Pb-enriched PbCO₃ obtained from Oak Ridge laboratories batch #116992 into 99.02 g of 2% v/v HNO₃ resulting in a roughly 16 μmol/L Pb solution. Using serial dilutions of no more than hundred-fold dilution at a time, this isotopically enriched solution was diluted to a final concentration of roughly 1 ppb (5 nmol/kg) to be spiked into seawater samples. The abundance of the stable isotopes is provided in Table 1. In order to determine the optimum ratio for determination by isotope dilution, the following equation was used (Heumann, 1988):

$$R_{\text{opt}} = \left[\left(\frac{h^{208}}{h^{207}} \right)_{\text{sample}} \left(\frac{h^{208}}{h^{207}} \right)_{\text{spk}} \right]^{1/2} = \left[\left(\frac{52.4}{22.1} \right) \left(\frac{4.68}{92.79} \right) \right]^{1/2} = 0.35 \quad [1]$$

where h^{208} is the abundance of ²⁰⁸Pb, h^{207} is the abundance of ²⁰⁷Pb and s and sp refer to sample (natural) and spike material, respectively. The result of 0.35 indicates that the lowest error during analysis will occur when the ²⁰⁸Pb:²⁰⁷Pb ratio is 0.35. The nature of sector-field mass spectrometers provide more precise measurements when the ratio is closer to 1, so an attempt was made to get the ratio between 0.35 and 1 during sample preparation for the lowest error during measurement.

Table 1. The relative abundance of Pb isotopes in natural samples and the ²⁰⁷Pb-enriched material used for isotope dilution.

Isotope	Natural Abundance (%)	Enriched Abundance (%)
²⁰⁴ Pb	1.4	0.01
²⁰⁶ Pb	24.1	2.51
²⁰⁷ Pb	22.1	92.79
²⁰⁸ Pb	52.4	4.68

Samples were transferred into clean centrifuge tubes by pouring directly from the sample bottle, using the graduations on the centrifuge tubes to determine volume. By not pipetting the sample into the tube, supplies can be conserved and a possible contamination source is removed from the procedure. The method used in the determinations in this thesis used 13 ml of seawater, the mass of which was then determined gravimetrically on a balance accurate to 1 mg and recorded. Depending on the expected concentration of Pb in the sample, either 30 or 50 µl of the 5 nmol/kg ²⁰⁷Pb-enriched solution was pipetted into the seawater sample and weighed once more to verify proper spike addition (i.e. an increase in mass of 0.030 or 0.050 mg). The spiked solution was allowed to sit for an hour to ensure isotopic equilibration (Wu and Boyle, 1997b). In order to precipitate Mg(OH)₂, 175 µl of concentrated Seastar Baseline ammonium hydroxide (NH₄OH) was added to the sample, capped and shaken vigorously for roughly five seconds and allowed to react for five to fifteen minutes. It was found that there was little difference in the amount of precipitate between these times. The sample was then centrifuged in a Thermo Scientific Sorvall benchtop centrifuge at 4,000 rpm for two minutes outside a cleanroom, care was taken to wipe all tubes with a kimwipe when returning to the cleanroom to avoid contamination. A small Mg(OH)₂ pellet should be clearly visible at the bottom of the tube. The supernatant can be decanted to waste, and what remains is centrifuged once more under the same conditions. The supernatant is discarded once more, and 2.0 – 2.5 ml of 1% v/v HNO₃ is added to the centrifuge tube and shaken vigorously to redissolve the Mg(OH)₃. The sample is now ready for analysis by ICP-MS.

Most preliminary work and method development was done on a Thermo X-Series II (X7) quadrupole ICP-MS operated by Dr. Jody Spence. Analysis of seawater samples were performed on a Thermo Element 2 high-resolution mass spectrometer at the Fipke Laboratory for Trace Element Research (FiLTER) at the Okanagan campus of the University of British Columbia. A Conikal glass expansion nebulizer introduced the sample to a Glass Expansion Twinnabar cyclonic spray chamber. Nickel cones were used. Sample operating conditions can be seen in Table 2. A tuning solution containing 1 ppb ²³⁸U gave a response of 1.4 x 10⁶ counts per second (cps), a blank solution containing only 1% HNO₃ gave a response of 300 cps. Samples were introduced to the system using an ESI model SC-2 autosampler.

Table 2. Typical operating conditions for the Element 2 during analysis.

Parameter	Setting
Forward Power	1100 W
Reflected RF Power	3 W
Cooling Gas	16.0 L/min
Auxiliary Gas	0.9 L/min
Sample Gas	1.125 L/min

To accurately determine the concentration of the ^{207}Pb -enriched solution, three replicate reverse-isotope dilution solutions were analyzed prior to determination of unknown concentrations (seawater samples). The standard isotope dilution equation is:

$$C_{sample} = C_{spk} \times \left[\frac{M_{spk}}{M_{sample}} \cdot \left(\frac{h_{spk}^{207} - (h_{spk}^{208} \cdot R_{measure})}{(h_{sample}^{208} \cdot R_{measure}) - h_{sample}^{207}} \right) \cdot R_{atw} \right] \quad [2]$$

where C is concentration (in mol/kg), M is mass, $R_{measure}$ is the measured ratio of the isotopes and R_{atw} is the ratio of the atomic weights of the sample and spike Pb, which differ as a result of the changed isotopic abundance. In the present case, this ratio is almost negligibly different ($R_{atw} = 1.001$). Reverse isotope dilution is performed by rearranging this equation to isolate C_{spk} and using a known standard for C_{sample} . The standard was diluted from $1,000 \pm 3 \mu\text{g/ml}$ High-Purity Standard to 200 pmol/kg and spiked with 100 μl of ^{207}Pb -enriched spike. This concentration was higher than any values seen in seawater, but was high enough that imprecision from the instrument was largely removed (instrumental precision increases with increasing concentration when working near the lower reaches of the instruments detection ability). The rearranged Equation [2] can then be solved treating C_{spk} as unknown which will provide an accurate concentration measurement for the spike. Several batches of working spike standard were prepared from a higher-concentration stock standard, the concentration of the working spike was generally 4.5 nmol/kg (0.9 ppb).

Once the concentration of the spike has been determined accurately, Equation [2] can be used with instrument output in order to determine [Pb] in the seawater samples. Mass bias corrections were not performed at the instrument as this artifact inherent to mass spectrometry would be accounted for during the reverse isotope dilution procedure. Pb concentrations was calculated manually using the instrumental output and compared with the concentration calculated by the instrument software and variation between the two values was on the order of 0.5%, well within the error of analysis.

This method has been shown to be rapid, accurate and precise in the determination of Pb in seawater with salinity as low as 26 psu in the surface layer of the Beaufort Sea. Occasionally a sample would show concentrations higher than expected or which was not oceanographically consistent and was prepared from the acidified sample in a new centrifuge tube. If the value was consistently excessively high the sample was deemed

contaminated, otherwise the reanalysis would yield a result consistent with an oceanographically consistent profile.

Appendix II

Data Tables

Table A2.1. Results of Pb determination for stations along Line P including historic data from archived samples collected in 1992 and 2003. Depth is reported in meters (m), potential density (sigma-0) and spiciness are presented in units of kg/m³ and [Pb] is reported as pmol/kg. Duplicate and triplicate Pb determinations are separated by commas.

Station	Latitude	Longitude	Depth	Sigma-0	Spiciness	[Pb]
P4	48°39.0	126°40.0	0	24.39	-0.824	21.4
			5	24.39	-0.824	10.4, 10.2
			10	24.39	-0.824	12.2
			25	25.07	-1.074	11.1
			40	25.28	-1.158	43.8
P12	48°58.2	130°40.0	0	23.42	-0.523	16.3
			5	23.42	-0.522	14.8
			10	23.42	-0.523	9.6
			25	23.48	-0.586	16.3
			40	24.72	-1.140	15.6
			75	25.30	-1.172	38.2
			100	25.61	-1.043	33.8, 34.2, 33.9
			150	26.39	-0.488	72.8
			200	26.59	-0.338	76.4
P16	49°17.0	134°40.0	0	24.02	0.163	44.8
			5	24.02	0.163	27.0
			10	24.03	0.160	30.4
			25	24.05	0.127	37.7
			40	24.82	-0.683	44.5
			75	25.62	-1.088	58.3
			100	25.94	-0.922	81.4
			150	26.54	-0.334	76.5
			200	26.67	-0.451	72.9, 69.8
			300	26.83	-0.516	59.9
			400	26.96	-0.455	55.3

Station	Latitude	Longitude	Depth	Sigma-0	Spiciness	[Pb]
P20	49°34.0	138°40.0	5	23.91	0.288	36.3
			10	23.91	0.288	33.0
			25	24.02	0.193	34.5
			40	25.09	-0.741	43.5
			75	25.61	-1.136	58.5
			100	25.95	-0.944	67.8
			150	26.58	-0.390	74.5
			200	26.7	-0.498	63.8
			300	26.87	-0.545	63.7
			400	26.99	-0.463	56.6
P26	50°00.0	145°00.0	0	24.44	-0.087	40.5
			5	24.44	-0.088	47.2
			10	24.44	-0.087	43.1
			25	24.76	-0.363	48.4
			40	25.42	-0.937	40.5, 40.2, 40.3
			75	25.78	-1.133	60.3
			100	26.01	-1.142	53.4
			150	26.71	-0.624	61.2
			200	26.82	-0.636	60.3
			300	26.95	-0.551	56.5
			400	27.05	-0.470	56.1
			600	27.20	-0.372	49.0
			800	27.33	-0.322	45.6
P26 (1992)	50°00.0	145°00.0	25	24.29	-0.363	51.7
			50	25.02	-0.910	41.6
			75	25.53	-1.326	48.3
			100	25.73	-1.351	44.7
			150	26.46	-0.797	54.6, 54.2
			200	26.74	-0.607	58.0
			2000	27.66	-0.208	20.0
P26 (2003)	50°00.0	145°00.0	10	24.34	-0.293	38.4

Station	Latitude	Longitude	Depth	Sigma-0	Spiciness	[Pb]
			40	25.07	-0.938	37.8
			100	26.23	-1.069	55.0
			200	26.79	-0.597	56.8
			600	27.19	-0.369	45.2, 44.5

Table A2.2. Results from the stations occupied during the coastal cruise along transects off the coast of British Columbia and southern Alaska during August 2010. Depth is reported in meters (m), potential density (Sigma-0) and spiciness are in kg/m³ and [Pb] is reported as pmol/kg. Multiple values for [Pb] separated by commas are replicate measurements as outlined in the methods section.

Station	Latitude	Longitude	Depth	Sigma-0	Spiciness	[Pb]
W2	56°15.2	135°01.5	10	24.14	-1.510	46.7
			31	24.61	-1.704	24.6
			50	24.85	-1.565	31.6
			90	25.51	-1.257	35.1
			120	26.16	-0.876	32.9, 33.7
W7	56°01.6	135°34.4	12	24.38	-0.825	67.3
			70	25.37	-1.409	45.8
			148	26.22	-0.999	63.0
			401	26.98	-0.443	56.9
			701	27.23	-0.311	55.5
W12	55°18.5	137°09.0	10	24.07	-0.868	79.2, 81.4, 78.8
			99	25.50	-1.283	58.9
			375	26.84	-0.557	60.6
			1001	27.35	-0.283	45.5
			2002	27.65	-0.209	37.9
CS2	50°40.8	128°45.5	16	25.28	-1.023	37.5
			51	25.89	-0.685	43.6
			92	26.53	-0.380	59.9
			120	26.64	-0.323	62.7
			151	26.72	-0.340	67.5
CS4	50°36.9	128°53.8	21	24.87	-1.195	35.9
			100	26.53	-0.417	50.1
			300	26.84	-0.326	66.0

Station	Latitude	Longitude	Depth	Sigma-0	Spiciness	[Pb]
CS8	50°06.0	130°03.0	600	27.06	-0.298	55.8, 55.5, 56.2
			1000	27.34	-0.240	46.0
			51	24.89	-1.278	41.7
			150	26.41	-0.397	67.2
			300	26.79	-0.329	68.3
			1001	27.37	-0.248	47.7
			1801	27.63	-0.212	31.3
G5	49°07.3	126°55.2	30	26.37	-0.468	67.2
			100	26.64	-0.263	66.5
			248	26.79	-0.283	64.0
G7	48°59.4	127°07.2	20	25.08	-1.172	42.1, 41.5
			102	26.44	-0.323	66.7
			397	26.89	-0.290	60.5
			1000	27.37	-0.222	42.6
			1701	27.60	-0.209	27.6
G9	48°35.8	127°42.7	50	25.23	-1.107	42.4
			200	26.59	-0.243	57.0
			600	27.09	-0.298	47.2
			1400	27.52	-0.219	31.5
			2001	27.66	-0.199	17.8
A10	47°59.0	125°43.4	27	24.90	-0.910	43.0
			127	26.29	-0.330	56.5
			202	26.60	-0.249	68.5
			601	27.05	-0.260	48.8, 46.7
			801	27.21	-0.231	47.8
WH5	47°08.5	124°58.8	10	24.24	-0.293	41.2
			50	25.33	-1.087	61
			100	26.26	-0.406	62.8
			150	26.60	-0.200	57.8
			200	26.68	-0.214	59.1, 59.2, 59.1
WH7	47°08.5	125°15.4	22	24.99	-0.931	46.3
			201	26.60	-0.227	63.9

Station	Latitude	Longitude	Depth	Sigma-0	Spiciness	[Pb]
			300	26.76	-0.284	60.6
			603	27.09	-0.255	45
			1451	27.55	-0.204	22.9

Table A2.3. Results of Pb determinations in the Haida eddy along with relevant physical parameters. Latitude and longitude are presented as degrees north and west respectively, depth is in metres (m), potential density (Sigma-0) and spiciness are reported as kg/m³ and [Pb] is in pmol/kg. [Pb] separated by commas are replicates from the same subsampled container. Values reported in brackets were prepared and analyzed a second time and replaced with the value of the second determination.

Station	Latitude	Longitude	Depth	Sigma-0	Spiciness	[Pb]
Haida Reference	51°24.0	134°00.1	10	25.11	-1.250	43.5
			20	25.11	-1.252	35.4
			30	25.11	-1.272	37.1
			40	25.19	-1.296	35.6
			50	25.28	-1.323	40.6
			75	25.64	-1.003	41.3
			95	26.21	-0.661	48.1
			170	26.63	-0.436	67.4
			200	26.69	-0.407	68.7
			300	26.82	-0.414	55.5, 55.3
			400	26.92	-0.412	55.2
			600	27.11	-0.345	48.1
			800	27.26	-0.298	42.3
				51°50.0	133°39.4	10
40	25.18	-1.345				32.4
52°05.0	133°28.4	10		24.93	-1.411	24.5
		40		24.98	-1.372	26.2
Haida Centre	52°20.0	133°17.4	10	24.96	-1.403	22.0
			20	24.97	-1.407	21.4
			30	24.99	-1.423	20.9, 20.6, 21.4

Station	Latitude	Longitude	Depth	Sigma-0	Spiciness	[Pb]
			40	25.00	-1.435	21.3
			50	25.05	-1.462	21.1
			75	25.30	-1.273	(28.0), 24.6
			100	25.64	-0.930	18.8
			150	26.15	-0.518	22.7
			200	26.46	-0.310	29.2
			300	26.58	-0.269	37.4
			400	26.63	-0.259	39.2
			600	26.91	-0.359	48.9
			800	27.11	-0.339	45.8, 43.1
	52°30.8	133°08.9	10	24.95	-1.414	26.0
			40	24.96	-1.417	22.6
Haida Edge	52°47.1	132°56.2	10	24.89	-1.334	24.0
			20	24.93	-1.381	25.8
			30	24.99	-1.385	27.4
			40	25.03	-1.395	29.4
			50	25.09	-1.391	(38.0), 30.9
			75	25.25	-1.320	30.1
			100	25.64	-0.934	29.6, 28.7, 29.2
			150	26.25	-0.568	36.8
			200	26.51	-0.460	56.5
			300	26.72	-0.363	55.5
			400	26.83	-0.375	51.9
			600	27.05	-0.357	21.2
			800	27.22	-0.315	21.0

Table A2.4. Results of Pb determinations in the Sitka and Yakutat eddy along with relevant physical parameters. Latitude and longitude are presented as degrees north and west respectively, depth is in metres (m), potential density (Sigma-0) and spiciness are reported as kg/m³ and [Pb] is in pmol/kg. [Pb] separated by commas are replicates from the same subsampled container. [Pb] values with an asterisk are instrument replicates (same sample run on the instrument on consecutive days). Values reported in brackets were prepared and analyzed a second time and replaced with the value of the second determination.

Station	Latitude	Longitude	Depth	Sigma-0	Spiciness	[Pb]
Sitka Reference	54°37.2	135°00.0	20	25.00	-1.384	22.5
			30	25.04	-1.359	26.7
			40	25.18	-1.362	(57.1), 35.9
			50	25.22	-1.359	31.7
			75	25.36	-1.411	33.6
			100	25.49	-1.342	37.2
			150	26.17	-0.656	52.7
			200	26.55	-0.390	56.6
			300	26.75	-0.406	57.3
			400	26.89	-0.409	50.0
			600	27.09	-0.361	56.8
800	27.24	-0.310	46.8			
Sitka Edge	56°28.2	138°19.4	10	25.08	-1.387	20.8
			20	25.10	-1.381	20.8
			30	25.16	-1.420	21.0
			40	25.30	-1.498	22.1
			50	25.36	-1.458	28.4
			75	25.45	-1.471	30.9, 31.3*
			100	25.57	-1.292	29.4, 29.6*
			150	26.23	-0.629	31.7, 31.7*
			200	26.51	-0.454	48.4, 51.6, 47.9
			300	26.74	-0.399	53.4
			400	26.87	-0.433	60.4
600	27.06	-0.373	47.1			
800	27.21	-0.326	40.9			
Sitka Centre	56°03.0	138°48.8	10	24.99	-1.537	13.9
			20	25.03	-1.651	(25.3), 17.8

Station	Latitude	Longitude	Depth	Sigma-0	Spiciness	[Pb]
			30	25.12	-1.749	13.0
			40	25.16	-1.775	16.1
			50	25.19	-1.769	15.7
			75	25.25	-1.722	14.0
			100	25.32	-1.648	20.7
			150	25.77	-1.061	22.5
			200	26.24	-0.658	22.7
			300	26.49	-0.463	37.4
			400	26.65	-0.398	36.9
			600	26.94	-0.412	47.5
			800	27.14	-0.348	42.1
Yakutat Centre	57°57.0	140°03.0	10	24.89	-1.659	12.4
			20	25.00	-1.755	13.8
			30	25.07	-1.848	11.5
			40	25.10	-1.861	13.0
			50	25.14	-1.854	12.2
			75	25.22	-1.771	13.4
			100	25.26	-1.729	13.3, 13.0, 13.0
			150	25.53	-1.346	19.6
			200	26.01	-0.841	19.3
			300	26.60	-0.418	50.5
			400	26.80	-0.409	45.7
			600	27.02	-0.389	45.7
			800	27.17	-0.339	59.2, 61.2
	56°35.1	139°28.7	10	25.07	-1.376	22.7
			100	25.47	-1.395	25.1
	56°45.4	139°14.2	10	25.02	-1.637	17.4
			100	25.45	-1.509	26.5
	56°55.7	138°59.6	10	25.03	-1.527	15.3
			100	25.40	-1.548	21.4
	57°06.0	138°45.0	10	24.97	-1.642	18
			100	25.28	-1.697	18.3

Station	Latitude	Longitude	Depth	Sigma-0	Spiciness	[Pb]
	57°10.4	138°25.0	10	24.97	-1.559	25.1
			100	25.37	-1.587	24.9
	57°15.0	138°05.0	10	24.89	-1.549	12.9
			100	25.45	-1.492	20.5

Table A2.5. Results of Pb determinations in the Canada Basin along with relevant physical parameters. Latitude and longitude are presented as degrees north and west respectively, depth is in metres (m), potential density (Sigma-0) is reported as kg/m³, salinity is reported in psu and [Pb] is in pmol/kg. [Pb] separated by commas are replicates from the same subsampled container.

Station	Latitude	Longitude	Depth	Sigma-0	Salinity	[Pb]
L1	71°06.9	139°19.9	8	20.57	25.64	29.7
			15	21.89	27.27	40.6
			40	23.75	29.57	14.0
			90	25.65	31.91	54.1
			160	26.54	32.99	20.1
			250	27.66	34.43	18.8
			400	27.91	34.81	32.7
			599	27.96	34.85	21.9, 22.5
			800	27.99	34.87	4.6
			1100	28.02	34.89	19.6
			1400	28.05	34.91	18.1
			1750	28.07	34.93	10.9
L1.1	72°30.6	136°35.5	8	20.47	25.51	12.7
			40	23.33	29.04	7.8
			75	24.91	30.99	5.9
			111	25.82	32.12	6.0
			170	26.47	32.91	1.8
			270	27.70	34.49	10.3
			425	27.92	34.83	23.4
			600	27.96	34.85	7.7
			1000	28.01	34.88	8.4
			1500	28.06	34.92	3.2
			2000	28.08	34.94	10.5
			2400	28.09	34.95	7.0, 7.0, 8.4

Station	Latitude	Longitude	Depth	Sigma-0	Salinity	[Pb]
L1.5	73°19.2	139°23.4	10	20.32	25.33	31.7
			19	22.04	27.46	34.0
			40	22.97	28.60	20.4
			90	25.30	31.47	41.1
			140	26.10	32.45	19.3
			280	26.76	33.27	29.7
			380	27.72	34.52	27.6
			450	27.92	34.83	7.7, 9.0
			600	27.95	34.85	37.8
			800	27.99	34.87	35.0
			1001	28.01	34.88	18.3
L2	74°23.6	136°09.6	8	21.37	26.62	9.8
			25	22.87	28.47	13.4
			55	24.48	30.46	5.4
			120	25.97	32.29	14.3
			180	26.66	33.15	9.6
			271	27.71	34.51	11.3
			360	27.89	34.78	13.8, 14.4
			421	27.92	34.82	7.7
			501	27.94	34.85	4.2
			648	27.97	34.86	16.8
			800	27.99	34.87	13.4
			899	28.00	34.88	(101.3), (102.7)
			1100	28.02	34.89	8.6
			1300	28.04	34.90	23.7
			1500	28.05	34.92	35.5
			1700	28.07	34.93	41.7
			1900	28.08	34.94	25.6
			2100	28.08	34.94	66.6, 67.6, 67.0
			2300	28.09	34.95	3.8
			2501	28.09	34.95	36.4
2701	28.09	34.96	11.2			
2950	28.09	34.96	14.4			
L3	75°16.8	137°33.6	10	21.28	26.52	15.0
			32	23.12	28.78	30.6

Station	Latitude	Longitude	Depth	Sigma-0	Salinity	[Pb]
			55	24.63	30.65	8.1
			140	26.15	32.51	22.5
			180	26.71	33.20	8.9, 7.8, 8.3
			260	27.67	34.45	8.3
			349	27.89	34.78	13.2
			440	27.92	34.83	10.0
			600	27.96	34.85	8.8
			801	27.99	34.87	15.3
			1000	28.01	34.88	20.6
			1201	28.03	34.90	20.1
S4	71°11.0	132°56.6	7	21.00	26.24	16.1
			17	23.00	28.72	12.6
			50	25.03	31.14	8.5
			90	25.93	32.25	16.6
			150	26.60	33.07	3.8
			240	27.68	34.46	7.4

Table A2.6. Results from archived samples collected along Line P in June 2000. Results are not presented or discussed in text as a result of a number of elevated values, which arouse suspicion of possible sample contamination. Latitude and longitude are presented as degrees north and west respectively, depth is in metres (m), potential density (Sigma-0) is reported as kg/m³, salinity is reported in psu and [Pb] is in pmol/kg. [Pb] separated by commas are replicates from the same subsampled container.

Station	Year	Latitude	Longitude	Depth	[Pb]
P04	2000	48°39.0	126°40.0	10	52.7
				25	56.3
				40	122.0
				75	41.5
				200	66.7
				300	90.1
				400	83.8, 88.3
				600	55.5
				1000	46.1
P12	2000	48°58.2	130°40.0	10	49.0

Station	Year	Latitude	Longitude	Depth	[Pb]
				25	52.6
				40	76.3
				75	57.8
				100	93.5
				200	77.6, 80.5, 97.8*
				300	68.9
				400	62.0
				600	59.8
				800	160.5
				1000	50.0
P16	2000	49°17.0	134°40.0	10	50.3
				25	59.0
				40	44.2, 43.9
				75	64.2
				100	79.7
				200	74.8
				300	144.6
				600	54.2
				800	55.6
P20	2000	49°34.0	138°40.0	10	65.9
				25	40.3
				40	36.4
				75	67.3
				100	174.0
				200	225.7
				300	220.0
				400	211.4
				600	48.9
				800	42.2
				1000	204.0